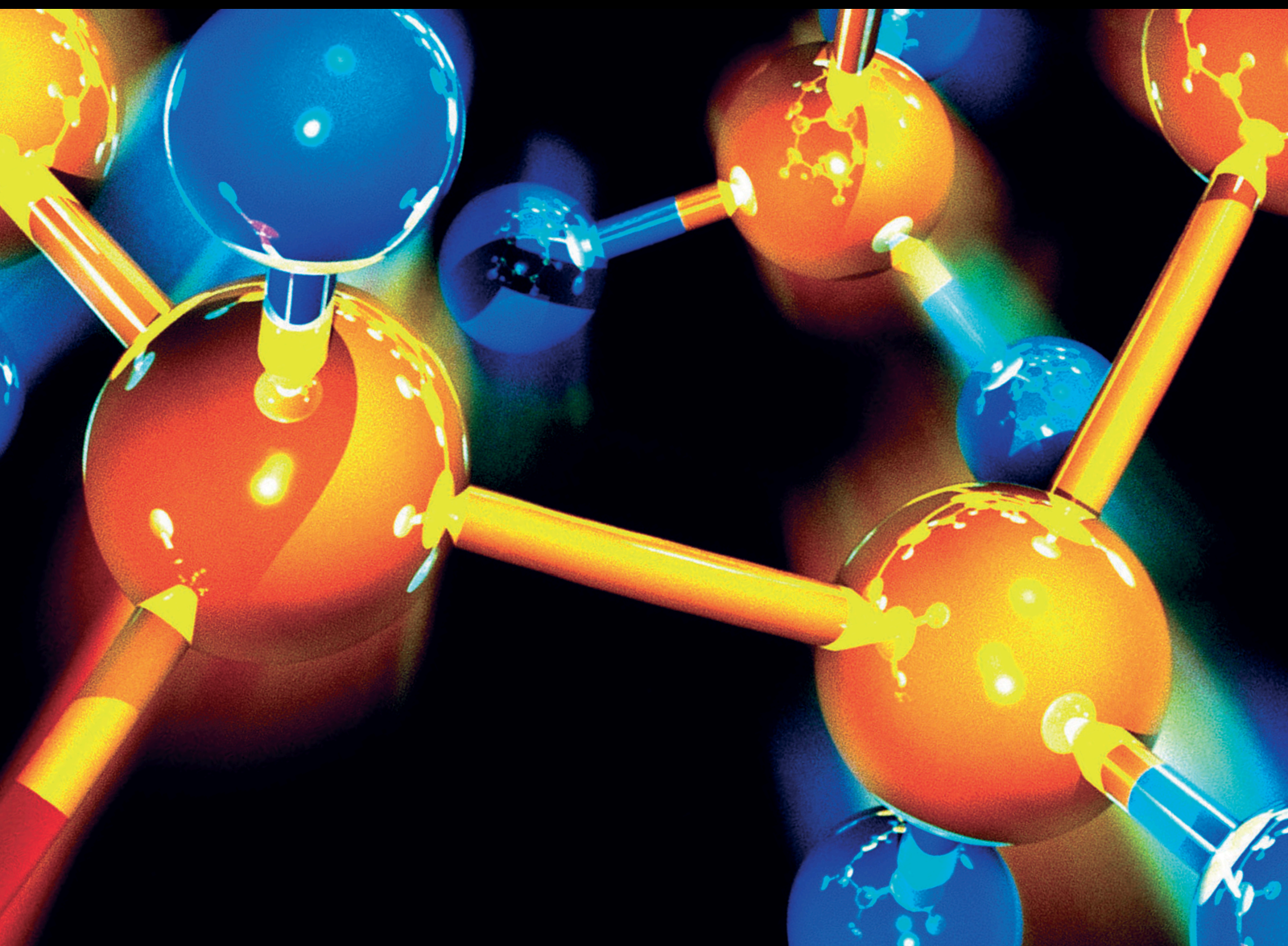# Challenges and Opportunities in the Application of Chemometrics in the Pharmaceutical and Food Science Industries

Lead Guest Editor: Alina Barbulescu
Guest Editors: Lucica Barbes and Cristiana Ra#dulescu

Challenges and Opportunities in the Application of Chemometrics in the Pharmaceutical and Food Science Industries

Challenges and Opportunities in the Application of Chemometrics in the Pharmaceutical and Food Science Industries

Lead Guest Editor: Alina Barbulescu
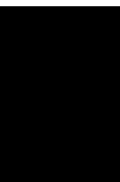Guest Editors: Lucica Barbes and Cristiana Ra#dulescu

Chief Editor

Pasquale Longo, Italy
Pablo Lorenzo-Luis, Spain
Zhang-Hui Lu, China
Devanand Luthria, USA
Konstantin V. Luzyanin, United Kingdom
Mari Maeda-Yamamoto, Japan
Isabel Mafra, Portugal
Dimitris P. Makris, Greece
Pedro M. Mancini, Argentina
Marcelino Maneiro, Spain
Giuseppe F. Mangiatordi, Italy
Casimiro Mantell, Spain
Ana B. Martin-Diana, Ireland
Carlos A Martínez-Huitle, Brazil
José M. G. Martinho, Portugal
Andrea Mastinu, Italy
Cesar Mateo, Spain
Georgios Matthaiolampakis, USA
Mehrab Mehrvar, Canada
Saurabh Mehta, India
Oinam Romesh Meitei, USA
Saima Q. Memon, Pakistan
Maurice Millet, France
Angelo Minucci, Italy
Liviu Mitu, Romania
Hideto Miyabe, Japan
Kaustubha Mohanty, India
Ana Moldes, Spain
Subrata Mondal, India
José Morillo, Spain
Giovanni Morrone, Italy
Marta E. G. Mosquera, Spain
Khaled Mostafa, Egypt
Ahmed Mourran, Germany
Markus Muschen, USA
Benjamin Mwashote, USA
Mallikarjuna N. Nadagouda, USA
Lutfun Nahar, United Kingdom
Mu. Naushad, Saudi Arabia
Gabriel Navarrete-Vazquez, Mexico
Jean-Marie Nedelec, France
Orazio Nicolotti, Italy
Nagatoshi Nishiwaki, Japan
Tzortzis Nomikos, Greece
Marjana Novic, Slovenia
Beatriz P. P. Oliveira, Portugal
Leonardo Palmisano, Italy

Mohamed Afzal Pasha, India
Dario Pasini, Italy
Angela Patti, Italy
Massimiliano F. Peana, Italy
Andrea Penoni, Italy
Franc Perdih, Slovenia
Jose A. Pereira, Portugal
Pedro Avila Pérez, Mexico
Maria Grazia Perrone, Italy
Silvia Persichilli, Italy
Thijs A. Peters, Norway
Christophe Petit, France
Marinos Pitsikalis, Greece
Rita Rosa Plá, Argentina
Fabio Polticelli, Italy
Josefina Pons, Spain
V. Prakash Reddy, USA
María Quesada-Moreno, Germany
Maurizio Quinto, Italy
Franck Rabilloud, France
Jamal Rafique, Brazil
C.R. Raj, India
Sanchayita Rajkhowa, India
Teodorico C. Ramalho, Brazil
Manzoor A. Rather, India
Julia Revuelta, Spain
Alberto Ritieni, Italy
Muhammad Rizwan, Pakistan
Manfredi Rizzo, Italy
Maria P. Robalo, Portugal
Maria Roca, Spain
Nicolas Roche, France
Samuel Lalthazuala Rokhum, India
Roberto Romeo, Italy
Antonio M. Romerosa-Nievas, Spain
Ioannis G. Roussis, Greece
Arpita Roy, India
Deniz ŞAHİN, Turkey
Nagaraju Sakkani, USA
Diego Sampedro, Spain
Shengmin Sang, USA
Eloy S. Sanz-Pérez, Spain
Vikram Sarpe, USA
Adrian Saura-Sanmartin, Spain
Stéphanie Sayen, France
Ewa Schab-Balcerzak, Poland
Hartwig Schulz, Germany

Contents

Editorial

Challenges and Opportunities in the Application of Chemometrics in the Pharmaceutical and Food Science Industries

Alina Bărbulescu [ID] [1] **and Lucica Barbeș** [ID] [2]

[1]*Transilvania University of Brașov, Department of Civil Engineering, 5, Turnului Street, 900152 Brașov, Romania*
[2]*Ovidius University of Constanța, Department of Chemistry and Chemical Engineering, 124, Mamaia Bd.,*
 900527 Constanța, Romania

Correspondence should be addressed to Alina Bărbulescu; alinadumitriu@yahoo.com

Nowadays, water, air, and soil pollution significantly impact the environment, the plants' growth, and food quality, given that many plants act as bioaccumulators. Therefore, consumers are concerned with food origin, authenticity, composition, and processing since its quality affects their health and lives [1–6].

Used for modeling problems from the environmental sciences, multivariate data analysis [4, 7–10], among which Principal Component Analysis and clustering became an important tool that, in combination with instrumental techniques, has a vital role in the control and monitoring of the various stages of the production chain. The most effective applications of chemometrics in the research and technology of functional foods and pharmaceuticals are those related to measuring compositional parameters based on instrumental analysis methods.

The advantages of the predictive capacity of multiple parameters have made significant contributions to the development of most applications currently used by the food and pharmaceutical industry and the emergence of new applications. With the development of new analysis tools and techniques, new analytical strategies, such as profiling and fingerprinting, contribute to obtaining a large data volume that characterizes the studied systems.

This special issue contains original research papers on developing multivariate and multidirectional methods, methodological aspects of chemometrics research were aimed at optimizing chemical systems, selection of process variables, and fusion of experimental data.

The article of Hssaini et al. [11] answers the question of whether pollination and pollen sources influence the fig seed set and their quality, using a combined approach of vibrational spectroscopy and ionomic fingerprinting. The topic treated is important since the pollination is required for fruit loading and has an important impact on fruit quality [12–15]. Results showed that pollination and pollen source significantly impacted seed set as it was higher in fertilized seeds than in control. Caprification displayed a significant effect on seeds' phenolic components. FTIR-ATR indicated that the fertilized sets have a high vibrational intensity than the control in all fingerprint regions.

Principal component analysis showed high throughput classification with similar patterns for FTIR-ATR fingerprinting and ionomic and biochemical analysis. The multivariate analysis provided identical samples' classification, indicating that vibrational spectroscopy may be accurate, fast, and cost-effective to investigate this effect on large samples further.

This study provides valuable information to understand better the impact of the mutualism between fig and its wasp on seed set.

The article of Park et al. [16] investigated the influence of the reaction conditions on the spectrophotometric and fluorometric assays using different substrates for optimizing for screening the lipase activity from *Chromobacterium viscosum*, *Pseudomonas fluorescens*, *Sus scrofa* pancreas, and *Triticum aestivum*. Different pH, temperature, and substrates have been considered. Experiments of 17 agricultural

products have confirmed the optimized conditions (pH = 7 and temperature = 30°C). The authors also proposed *P. eryngii* as a novel source of lipases. Factorial design is one of the most used methods for optimizing the extraction of different substances, applied to reduce the number of laboratory experiments or confirm the experimental findings [17–20].

In their article, Ngamkhae et al. [21] applied this method to optimize the Kleeb Bua Daeng extraction, one of the most used remedies used in Thailand. Its active components are *Centella asiatica* L., *Nelumbo nucifera* Gaertn., and *Piper nigrum* L, having mainly antioxidant, anti-inflammatory, analgesic, and antidepressant effects [22–25].

Seventeen laboratory experiments at three levels (−1, 0, +1) and three factors (type of solvent—ethyl acetate, ethanol, methanol—number of extraction times—1, 2, 4—and material-to-solvent ratio −1 : 3, 1 : 6, and 1 : 9) were used to evaluate the optimal conditions of the extraction process. In each experiment, different dependent variables were considered: percentage extraction yield, total phenolic content, total flavonoid content, total carotenoid content, and total anthocyanin content. The highest content of each total active compound was not obtained in the same conditions. Therefore, the optimal condition for each active content for product development should be chosen depending on the purpose because different types of active compounds express different biological activities.

Moreover, improving the variable factors from the study for the basic solvent extraction technique might be necessary to get the better suitable variable factors such as changing the type of organic solvent to the ratio of ethanol and water for the extraction.

The articles of Alhazmi et al. [26] and Bărbulescu et al. [27] employ chemometric methods [28–30] for analyzing new drugs. In [26], the amphetamine tables collected in some cities in Saudi Arabia have been studied to determine their content. The same techniques—GC-MS and ICP-MS—have been used by the authors to perform analysis of various other substances of abuse and determined a number of constituents [31–33] in the samples. Apart from the amphetamine, other psychoactive and nonpsychoactive additives were also identified (caffeine, lidocaine, diphenhydramine, and 8-chlorotheophylline), which may have been added to enhance the effects of amphetamine and to increase the dependence. The samples have finally been classified into six clusters, using hierarchical clustering with average linking, based on the percentage of different compounds found.

The appearance on the free market of synthetic cannabinoids raised the researchers' interest in establishing their molecular similarity. A rigorous criterion for classifying drugs is their chemical structure. In [27], the authors present their research on the structural similarity of two groups of drugs—benzoylindoles and phenylacetylindoles—using the facilities provided by rcdk and ChemmineR packages in R. Statistical analysis and clustering of the molecules are performed based on their numerical characteristics extracted using cheminformatics methods. Their similarities/dissimilarities have been emphasized using the Tanimoto index, dendrograms, and heat map. The highest discrepancies are found in the phenylacetylindoles group. Further practical studies should confirm the similarity of the actions and effects in the same cluster and the possible cure using the same inhibitors. The study is extended in [34] with the possible activities of the investigated drugs.

We hope that the readers will find new idea for their research in the related research fields.

Conflicts of Interest

The editors declare that they have no conflicts of interest regarding the publication of this special issue.

Acknowledgments

Alina Bărbulescu
Lucica Barbeş

References

[1] A. A. Georgescu, A. Danet, C. Radulescu, I. D. Dulama, and D. Elena, "Determination of several elements in edible mushrooms using ICP-MS," *Romanian Journal of Physics*, vol. 61, no. 5-6, pp. 1087–1097, 2016.

[2] A. Chilian, O. Bancuta, I. Bancuta et al., "Study of the influence of Zn concentration on the absorption and transport of Fe in maize by AAS and EDXRF analysis techniques," *Romanian Reports in Physics*, vol. 67, no. 3, pp. 1138–1151, 2015.

[3] A. Bărbulescu and C. Ş. Dumitriu, "Assessing water quality by statistical methods," *Water*, vol. 13, no. 8, p. 1026, 2021.

[4] A. Al-Taani, Y. Nazzal, F. Howari et al., "Contamination assessment of heavy metals in agricultural soil, in the Liwa Area (UAE)," *Toxics*, vol. 9, no. 3, p. 53, 2021.

[5] I. Manea, L. Manea, C. Radulescu et al., "Assessment of metals level in several meat products obtained through conventional and traditional methods," *Romanian Report in Physics*, vol. 69, no. 4, p. 711, 2017.

[6] N. M. Tanase, I. V. Popescu, C. Radulescu et al., "Occurrence, toxicological risks of heavy metals and possible agricultural consequences of sewage sludge from urban treatment plants," *Romanian Journal of Physics*, vol. 65, p. 812, 2020.

[7] A. Bărbulescu, L. Barbeş, and C. Ş. Dumitriu, "Assessing the water pollution of the Brahmaputra River using water quality indexes," *Toxics*, vol. 9, no. 11, p. 297, 2021.

[8] C. Costa, C. Taiti, M. C. Strano et al., "Chapter 8- multivariate approaches to electronic nose and PTR–TOF–MS technologies in agro-food products," in *Electronic Noses and Tongues in Food Science*, M. L. Rodríguez Méndez, Ed., pp. 73–82, Academic Press, 2016.

[9] S. L. C. Ferreira, M. M. Silva Junior, C. S. A. Felix et al., "Multivariate optimization techniques in food analysis - a review," *Food Chemistry*, vol. 273, pp. 3–8, 2019.

[10] A. Valdés, A. Beltrán, C. Mellinas, A. Jiménez, and M. C. Garrigós, "Analytical methods combined with multivariate analysis for authentication of animal and vegetable food products with high fat content," *Trends in Food Science & Technology*, vol. 77, pp. 120–130, 2018.

[11] L. Hssaini, R. Razouk, A. Irchad, R. Aboutayeb, and R. Ouaabou, "Do pollination and pollen sources affect fig seed

set and quality? First attempt using chemical and vibrational fingerprints coupled with chemometrics," *Journal of Chemistry*, vol. 2022, Article ID 3969165, 13 pages, 2022.

[12] M. Rahemi and M. Jafari, "Effect of caprifig type on quantity and quality of Estahban dried fig Ficus carica cv. Sabz," *Acta Horticulturae*, vol. 798, no. 798, pp. 249–252, 2008.

[13] B. Gaaliche, M. Trad, and M. Mars, "Effect of pollination intensity, frequency and pollen source on fig (*Ficus carica* L.) productivity and fruit quality," *Scientia Horticulturae*, vol. 130, no. 4, pp. 737–742, 2011.

[14] M. Trad, C. Le Bourvellec, B. Gaaliche, C. Ginies, C. M. G. C. Renard, and M. Mars, "Caprification modifies polyphenols but not cell wall concentrations in ripe figs," *Scientia Horticulturae*, vol. 160, pp. 115–122, 2013.

[15] Y. Rosianski, Z. E. Freiman, S. M. Cochavi, Z. Yablovitz, Z. Kerem, and M. A. Flaishman, "Advanced analysis of developmental and ripening characteristics of pollinated common-type fig (*Ficus carica* L.)," *Scientia Horticulturae*, vol. 198, pp. 98–106, 2016.

[16] J.-Y. Park, J. Ha, Y. Choi, P.-S. Chang, and K.-M. Park, "Optimization of spectrophotometric and fluorometric assays using alternative substrates for the high-throughput screening of lipase activity," *Journal of Chemistry*, vol. 2021, Article ID 3688124, 10 pages, 2021.

[17] O. Buriac, M. Ciopec, N. Duțeanu, A. Negrea, P. Negrea, and I. Grozav, "Platinum (IV) recovery from waste solutions by adsorption onto Dibenzo-30-crown-10 Ether Immobilized on Amberlite XAD7 Resin-Factorial Design Analysis," *Molecules*, vol. 25, no. 16, p. 3692, 2020.

[18] A. Gabor, C. M. Davidescu, A. Negrea et al., "Optimizing the lanthanum adsorption process onto chemically modified biomaterials using factorial and response surface design," *Journal of Environmental Management*, vol. 204, pp. 839–844, 2017.

[19] S. Al-Asheh, R. Jumah, F. Banat, and S. Hammad, "The use of experimental factorial design for analysing the effect of spray dryer operating variables on the production of tomato powder," *Food and Bioproducts Processing*, vol. 81, no. 2, pp. 81–88, 2003.

[20] A. Mihăilescu, M. Negrea, M. Ciopec et al., "Full factorial design for gold recovery from industrial solutions," *Toxics*, vol. 9, no. 5, p. 111, 2021.

[21] N. Ngamkhae, O. Monthakantirat, Y. Chulikhit et al., "Optimized extraction method for Kleeb Bua Daeng formula with the aid of the experimental design," *Journal of Chemistry*, vol. 2021, Article ID 1457729, 10 pages, 2021.

[22] Y. Deng, S. Sriwiriyajan, A. Tedasen, P. Hiransai, and P. Graidist, "Anti-cancer effects of *Piper nigrum* via inducing multiple molecular signaling *in vivo* and *in vitro*," *Journal of Ethnopharmacology*, vol. 188, pp. 87–95, 2016.

[23] Z. Zarai, E. Boujelbene, N. Ben Salem, Y. Gargouri, and A. Sayari, "Antioxidant and antimicrobial activities of various solvent extracts, piperine and piperic acid from Piper nigrum," *Lebensmittel-Wissenschaft und-Technologie-Food Science and Technology*, vol. 50, no. 2, pp. 634–641, 2013.

[24] J. H. Park, J. Y. Choi, D. J. Son et al., "Anti-Inflammatory effect of titrated extract of *Centella asiatica* in phthalic anhydride-induced allergic dermatitis animal model," *International Journal of Molecular Sciences*, vol. 18, no. 4, p. 738, 2017.

[25] F. Pittella, R. Dutra, D. Junior, M. T. Lopes, and N. Barbosa, "Antioxidant and cytotoxic activities of *Centella asiatica* (L)

urb," *International Journal of Molecular Sciences*, vol. 10, no. 9, pp. 3713–3721, 2009.

[26] H. A. Alhazmi, W. Ahsan, M. Al Bratty et al., "Chemo-profiling of illicit amphetamine tablets seized from Jazan, Saudi Arabia, using gas chromatography-mass spectrometry and chemometric techniques," *Journal of Chemistry*, vol. 2021, 10 pages, 2021.

[27] A. Bărbulescu, L. Barbeş, and C. Ş. Dumitriu, "Computer-aided classification of new psychoactive substances," *Journal of Chemistry*, vol. 2021, Article ID 4816970, 11 pages, 2021.

[28] A. Voicu, N. Duțeanu, M. Voicu, D. Vlad, and V. Dumitrascu, "The rcdk and cluster R packages applied to drug candidate selection," *Journal of Cheminformatics*, vol. 12, no. 1, p. 3, 2020.

[29] S. Mente and M. Kuhn, "The use of the R language for medicinal chemistry applications," *Current Topics in Medicinal Chemistry*, vol. 12, no. 18, pp. 1957–1964, 2012.

[30] R. Guha, "Chemical informatics functionality in R," *Journal of Statistical Software*, vol. 18, no. 6, 2007.

[31] H. A. Alhazmi, A. Khalid, S. Sultana et al., "Determination of phytocomponents of twenty-one varieties of smokeless tobacco using gas chromatography-mass spectroscopy (GC-MS)," *South African Journal of Chemistry*, vol. 72, no. 1, pp. 47–54, 2019.

[32] M. Al Bratty, W. Ahsan, H. A. Alhazmi, I. M. Attafi, I. A. Khardali, and S. I. Abdelwahab, "Determination of trace metal concentrations in different parts of the khat varieties (Catha edulis) using inductively coupled plasma-mass spectroscopy technique and their human exposure assessment," *Pharmacognosy Magazine*, vol. 15, no. 63, pp. 449–458, 2019.

[33] A. Khalid, H. A. Alhazmi, A. N. Abdalla et al., "GC-MS analysis and cytotoxicity evaluation of shammah (smokeless tobacco) samples of Jazan region of Saudi Arabia as promoter of cancer cell proliferation," *Journal of Chemistry*, vol. 2019, Article ID 3254836, 8 pages, 2019.

[34] A. Bărbulescu, L. Barbeş, and C. Ş. Dumitriu, "Computer-aided methods for molecular classification," *Mathematics*, vol. 10, no. 9, p. 1543, 2022.

Research Article

Do Pollination and Pollen Sources Affect Fig Seed Set and Quality? First Attempt Using Chemical and Vibrational Fingerprints Coupled with Chemometrics

Lahcen Hssaini [iD],[1] **Rachid Razouk** [iD],[1] **Ahmed Irchad,**[1]
Rachid Aboutayeb [iD],[1] **and Rachida Ouaabou** [iD][2]

[1]*National Institute of Agricultural Research, Avenue Ennasr, BP 415 Rabat Principale, 10090 Rabat, Morocco*
[2]*Cadi Ayyad University of Marrakech, Marrakech, Morocco*

Correspondence should be addressed to Lahcen Hssaini; hssaiini@gmail.com

This research investigates whether pollination and pollen sources separately and simultaneously influence fig seed set and quality, as being thus far the less studied part of the fig trees. This is the first research that tries to answer and verify the above hypothesis through a combined approach of vibrational spectroscopy along with lipo-biochemical and ionomic fingerprinting. Results showed that pollination and pollen source significantly impacted seed set as it was higher in fertilized seeds than that in the control. A similar pattern was obtained with oil yield, which generally ranged between 25.93 and 32.59%. Caprification also displayed a substantial effect on seeds' phenolic components, which was more driven by pollen carbohydrates, involved in the phenolic biosynthesis in the endosperm and embryo tissues. This biosynthesis is also activated by minerals, which are cofactors for large varieties of enzymes that are involved in the phenolic synthesis pathways. Ca and Zn did not follow this pattern and have recorded high levels in figs fertilized by the pollen of OZ and FD4 caprifigs pollen, respectively. Vibrational spectroscopy using Fourier transform infrared (FTIR) spectroscopy coupled with total attenuated reflectance (ATR) also showed a similar pattern to the seed sets and their lipo-biochemical attributes. Thus, the fertilized seeds displayed high vibrational intensity compared to the control in all fingerprint regions. Peaks at 2928 and 1747 cm^{-1} had a higher intensity and were attributed to lipids CH_2 and CH_3 stretching vibration and $C=O$ of the carbonyl groups belonging to the triacylglycerols, respectively. Principal component analysis showed high throughput classification with quite similar patterns for both FTIR-ATR fingerprinting and ionomic and bio-chemical analysis. As many areas of how caprification impacts other seed aspects still need to be investigated further, this research suggests the importance of caprification in seed valorization for oil extraction and as a functional ingredient.

1. Introduction

The pollination system in *Ficus carica* L. is based on a unique mutualism between the species and a symbiotic fig wasp called *Blastophaga psenes*, which has always been coexisted with the fig. This symbiosis symbolizes an outstanding example of very particular coevolution between the tree and its pollinator wasp in the kingdom Plantae [1, 2]. This pollination, also known as caprification, is generally required for fruit loading and has an important impact on fruit quality [3–5]. However, some types of female figs can partheno-carpically produce fruits without pollination. This particular

aspect divides female figs into three types. The first one is called common figs, which do not require caprification and can yield one (*unifera* variety) or two (*bifera* variety) crops [6]. The second is known as Smyrna-type figs, which require pollen from the male tree called caprifig. Then, the third type, named San Pedro, producing a first crop partheno-carpically (breba), is usually reaped in late June in Mediterranean countries and is the main crop only after caprification, which is generally harvested in the period between mid-August and early September [7, 8]. The fig pollination cycle is determined mutually by the cycles of wasp pollinator and caprifig production. Thus, a caprifig tree

yields three types of inedible syconia annually: "profichi," "mammoni," and "mamme." The "profichi" caprifigs initiate in the spring and mature in summer and are also called insectivorous since they host the fig wasp [9, 10]. The "mammoni" are small-sized fruits that mature in the fall. Then, the "mamme" fruits initiate in the fall, remain dormant during the winter, and ripen in the spring. The pollination (caprification) process, which occurs from the end of May into June, is assured by the adult female wasp, which emerges from the caprifig ("profichi") and enters receptive common fig through the ostiole, seeking egg-laying sites using its ovipositor. During this process, pollen carried on the female body is spread to female flowers, resulting in pollination, which is necessary to seeds yielding [4]. This unique mutualism cycle between this wasp and the edible and inedible figs is behind the transfer of pollen from caprifigs to edible figs, which helps produce high nutritive figs and yields seeds. Today it is well-known that caprification has a substantial impact on fruit load and quality. In the study carried out by Trad et al. [5], textural traits of ripened fig were moderately impacted by caprification, which significantly enhanced anthocyanins biogenesis in the syconium. Similarly, Trad et al. [7] demonstrated that caprification significantly increased fruit yield and volatile compounds content. Other studies reported that pollination has a significant effect on morphometric traits and storage aptitude of ripened figs alongside their aptitude for drying while safeguarding their organoleptic properties during the process [3, 4, 8, 11, 12]. The aforementioned effects are systematically driven by caprifig phenotypic variability previously assessed by several reports [1, 13]. Since many caprifig types exist, the effect on the common fig quality is dependent on its source [12]. So far, to the best of our knowledge, there is no single report on the caprification effect on fig seeds quality as the latter remains thus far the less studied part of the species. Based on previous studies, fig seeds are an important source of novel oil qualified as a minor source of atypical vegetable oil, with a yield of up to 30%. Furthermore, fig seeds oil was reported to have a higher desaturation rate and a significant phenotypic effect [14, 15]. Basically, as pollination is mainly involved in seeds formation [6], the main effect probably occurs over the attributes of seeds and, subsequently, the whole fruit quality. In this sense, the investigation of the caprification and source pollen effect on fresh figs must pass through its seeds' chemical and lipochemical attributes. For this reason, this study was designed to investigate whether caprification and pollen source impact fig seeds set and quality, separately and in combination of both. To answer this question, lipochemical vibrational fingerprinting through attenuated total reflectance-Fourier transformed infrared (ATR-FTIR) spectroscopy and biochemical and ionomic assessment were performed on "Nabout" variety, which is one of the main components of the Moroccan fig trees landscape, with two caprifig cultivars, all cultivated in the same orchard and under the same conditions.

2. Material and Methods

2.1. Plant Material and Experimental Design.
Caprification experiment was conducted in the national fig collection owned by the National Institute of Agricultural Research (INRA) and located in Meknes, northern Morocco ($x = 511,600$; $y = 370,250$; $z = 480$ m). Fig cultivars were trained to vase, spaced at 4×5 m, and conducted under the same cultural practices, with no use of pesticides. A pollination experiment was undertaken on the local variety "Nabout," which is a common-type fig defined as uniferous (*unifera* variety), and does not require caprification (parthenocarpic). Thus, uniform branches bearing fruits at a similar biological stage were randomly chosen around the canopy and were covered with bags (60×30 cm) made of sulfur a week before the caprification period. Meanwhile, two caprifig cultivars, "Ouzidane" and "Frond d'Oued N° 4," were selected; they had the same ripening stage (early June) that overlaps with the period of "Nabout" receptivity to pollen. The caprification process consisted of separately enclosing ten ripe profichi fruits (bearing pollen) harvested from each caprifig cultivar so that each branch covered with a single bag was pollinated with one type of caprifig fruit. The caprification process was repeated four times with four-day intervals [4]. In total, ten–fifteen bags were used for each pollen source, with a similar number of bags as a control (no caprification). It is noteworthy that these caprifigs were cultivated close to the fig trees collection and are subjected to the same conditions.

Once the caprification period was achieved, the sulfurized bags were removed. The experiment was conducted as a randomized complete block (RBC) design, where the pollen source was assigned as the main factor. Pollinated figs were harvested at their fully ripening stage, when their receptacle displayed reddish-purple coloration and when they were easily separated from the twig.

2.2. Samples Preparation.
Once pollinated and control figs were harvested, they were longitudinally cut and seeds were extracted using the spatula and then put in 5% of technical ethanol for 5 min to separate seeds from pulp filaments through agitation and decantation [14, 15]. Shortly afterward, seeds were abundantly washed with distilled water and then air-dried at room temperature before being ground into a fine powder using IKA A11 Basic Grinder (St. Louis, MO). It is noteworthy that seeds yield was determined per fruit, using the same extraction method, with five replicates. Fig seeds are round-shaped and yellowish, with an average thousand seed weight of about 1.14 ± 0.01 g.

2.3. Ionomic Analysis.
Nitrogen (N) contents were quantified using the Kjeldahl method (Buchi, Switzerland). Complexation with chromotropic acid helped to measure nitrate content using absorbance in a spectrophotometer (Spectronics, USA) fixed at 410 nm (Hadjidemetriou, 1982).

Protein content was calculated based on N content using the following relation: $P = 6.25 * N$. Phosphorus (P) content was determined by the yellow color method using the wet digestion method. The yellow color was measured at 410 WL by spectrophotometry (Shimadzu, Japan) [16]. Other elements (K, Na, Ca, Mg, Fe, Cu, Zn, and Mn) were analyzed using a dry-ashing method carried out at 550°C. Macroelements, namely, K, Na, and Ca, were assessed by flame photometry (Elico-CI378, India) [17]. Microelements, namely, Fe, Cu, Zn, and Mn, were assessed by atomic absorption spectrometry (AAS) (Perkin Elmer AAnalyst 300, USA) [18]. For each sample, three measures were undertaken to assess analysis reliability.

2.4. Vibrational Fingerprinting.

Vibrational fingerprinting of fig seeds was performed, using Vertex 70-RAM II Bruker spectrometer within wavenumber range from 4000 to $500 \, \text{cm}^{-1}$ with a spectral resolution of $4 \, \text{cm}^{-1}$, averaging 256 scans per spectrum and equipped with a diamond ATR accessory (Bruker Analytical, Madison, WI). Spectrum acquisition of each sample (50 mg) was repeated five times in room conditions; then, an average spectrum was obtained. Before FTIR spectra acquisition, ultrapure water was recorded, under the same conditions, as a background, which was automatically subtracted from each sample spectra. Between each measurement, ethyl alcohol and warm water were used to clean the ATR cell using soft paper.

2.5. Biochemical Assessment

2.5.1. Extraction of Phenolic Compounds.
In total, 2 g of seeds powder from pollinated and control samples was dissolved in 20 mL of methanol and ultrapure water (70 : 30, v/v) and then homogenized at 4°C for 15 min using an Ultra-Turrax homogenizer (IKA-Werke GmbH and Co., Staufen, Germany). Afterward, the mixture was centrifuged for 15 min at 4°C and 3000 ×g. For each sample, the supernatant was separated from the residue, which was subjected to a second extraction as described above and the supernatant was removed. Extracted supernatants were combined and then filtered using Whatman No. 1 filter paper.

2.5.2. Total Phenolics (TP).
Total phenolics were determined using Folin–Ciocalteu's micro method [19]. Briefly, an aliquot of 40 μL of each sample extract or standard solution was mixed with 3.16 mL of ultrapure water and 200 μL of 20% sodium carbonate solution. After 30 min of incubation at 40°C, the mixture absorbance was measured at 765 nm. The analysis was performed in triplicate and gallic acid was used as the standard solution.

2.5.3. Total Flavonoids (TF).
A volume of 250 μL of samples extracts or standard solution was homogenized with 1250 μL of ultrapure water and 75 μL of NaNO$_2$ solution (5%). The mixture was incubated for 6 min at room temperature and then 150 μl of 10% AlCl$_3$.6H$_2$O solution was added. After the second incubation of 5 min, 500 μL of 1 M NaOH solution was added to the mixture and then the final volume was made up to 2500 μL using ultrapure water. The absorbance against the blank was read at 510 nm. The results were expressed in terms of mg rutin equivalent (RE)/100 g seeds [20].

2.5.4. Total Anthocyanin (TA).
The pH differential method was used to quantify TA as described by Cheng and Breen [21]. Thus, the absorbance of fig seeds extracts was measured at the wavelength of 520 and 700 nm in solution buffers of hydrochloric acid-potassium chloride (0.2 M) and acetic acid-sodium acetate (1 M) at pH of 1.0 and 4.5, respectively. Absorbance (A) was calculated as follows:

$$A = (A520 - A700)pH1.0 - (A520 - A700)pH4.5. \quad (1)$$

TA content was determined as g cyanidin-3-rutinoside (cy-3-r) equivalents per 100 g of seeds [22], as cy-3-r are the major anthocyanin compounds in figs [23].

2.5.5. Total Proanthocyanins (TPA).
TPA content was determined following the acid hydrolysis and color formation method described by Porter et al. [24] and expressed in mg cyanidin equivalent per 100 g seeds.

2.6. Oil Extraction.
Oil extraction was performed following the ISO method 659 : 199 using Soxhlet extraction with n-hexane (99%) as a solvent, which was evaporated at 40°C using a Rotavapor after a cycle of 4 h [14]. The resulting oils were stored in a dark flask at 4°C until analysis.

2.7. Data Analysis.
Data were verified for normality and homogeneity of variance before statistical processing to ensure the validity of chemometric analyses using SPSS software v27. Biochemical and ionomic data were subjected to analysis of variance (ANOVA) to inspect differences among fig seeds samples. FTIR data were also subjected to the standard normal variate (SNV) alongside multiplicative scattering correction (MSC) procedures. Corrected spectrum and the main area of vibration were plotted using OriginLab Pro. In the second step, FTIR and biochemical and ionomic data were separately subjected to principal component analysis (PCA) to determine the variables and spectral signatures most contributing to explaining the pollination effect and pollen source. Later, 2D scatter plots were drawn to display the classification pattern, as affected by pollination and pollen source, separately based on FTIR fingerprints and biochemical and ionomic data.

3. Results and Discussion

3.1. Oil Yield and Seeds Set.
The weight of seeds per fruit displayed a significant impact of pollination and pollen, as it was higher in pollinated fig seeds than the control (unpollinated figs), with a substantial difference noticed based on the following profichi sources (Figure 1). Thus, fruits pollinated with "Frond d'Oued N° 4" (FD4) profichis exhibited the highest seeds yield per fruit (2.441 g), while it
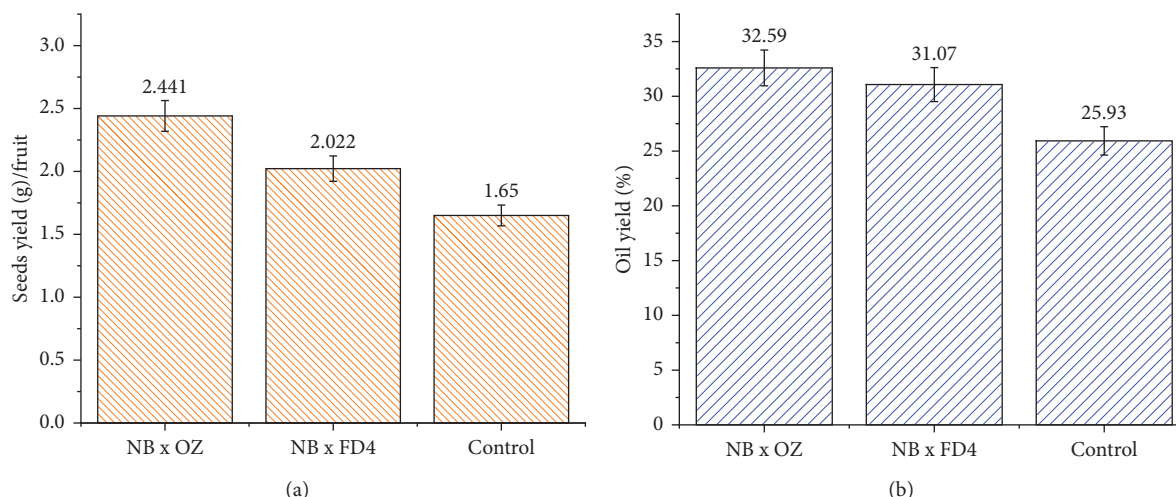
FIGURE 1: Effect of pollination and pollen source on seeds (a) and oil (b) yields. NB refers to the variety "Nabout," while OZ and FD4 are the two caprifigs used as a source of pollen and denote "Ouzidane" and "Frond d'Oued N° 4," respectively.

was 2.022 g in figs, which received "Ouzidane" (OZ) pollen. Unpollinated figs presented a very low seeds yield (1.65 g), which was about 1.48 and 1.22 times lower than the level recorded in figs pollinated by OZ and FD4, respectively. These results are due to the production of small empty seeds, as pollen is required for seeds sporophyte (embryo) development and subsequently its impact on the seeds loading and weight [25]. Thus, fig seeds are generally hollow unless they are successfully pollinated [14, 26]. This trait of hollowness seems to be common between the fig receptacle and unpollinated seeds. These seeds, especially pollinated ones, are well-known for their contribution to the fruit taste and flavor and antioxidant properties and dried ones to which pollinated seeds deliver the characteristic nutty taste [15, 26]. This close relationship between pollination and seed set has also been linked with the pollination intensity, as reported by [4], who found that sterile seeds are likely to be abundant as the pollination frequency is low. Similar results were reported on other trees such as apple [27, 28] and kiwi [29], where the absence of pollen leads to seed abortion.

A similar effect pattern was observed on oil yield, which showed a significant sensibility to pollination and pollen sources. Thus, unfertilized seeds exhibited an oil yield of 25.93%, which is about 20% lower than the rate recorded by pollinated seeds (Figure 1). The pollen source also had a significant effect on this trait, which is quite similar to that on seeds loading. Indeed, seeds that received OZ pollen gave the highest oil yield (32.59%) compared to those pollinated by FD4 (31.07%). The effect of pollination on grain set and oil yield was also reported in several crop seeds species, including sunflower [30, 31], rapeseeds [32, 33], and soybean [34], where the simultaneous effects of pollen source and quality have enhanced seeds development and their oil content. Lately, more attention has been paid to the irradiation effect on pollen and seeds set in several species, such as pomelo [35], apple [36], and citrus [37], where irradiated pollen displayed a significant effect on seeds sets and that an increasing irradiation level showed a tendency to stimulate the parthenocarpy property in fruits.

3.2. Biochemical Attributes. The results of fig seeds biochemical attributes as affected by pollination and pollen source are summarized in Table 1. The pollination source significantly affected biochemical traits of "Nabout" fruits seeds ($p < 0.05$); hence, fertilized figs exhibited high levels of total phenolic content (TPC) compared to unfertilized samples (117.71 ± 10 mg GAE/100 g). Likewise, pollen sources displayed a significant effect on TPC; henceforward, they were higher in fig seeds fertilized with "Ouzidane" pollen (185.93 ± 8.21 mg GAE/100 g) than those pollinated with "Frond d'Oued N° 4" pollen (185.93 ± 8.21 mg GAE/100 g) (Table 1). Although little attention was paid to the pollination impact on total phenolics of fig seeds, this behavior was in agreement with a study conducted in Iran, where the interaction "pollen sources × female cultivars" showed a significant impact on the fruit total phenolics (Pourghayoumi et al., 2012). In the same way, Trad et al. [38] reported that caprification had a significant influence on fresh figs' polyphenols composition. This result agrees with that of Rahemi et al. [3] and Pourghaymi et al. [12], who reported that the pollen source has a substantial effect on the fig biochemical traits alongside the fruit peel and pulp color. Some major phenolic compounds such as catechin, quercetin-3-glucoside, quercetin, and chlorogenic acid were also reported to be influenced by the pollination process and pollen source [12]. In fact, the caprifig pollen might probably present many differences following their origins, which drives their levels of carbohydrates, affecting the total phenolic compounds biosynthesis by transferring those carbohydrates supplements to the endosperm and embryo tissues, which are necessary as the precursors in phenolic compounds production [39]. This suggests that the biosynthesis of phenolic compounds occurs later after pollination and could be under the effect of caprification and pollen sources. However, higher TPC levels could be recorded without pollination, which could most likely be explained by physiological and environmental conditions during the fruit ripening period [38].

TABLE 1: Statistical analysis of biochemical traits of fig seeds as affected by pollination.

Variables	NB x FD4	NB x OZ	Control	ANOVA		
				Overall mean	Mean square	Sig.
Total phenolics (mg GAE/100 g)	176.64 ± 6.07	185.93 ± 8.21	117.71 ± 10	160.10	4105.99	.000
Total flavonoids (mg RE/100 g)	53.38 ± 2.35	59.59 ± 0.55	41.36 ± 6.91	51.44	257.72	.005
Total anthocyans (mg cy-3-r/100 g)	31.41 ± 6.61	48.77 ± 8.27	16.77 ± 0.23	32.32	770.16	.002
Total proanthocyanidins (mg cyan/100 g)	3.91 ± 0.01	4.05 ± 0.02	3.87 ± 0	3.94		.026	.000

NB: Nabout; FD4: Frond d'Oued N° 4; OZ: Ouzidane; ANOVA: analysis of variance; cyan: cyanidin; cy-3-r: cyanidin-3-rutinoside; GAE: gallic acid equivalent; QE: quercetin equivalent. Sig.: significance of ANOVA.

Total flavonoids content (TFC) displayed a similar pattern to TPC; hence, fertilized seeds recorded the highest levels compared to unfertilized ones (41.36 ± 6.91 mg CE/100 g). TFC was also sensitive to pollen source since, once again, seeds fertilized with OZ pollen exhibited higher levels in comparison to those pollinated with FD4 (59.59 ± 0.55 and 53.38 ± 2.35 mg CE/100 g, respectively). A similar effect has also been reported in Iranian dried figs varieties [38]. Undoubtedly, fig is a suitable example through which the relationship between pollination and major factors of quality has already been demonstrated [5, 40].

Effect of pollination and pollen source, separately and in combination of both, followed the same above-described pattern on total anthocyanins content (TAC), which is the main responsible for the fruit peel color [23, 41]. Unfertilized seeds showed the lowest TAC levels, 16.77 ± 0.23 mg cy-3-r/100 g, compared to pollinated ones, where the recorded levels were of 48.77 ± 8.27 and 31.41 ± 6.61 mg cy-3-r/100 g for pollen source of OZ and FD4 (Table 1). A similar tendency of pollen source effect on antioxidant capacity along with some phenolic components such as chlorogenic acid catechin, quercetin-3-glucoside, catechin, and quercetin was previously reported in dried figs belonging to "Payves" and "Sabz" cultivars growing in Kazerun, Iran [12]. This pattern has also been reported by Trad et al. [38], who examined the anthocyanins levels in ripened fresh figs and found that caprified syconium was richer in TAC compared to unfertilized ones. The effect of caprification on anthocyanins biosynthesis was indirectly interpreted by some authors (Sullivan, 1998; Nakajima et al., 2001), and it is associated with two different streams of chemical raw material in the cell. The first involves the shikimate pathway to produce the amino acid phenylalanine. The second produces three molecules of malonyl-CoA, a C3 unit from a C2 unit (acetyl-CoA) [38].

Once again, total proanthocyanidins content (TPAC) was higher in fertilized seeds compared to unfertilized ones, with a significant difference following the pollen sources ($p < 0.05$). Hence, TPAC was 3.87 mg cyanidin/100 g of seeds in control samples, whereas it was slightly higher in those fertilized with FD4 (3.91 ± 0.01 mg cyanidin/100 g) but greater in seeds pollinated with OZ caprifig pollen (4.05 ± 0.02 mg cyanidin/100 g). Obviously, very little data was found on the separate and simultaneous effect of pollination and pollen source on the fig seeds' biochemical traits. Therefore, the herein reported findings are very promising since fig seeds remain thus far the less studied part of the species and are being considered a novel source of fats

and functional properties. Considering the efficiency of pollen source effect on above-described attributes of fig seeds, it seems that the use of caprifig "Ouzidane" as pollinator could be more appropriate to enhance fig seeds set, oil yield, and quality.

3.3. Mineral Content. Inorganic elements are remarkable constituents of figs; they play a vital role in biological systems and body development. However, minerals can have a toxic effect when their intake exceeds functional levels [42]. Several authors have reported the quantitative estimation of mineral element concentrations in the different parts of plants Ficus carica L., including leaves, aerial roots, and bark [43]; however, most studies have been performed on the whole fruit especially dried figs [42–46]. To the best of our knowledge, one report has mentioned mineral composition in fig seeds, one of the fig fruit parts responsible for beneficial health effects hitherto unknown. Results given in Table 2 summarize the separate and simultaneous influence of pollination and pollen source on the fig seed mineral contents. Overall, results showed that ten mineral elements were identified in fig seeds, among which N, Ca, P, and K were, in order of importance, the major elements, and showed in addition to proteins significant differences among samples. We also found minerals such as Na, Fe, Zn, Mn, Cu, and Mg, which did not display statistically significant differences among samples taking into consideration pollination and pollen source ($p > 0.05$). The mineral composition herein reported was similar to that of Nakilcioğlu [47]. Unexpectedly, concentrations in mineral elements were substantially lower in fertilized seeds compared to control samples. Only calcium (Ca) escaped to this rule, as it was higher in fertilized seeds with OZ pollen (8.16 ± 0.92 g/kg) compared to other samples, where recorded values were generally lower than 8 g/kg. It is noteworthy that the pollination impact revealed a clear pattern, while the pollen source did not display an obvious tendency, as the levels recorded in N (2.26 ± 0.06%) and Ca (8.16 ± 0.92 g/kg) were slightly higher in seeds pollinated by OZ, whereas the other mineral elements were somewhat greater in seeds fertilized with FD4 pollen. The highly significant impact of pollen source could be particularly noticed on several minerals, e.g., Fe, Zn, and Mn, which were higher in seeds fertilized by FD4 pollen and where values were of 94.23 ± 7.53, 20.13 ± 1.43, and 8.18 ± 0.78, respectively, while they were of 60.13 ± 29.33, 14.78 ± 12.43, and 6.58 ± 2.93, respectively, in seeds pollinated by OZ pollen. It seems that fig seeds'

TABLE 2: Statistical analysis of the mineral composition of fig seeds as affected by pollination.

Samples	NB x FD4	NB x OZ	Control	ANOVA		
				Overall mean	Mean square	Sig.
N (%)	2.19 ± 0.02	2.26 ± 0.06	2.65 ± 0.11	2.37	.180	.001
Proteins (%)	13.69 ± 0.13	14.13 ± 0.39	16.54 ± 0.7	14.79	7.034	.001
P (g/kg)	4.88 ± 0.23	4.41 ± 0.23	7.04 ± 0	5.44	5.868	.000
K (g/kg)	3.6 ± 0.12	2.48 ± 0.04	4.42 ± 0.1	3.50	2.845	.000
Ca (g/kg)	6.66 ± 0.74	8.16 ± 0.92	7.98 ± 0.38	7.60	2.012	.081
Na (g/kg)	0.6 ± 0.16	0.6 ± 0.12	0.9 ± 0.02	0.70	.090	.030
Fe (ppm)	94.23 ± 7.53	60.13 ± 29.33	122.2 ± 3	92.18	2899.358	.014
Zn (ppm)	20.13 ± 1.43	14.78 ± 12.43	17.65 ± 0.85	17.52	21.507	.681
Mn (ppm)	8.18 ± 0.78	6.58 ± 2.93	8.48 ± 0.43	7.74	3.130	.420
Cu (ppm)	24.43 ± 0.58	25.1 ± 2.8	26.73 ± 0.13	25.42	4.193	.289
Mg (ppm)	713.5 ± 0.5	714 ± 13.5	715 ± 1	714.17	1.750	.972

NB : Nabout; FD4 : Frond d'Oued N° 4; OZ : Ouzidane; ANOVA: analysis of variance; N : nitrogen; P: phosphorus; K : potassium; Ca: calcium; Na : sodium; Fe : iron; Zn: zinc; Mn : manganese; Mg : magnesium; Cu : copper.

mineral contents are proprietary dependent on pollination and then pollen source, which needs further investigation to be clearly stated. As no previous study has been interested in this aspect, these findings herein reported remain the first to mention the caprification effect on the mineral composition of fig seeds.

3.4. Impact of Pollination on the Correlations between Minerals and Phenolic Components. Heatmap correlation matrix shown in Figure 2 displays particularly strong correlations between minerals and phenolics components. In fact, all mineral elements showed strong negative correlations, with all phenolics components herein studied, with the exception of calcium, which showed a weak positive correlation with TPAC and TAC ($r = 0.15$ and $r = 0.42$, respectively) and a very weak negative correlation with TPC ($r = -0.28$). Similarly, zinc showed weak correlations with phenolic compounds, except with TAC and TPAC ($r = -0.57$ and -0.78, respectively). Similar patterns of correlations between phenolics and minerals were previously reported in several studies, where the increase in phenolic compounds is negatively associated with the minerals levels [48–50]. Based on the results described in the sections above, it was shown that pollination had a large size effect on the correlation between minerals and phenolics content. Hence, unfertilized seeds exhibited low phenolics components compared to pollinated ones but higher mineral elements level with only a single exception of Ca. Contrariwise, fertilized seeds displayed a low level of minerals compared to control, while they recorded high amounts of phenolics. This relationship pattern driven by pollination can be explained by the fact that those minerals are actively involved in activating phenolic compounds' biosynthesis [51]. This relationship was previously explained by the fact that minerals play a key role in providing cofactors for large varieties of enzymes involved in the phenylpropanoid and flavonoid pathways. Particularly, Fe, Mg, and Mn cations are essential for phenylalanine ammonia-lyase (PAL) activation, one of the key enzymes responsible for phenol biosynthesis [52, 53]. Furthermore, limited minerals supply is usually associated with phenolic accumulation. For instance, nitrogen

deficiency is especially linked to higher phenolic levels. Finally, in plants, there is a general trend towards increased phenolics whensoever minerals availability is low [54, 55].

4. FTIR Signatures

FTIR-ATR fingerprinting has proven itself as a powerful tool for chemical screening and discrimination purposes of biological samples. In the study of Hssaini et al. [15], this technique has provided a high throughput screening framework over the oil sample of fig seeds. In this work, FTIR was employed to determine fig seeds' molecular signatures and to investigate their sensitivity to pollination and pollen source separately and in combination of both. To this end, fertilized and control samples were scanned within a wave numbers interval of 4000 and 500 cm^{-1}. Detailed band assignments are given in Table 3 revealing fifteen fingerprints represented in Figure 3. The influence of pollination and pollen sources separately and jointly was significant on samples' spectrum vibrational intensity (Figures 3 and 4). The first FTIR fingerprint appeared around 3411 cm^{-1} which would be assigned to O–H stretching vibration, most likely attributed to fibers, which have been reported to be present in large quantities in fig trees [15]. This flattened peak occurred within the vibration region of 3750 and 3100 cm^{-1} associated with the intramolecular hydrogen bond between C(3) OH···O(5) and C(6) O···O(2) H according to Schwanninger et al. [69] and Oh et al. [70]. The second peak occurred around 3071 cm^{-1}, which is most likely assigned to C–H stretching of olefinic double bonds related to long carbon chains containing a relatively high number of CH_2 groups of unsaturated fatty acids [57, 70–72]. The vibration around the wavenumber of 3013 cm^{-1} has been attributed to the symmetrical and asymmetrical stretching of C–H, O–H and NH_3, which is probably typical to carboxylic acids, carbohydrates, and phenolic compounds [70, 71]. The sharp and distinct peak at 2928 cm^{-1} is due to the asymmetric and symmetric stretching of the aliphatic C–H in the $–CH_2$ and terminal groups $–CH_3$, respectively [58, 72]. The same goes for the peak that occurred at 2660 cm^{-1}. The bands in the region between 1800 and 1700 cm^{-1} are ascribed to stretching of

* p<=0.05 ** p<=0.01 *** p<=0.001
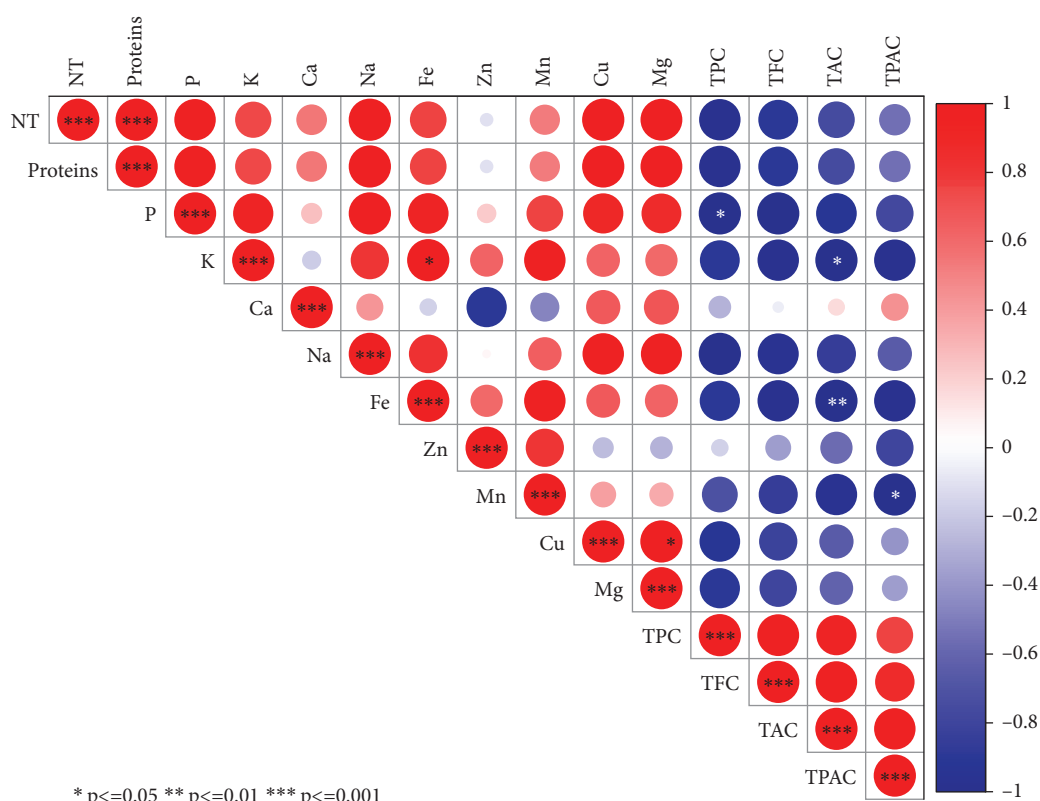
FIGURE 2: Correlation heatmap showing the relationship between mineral elements and phenolic components.

TABLE 3: FTIR peaks assignments for functional groups found in the spectrum of fig seeds.

Wavenumber (cm^{-1})	Functional group	Mode of vibration	Assignments	References
3411	δ(O–H)	Stretching vibration	Hydroxyl group	[56]
3071	ν(=C–H)	Bending vibration	Lipids	[57]
3013	δ(C–H), δ(N–H)	Stretching vibration		
2928	δ (–CH2–), δ(–CH3)	Stretching vibration	Methylene and methyl groups (lignins, lipids)	[58]
2660	δ(C–H)	Stretching vibration		
1747	δ(COH), δ(CCH), δ(OCH), ν(C–O)	Stretching and bending vibration	β-Sheet of amide I	[59–61]
1652	δ(N–H), ν(C–N)	Bending vibration	Amide II (α-helix)	[62]
1544				
1457	δ(C–H), δ(N–H), ν(C–H)	Stretching and bending vibration	β-Sheet of amide II	[59–61]
1386				
1239	δ(N–H), ν(C–H)	Stretching and bending vibration	β-Sheet of amide III	[59–61]
1164	δ(C–O), ν(C–C)	Bending vibration	Ester	[63–65]
1102	δ(C–O)	Stretching vibration	Methyl-carbon stretching (polypeptides)	[66]
720	δ(COH), δ(CCH), δ(OCH)	Stretching vibration	(Phenolics)	[67]
611	δ (C–H)	Stretching vibration	Out-of-plane bending vibrations	[68]

carbonyl groups and that of esters. This vibration region is related to the C=O extension of the carboxylic ester type. The sharp and acute peak at 1747 cm^{-1} is due to the stretching vibration of the C=O of the carbonyl groups belonging to the triacylglycerols. It is probably associated with the lipids and fatty acids contained in the seeds

[70, 73]. Nevertheless, according to several authors, this peak could be attributed to proteins [59–61, 74]. Vibration within the wavenumber range of 1700 to 1550 cm^{-1} is possibly related to the amide I and II secondary structure of the protein. The peaks at 1652 cm^{-1} and 1544 cm^{-1} are attributed to the stretching vibration of the C–C group of
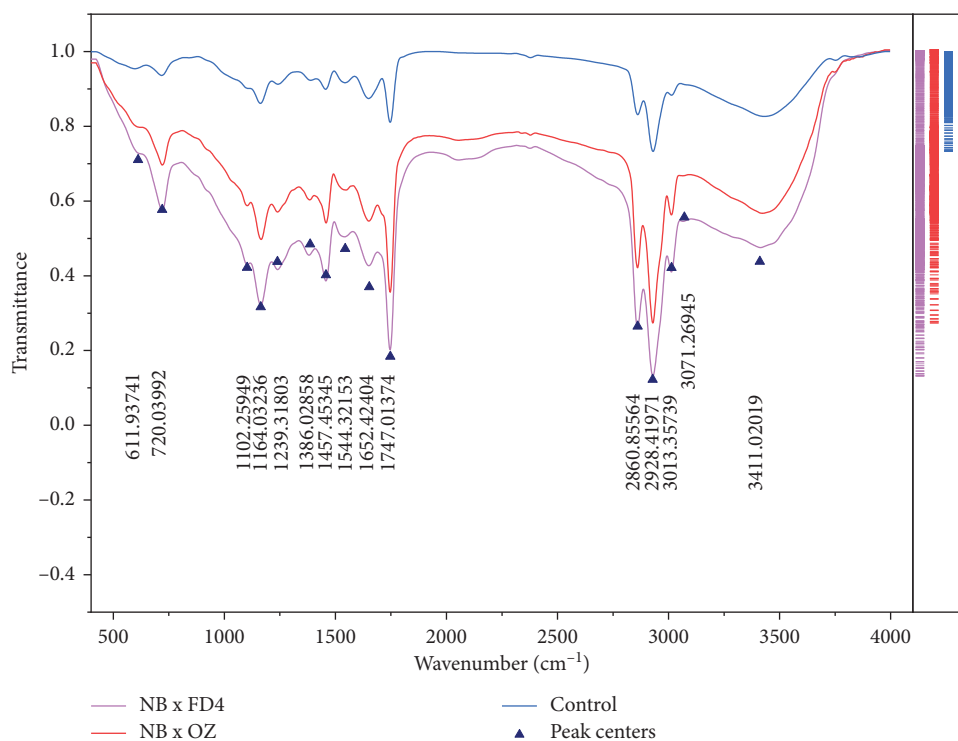
FIGURE 3: ATR-FTIR spectrum of fig seeds showing major peaks in the range of 4000–450 cm^{-1}. FD4 : Frond d'Oued N° 4; OZ : Ouzidane.
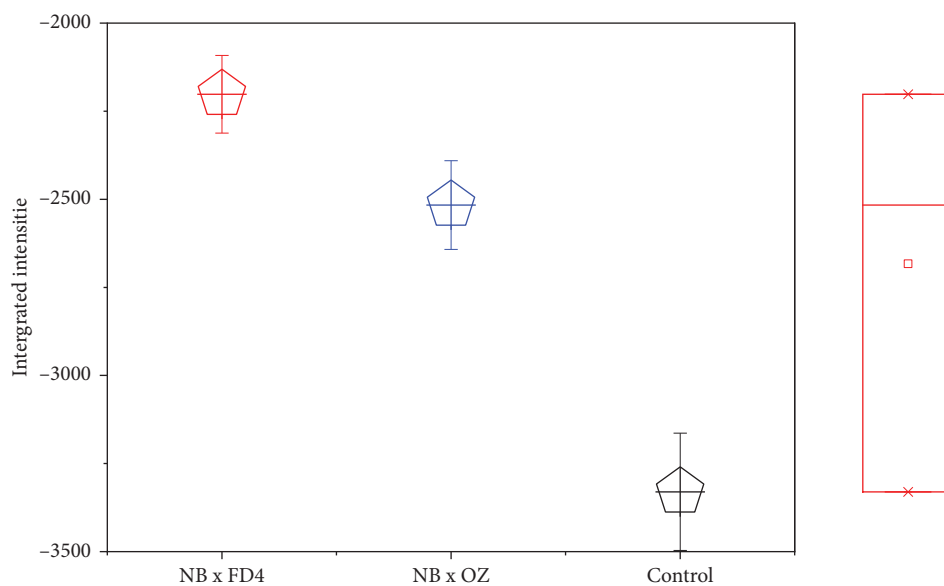
FIGURE 4: Overall integrated intensities of fig seeds IR spectrum as affected by pollination. FD4 : Frond d'Oued N° 4; OZ : Ouzidane.

the cis-alkene [62, 72]. The transmittance bands between 1500 and 1100 cm^{-1} would correspond to the phosphodiester groups and are probably the result of several weak peaks, which could not be differentiated in the samples analyzed according to several studies. The spectral band at 1457 cm^{-1} could probably be associated with the curvature of CH$_2$ and the deformation of methylene of lipids, proteins, or cholesterol esters [59–61, 75]. The vibrations that

occurred around 1386 cm^{-1} and 1239 cm^{-1} could probably be attributed to C–N elongation combined with N–H flexion and small vibrations of C–C elongation and C–O flexion in the plan. This group has been assigned to amides III [59–61, 76]. The band appearing at 1164 cm^{-1} was associated with the bending vibration of the C–O ester group [63–65, 72]. Approximately, a very weak vibration around 1102 cm^{-1} is most likely ascribed to a C–O stretch of
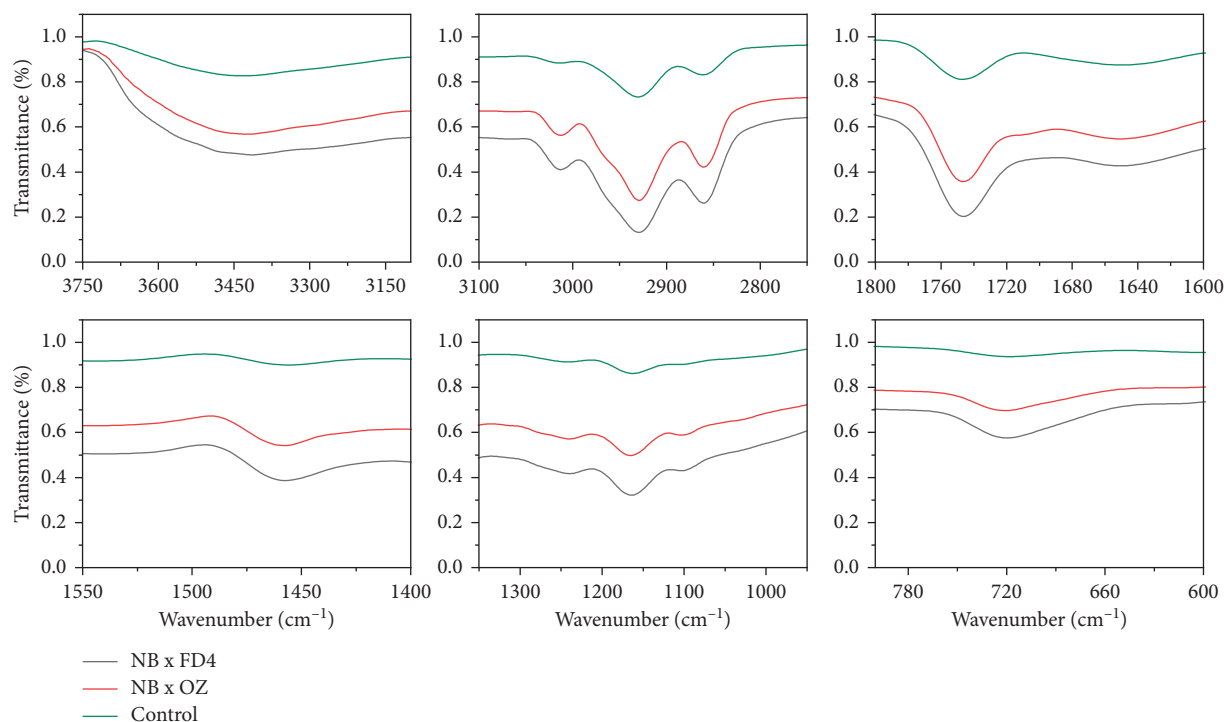
FIGURE 5: Major vibrational regions of fig seeds ATR-FTIR spectrum as affected by pollination. FD4 : Frond d'Oued N° 4; OZ : Ouzidane.

methyl-carbon (polypeptides) [66]. Finally, the vibration around $720\,cm^{-1}$ is probably assigned to C–OH group and C–C and C–O segments in the carbohydrate structure and C–O in the phenols [67]. The last region of vibration between 700 and $400\,cm^{-1}$ shows a peak near $611\,cm^{-1}$, which has been attributed to the overlap of the methylene ($-CH_2$) vibrations and the out-of-plane vibrations of the C–H bonds of the cis-alkenes disubstituted [68, 73].

In order to visualize the pollination impact between the samples according to their vibrational intensities, the integrated intensities of the main peaks in the range $3500-1000\,cm^{-1}$ were analyzed individually using the OriginLab Pro v9 software and a marginal plot (Figure 5). Thus, unfertilized seeds recorded a very low vibrational intensity within the entire wavenumber length, compared to pollinated seeds, which displayed a remarkable impact of the pollen source. Figure 4 displays the overall vibrational intensity of all samples' spectrum, where the higher level was reordered by seeds fertilized with OZ pollen, followed by those pollinated by FD4 pollen and then the control. Although sometimes considered minor, these differences indicate the high impact of pollination and pollen source on the fig seeds' molecular signatures. Obviously, the results herein reported join those described above by displaying a similar pattern of pollination and pollen source impact on fig seeds set and quality, including phenolic compounds and minerals. Being a highly sensitive, nondestructive, fast, cost-effective, and safeguarding technique, FTIR fingerprinting seems highly accurate to assess fig seeds, especially with larger sample length.

5. Multivariate Analysis

The principal components analysis (PCA) model was employed to reveal the separate and simultaneous impact of pollination and pollen source on the throughput resolution of fig seeds classification. Being an unsupervised learning approach, it was also used to verify whether FTIR-ATR spectrum data can provide a similar classification pattern as that of phenolic compounds and mineral composition, combined. Figure 6 shows two biplots constructed based on the first two PCA components of FTIR fingerprints (Figure 6(a)) and phenolics combined with minerals (Figure 6(c)). The figure also presents the loading plots displaying vibrational regions (Figure 6(b)) along with phenolic and ionomic variables (Figure 6(d)) contribution (weight) to the samples' classifications. Both models exhibited high total variance, where all major infrared peaks previously described were dominated by lipids, amids, and phenols vibration signature, which displayed high loadings on biplot clustering. In PCA generated by phenolics and minerals data, Ca and Zn had the highest loadings value, which means that they were the main contributors in samples classification. It is noteworthy that Ca and Zn were negatively correlated and were the only elements that did not follow the negative association pattern between minerals and phenolics accumulation previously described as being driven by pollination and pollen source. This relationship pattern suggests that limited minerals supply is usually associated with phenolic accumulation. Outstandingly, both biplots

(a)

(b)

(c)

(d)
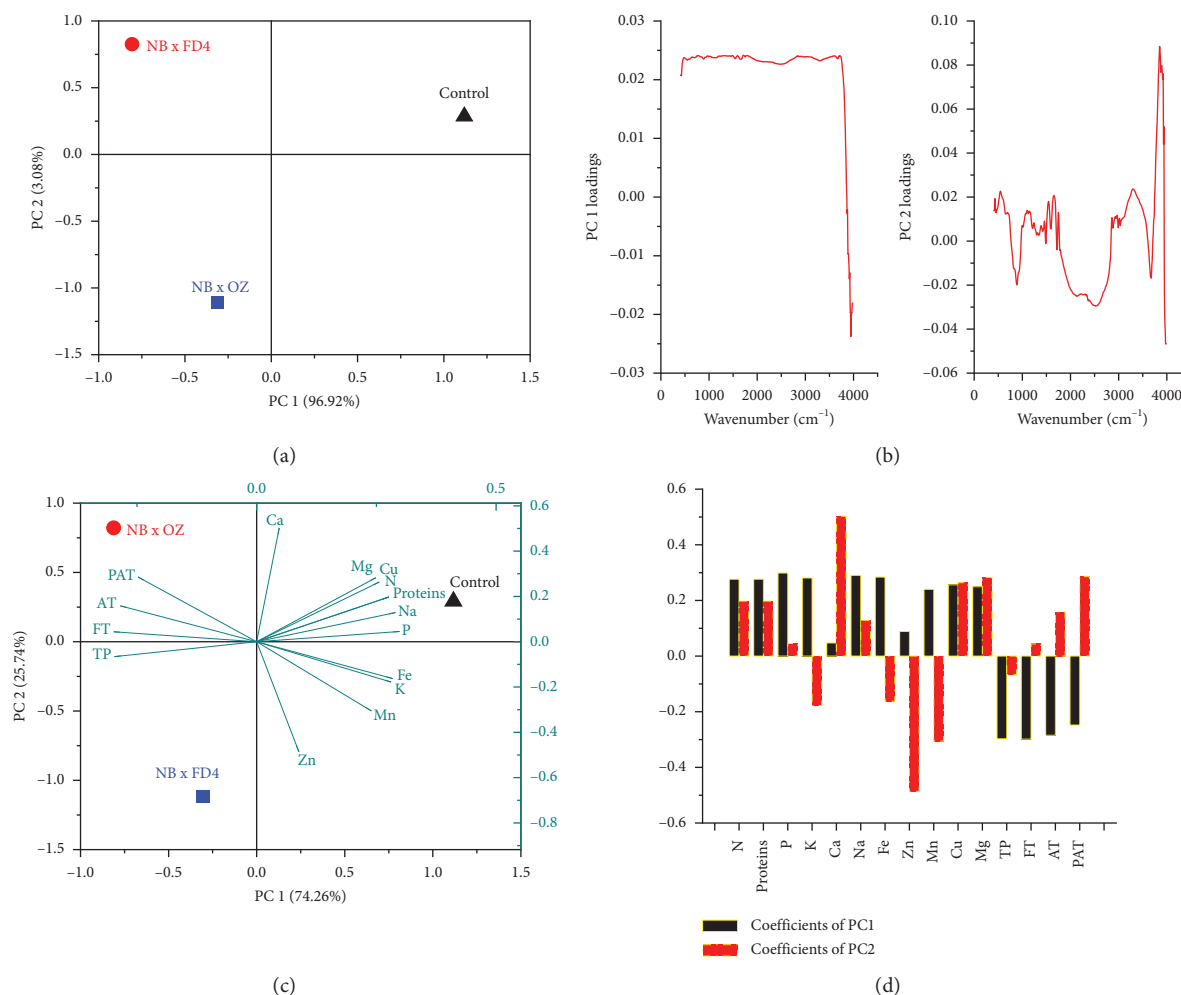
FIGURE 6: PCA 2D plot showing the effect of separate and simultaneous effect on fig seeds vibrational fingerprints (a) and biochemical attributes alongside minerals (b) with components most contributing to both PCA patterns (b and d). FD4 : Frond d'Oued N° 4; OZ : Ouzidane.

displayed quite similar samples repartitions with high inertia rate showing thus a remarkable influence of pollination and pollen source, separately and simultaneously. This result makes sense due to the fact that FTIR-ATR fingerprinting is a highly accurate qualitative technique of which absorbances are proportionally linked to concentrations in bioactive molecules as the Lambert–Beer law stipulates [77]. Similar classification patterns using a comparable approach were recently used for the first time on fig seeds oil in order to determine whether vibrational spectroscopy can provide high throughput discrimination resolution of a minor vegetable source that is so far scarcely investigated [15].

6. Conclusion

Fig caprification symbolizes an outstanding mutualism between the species and its wasp pollinator. This unique coevolution has a substantial impact on fruit load and quality. However, very limited works have attempted to explore its impact on seeds' set and quality. Perhaps, this is why those seeds are thus far the less studied part of the tree

and their metabolites and nutraceutical attributes are barely known. This article attempts to answer the following question: do pollination and pollen source affect simultaneously or separately the fig seeds set and quality? The article uses an analytical approach scheme combining lipo-biochemical with ionomic analysis and FTIR-ATR fingerprinting. Results displayed a significant effect of caprification and pollen source on all the above-mentioned attributes. Minerals, except Ca and Zn, showed a decreased pattern in response to pollination, which is an opposed tendency to the seeds set, oil yield, and phenolic compounds, as they recorded higher levels in fertilized seeds. These patterns were explained by the fact that minerals are key factors in activating some enzymes accurately involved in phenols biosynthesis. Pollination and pollen source effects were also revealed using FTIR-ATR that showed two sharp and acute peaks around 2928 and 1747 cm^{-1}, which were ascribed to CH$_2$ and CH$_3$ stretching in lipids and to C=O of carbonyl groups belonging to the triacylglycerols, respectively. Multivariate analysis of the above-described approaches showed identical classification of samples, suggesting that vibrational

spectroscopy may be accurate, fast, and cost-effective to further investigate this effect on a large sample size. This first study does not answer all questions related to the caprification effect, but it obviously provides valuable data and opens up new possibilities for future directions for more understanding of the impact of the mutualism between fig and its wasp on seeds set and quality as being an atypical functional food.

Data Availability

The data used to support the findings of this study are available upon request from the corresponding author.

Disclosure

This research did not receive any specific grant from funding agencies in the public, commercial, or not-for-profit sectors.

Conflicts of Interest

The authors declare no conflicts of interest.

Authors' Contributions

Lahcen Hssaini conceptualized the study, developed the methodology, performed validation, performed formal analysis, performed investigation, provided the resources, performed data curation, wrote the original draft, reviewed and edited the article, performed visualization, and performed project administration. Ahmed Irchad contributed to visualization and data curation. Rachid Aboutayeb and Rachida Ouaabou conducted the formal analysis.

Acknowledgments

References

[1] O. Caliskan, S. Bayazit, M. Ilgin, and N. Karatas, "Morphological diversity of caprifig (Ficus carica var. caprificus) accessions in the eastern Mediterranean region of Turkey: potential utility for caprification," *Scientia Horticulturae*, vol. 222, pp. 46–56, 2017.

[2] A. Khadivi-Khub and K. Anjam, "Characterization and evaluation of male fig (caprifig) accessions in Iran," *Plant Systematics and Evolution*, vol. 300, no. 10, pp. 2177–2189, 2014.

[3] M. Rahemi and M. Jafari, "Effect of caprifig type on quantity and quality of Estahban dried fig Ficus carica cv. Sabz," *Acta Horticulturae*, vol. 798, pp. 249–252, 2008.

[4] B. Gaaliche, M. Trad, and M. Mars, "Effect of pollination intensity, frequency and pollen source on fig (Ficus carica L.) productivity and fruit quality," *Scientia Horticulturae*, vol. 130, no. 4, pp. 737–742, 2011.

[5] M. Trad, C. Le Bourvellec, B. Gaaliche, C. Ginies, C. M. G. C. Renard, and M. Mars, "Caprification modifies polyphenols but not cell wall concentrations in ripe figs," *Scientia Horticulturae*, vol. 160, pp. 115–122, 2013.

[6] I. Marcotuli, A. Mazzeo, P. Colasuonno et al., "Fruit development in ficus carica L.: morphological and genetic approaches to fig buds for an evolution from monoecy toward dioecy," *Frontiers of Plant Science*, vol. 11, Article ID 1208, 2020.

[7] M. Trad, C. Ginies, B. Gaaliche, C. M. G. C. Renard, and M. Mars, "Does pollination affect aroma development in ripened fig [Ficus carica L.] fruit?" *Scientia Horticulturae*, vol. 134, pp. 93–99, 2012.

[8] M. Mars, M. Trad, and B. Gaaliche, "The unique fig caprification system and its effects on productivity and fruit characteristics," *Acta Horticulturae*, vol. 1173, pp. 127–135, 2017.

[9] H. Crisosto, L. Ferguson, V. Bremer, E. Stover, and G. Colelli, "Fig (Ficus carica L.)," *Postharvest Biology and Technology of Tropical and Subtropical Fruits: Cocona to Mango*, pp. 134–160e, 2011.

[10] P. Note, "Identification and characterization of microsatellite loci in the common fig (Ficus carica L .) and representative species of the genus Ficus," *Molecular Ecology Notes*, vol. 1, pp. 191–193, 2001.

[11] Y. Rosianski, Z. E. Freiman, S. M. Cochavi, Z. Yablovitz, Z. Kerem, and M. A. Flaishman, "Advanced analysis of developmental and ripening characteristics of pollinated common-type fig (Ficus carica L.)," *Scientia Horticulturae*, vol. 198, pp. 98–106, 2016.

[12] M. Pourghayoumi, D. Bakhshi, M. Rahemi, and M. Jafari, "Effect of pollen source on quantitative and qualitative characteristics of dried figs (Ficus carica L.) cvs 'Payves' and 'Sabz' in Kazerun – Iran," *Scientia Horticulturae*, vol. 147, pp. 98–104, 2012.

[13] A. Essid, F. Aljane, A. Ferchichi, and J. I. Hormaza, "Analysis of genetic diversity of Tunisian caprifig (Ficus carica L.) accessions using simple sequence repeat (SSR) markers," *Hereditas*, vol. 152, pp. 1–7, 2015.

[14] L. Hssaini, H. Hanine, J. Charafi et al., "First report on fatty acids composition, total phenolics and antioxidant activity in seeds oil of four fig cultivars (Ficus carica L.) grown in Morocco," *OCL*, vol. 27, p. 8, 2020.

[15] L. Hssaini, R. Razouk, J. Charafi, K. Houmanat, and H. Hanine, "Fig seeds: combined approach of lipochemical assessment using gas chromatography and FTIR-ATR spectroscopy using chemometrics," *Vibrational Spectroscopy*, vol. 114, Article ID 103251, 2021.

[16] A. p. Gupta, H. U. Neue, and V. P. Singh, "Phosphorus determination in rice plants containing variable manganese content by the phospho-molybdo-vanadate (yellow) and phosphomolybdate (blue) colorimetric methods," *Communications in Soil Science and Plant Analysis*, vol. 24, no. 11-12, pp. 1309–1318, 2008.

[17] D. Knudsen, G. A. Peterson, and P. F. Pratt, "Lithium, sodium, and potassium," *Agronomy Monographs*, John Wiley & Sons, New York, NY, USA, pp. 225–246, 2015.

[18] G. Estefan, *Methods of Soil, Plant, and Water Analysis: A Manual for the West Asia and North Africa Region*, International Center for Agricultural Research in the Dry Areas, Beirut, Lebanon, 3rd edition, 2013.

[19] A. L. Waterhouse, "Determination of total phenolics," *Current Protocols in Food Analytical Chemistry*, vol. 6, no. 1, pp. I1.1.1–I1.1.8, 2002.

[20] D. O. Kim, O. K. Chun, Y. J. Kim, H. Y. Moon, and C. Y. Lee, "Quantification of polyphenolics and their antioxidant capacity in fresh plums," *Journal of Agricultural and Food Chemistry*, vol. 51, no. 22, pp. 6509–6515, 2003.

[21] G. W. Cheng and P. J. Breen, "Activity of phenylalanine ammonia-lyase (PAL) and concentrations of anthocyanins and phenolics in developing strawberry fruit," *Journal of the American Society for Horticultural Science*, vol. 116, no. 5, pp. 865–869, 1991.

[22] A. Solomon and S. Golubowicz, "Antioxidant activities and anthocyanin content of fresh fruits of common fig (Ficus carica L.)," *Journal of Agricultural*, vol. 54, 2006.

[23] L. Hssaini, F. Hernandez, M. Viuda-Martos et al., "Survey of phenolic acids, flavonoids and in vitro antioxidant potency between fig peels and pulps: chemical and chemometric approach," *Molecules*, vol. 26, no. 9, Article ID 2574, 2021.

[24] L. J. Porter, L. N. Hrstich, and B. G. Chan, "The conversion of procyanidins and prodelphinidins to cyanidin and delphinidin," *Phytochemistry*, vol. 25, no. 1, pp. 223–230, 1985.

[25] C. L. Quarin, "Effect of pollen source and pollen ploidy on endosperm formation and seed set in pseudogamous apomictic Paspalum notatum," *Sexual Plant Reproduction*, vol. 11, no. 6, pp. 331–335, 1999.

[26] S. B. Badgujar, V. V. Patel, A. H. Bandivdekar, and R. T. Mahajan, "Traditional uses, phytochemistry and pharmacology of Ficus carica: a review," *Pharmaceutical Biology*, vol. 52, no. 11, pp. 1487–1503, 2014.

[27] E. J. Blitzer, J. Gibbs, M. G. Park, and B. N. Danforth, "Pollination services for apple are dependent on diverse wild bee communities," *Ecosystems & Environment*, vol. 221, pp. 1–7, 2016.

[28] L. Russo, M. G. Park, E. J. Blitzer, and B. N. Danforth, "Flower handling behavior and abundance determine the relative contribution of pollinators to seed set in apple orchards," *Agriculture, Ecosystems & Environment*, vol. 246, pp. 102–108, 2017.

[29] R. Goodwin, H. McBrydie, and M. Taylor, "Wind and honey bee pollination of kiwifruit (Actinidia chinensis 'HORT16A')," *New Zealand Journal of Botany*, vol. 51, no. 3, pp. 229–240, 2013.

[30] A. M. Chamer, D. Medan, A. I. Mantese, and N. J. Bartoloni, "Impact of pollination on sunflower yield: is pollen amount or pollen quality what matters?" *Field Crops Research*, vol. 176, pp. 61–70, 2015.

[31] A. M. Bartual, G. Bocci, S. Marini, and A. C. Moonen, "Local and landscape factors affect sunflower pollination in a Mediterranean agroecosystem," *PLoS One*, vol. 13, no. 9, Article ID e0203990, 2018.

[32] R. Bommarco, L. Marini, and B. E. Vaissière, "Insect pollination enhances seed yield, quality, and market value in oilseed rape," *Oecologia*, vol. 169, no. 4, pp. 1025–1032, 2012.

[33] D. P. Abrol, "Honeybees and rapeseed: a pollinator–plant interaction," *Advances in Botanical Research*, vol. 45, pp. 337–367, 2007.

[34] D. P. Abrol and U. Shankar, "Pollination in oil crops: recent advances and future strategies," *Technological Innovations in Major World Oil Crops*, vol. 2, pp. 221–267, 2012.

[35] L. Yang, D. Liu, W. Hu, Y. Chun, J. Zhang, and Y. Liu, "Fruit characteristics and seed anatomy of 'Majia' pomelo pollinated with cobalt-60 gamma-ray-irradiated pollen," *Scientia Horticulturae*, vol. 267, Article ID 109335, 2020.

[36] Y. X. Zhang and Y. Lespinasse, "Pollination with gamma-irradiated pollen and development of fruits, seeds and parthenogenetic plants in apple," *Euphytica*, vol. 54, no. 1, pp. 101–109, 1991.

[37] M. Kundu, A. Dubey, and S. Malik, "Effect of Gamma Ray Irradiation Doses on Pollen Viability and In-Vitro

[38] M. Trad, C. Le Bourvellec, B. Gaaliche, C. Ginies, C. M. G. C. Renard, and M. Mars, "Caprification modifies polyphenols but not cell wall concentrations in ripe figs," *Scientia Horticulturae*, vol. 160, pp. 115–122, 2013.

[39] W. Vermerris and R. L. Nicholson, *Phenolic Compound Biochemistry*, p. 276, Springer-Verlag, Dordrecht, Netherlands, 2006.

[40] G. Adiletta, L. Zampella, C. Coletta, and M. Petriccione, "Chitosan coating to preserve the qualitative traits and improve antioxidant system in fresh figs (Ficus carica l.)," *Agriculture*, vol. 94 pages, 2019.

[41] L. Hssaini, J. Charafi, H. Hanine et al., "Correction to: comparative analysis and physio-biochemical screening of an ex-situ fig (Ficus carica L.)," *Horticulture Environment and Biotechnology*, vol. 60, no. 5, pp. 671–683, 2019.

[42] V. Lo Turco, A. G. Potortì, A. Tropea, G. Dugo, and G. Di Bella, "Element analysis of dried figs (Ficus carica L.) from the Mediterranean areas," *Journal of Food Composition and Analysis*, vol. 90, Article ID 103503, 2020.

[43] K. Y. Khan, "Element content analysis of plants of genus Ficus using atomic absorption spectrometer," *African Journal of Pharmacy and Pharmacology*, vol. 5, no. 3, pp. 317–321, 2011.

[44] F. Aljane and A. Ferchichi, "Morphological, chemical and sensory characterization of Tunisian fig (Ficus carica L.) cultivars based on dried fruits," *Acta Horticulturae*, vol. 741, pp. 81–86, 2007.

[45] F. Aljane and A. Ferchichi, "Postharvest chemical properties and mineral contents of some fig (Ficus carica L.) cultivars in Tunisia," *Journal of Food Agriculture and Environment*, vol. 7, no. 2, pp. 209–212, 2009.

[46] H. Sadia, M. Ahmad, S. Sultana et al., "Nutrient and mineral assessment of edible wild fig and mulberry fruits," *Fruits*, vol. 69, no. 2, pp. 159–166, 2014.

[47] T. Bil Der and E. Nakïlcïoglu Tas, "Biochemical characterization of fig (Ficus carica L.) seeds," *Tarım Bilimleri Dergisi*, vol. 25, no. 2, pp. 232–237, Jun. 2019.

[48] M. J. Giertych, P. Karolewski, and L. O. De Temmerman, "Foliage age and pollution alter content of phenolic compounds and chemical elements in pinus nigra needles," *Water, Air, and Soil Pollution*, vol. 110, no. 3, pp. 363–377, 1999.

[49] I. Esparza, I. Salinas, I. Caballero et al., "Evolution of metal and polyphenol content over a 1-year period of vinification: sample fractionation and correlation between metals and anthocyanins," *Analytica Chimica Acta*, vol. 524, no. 1–2, pp. 215–224, 2004.

[50] A. Perna, A. Simonetti, I. Intaglietta, A. Sofo, and E. Gambacorta, "Metal content of southern Italy honey of different botanical origins and its correlation with polyphenol content and antioxidant activity," *International Journal of Food Science and Technology*, vol. 47, no. 9, pp. 1909–1917, 2012.

[51] B. Gordon, "Manganese nutrition of glyphosate-resistant and conventional soybeans," *Better Crops*, vol. 91, no. 4, pp. 12-13, 2007.

[52] I. Pasković, "Temporal variation of phenolic and mineral composition in olive leaves is cultivar dependent," *Plants*, vol. 9, no. 9, Article ID 1099, 2020.

[53] J. Kováčik, B. Klejdus, J. Hedbavny, F. Štork, and M. Bačkor, "Comparison of cadmium and copper effect on phenolic metabolism, mineral nutrients and stress-related parameters in Matricaria chamomilla plants," *Plant and Soil*, vol. 320, no. 1, pp. 231–242, 2009.

[54] A. J. Parr and P. Bolwell, "Review Phenols in the plant and in man. The potential for possible nutritional enhancement of the diet by modifying the phenols content or profile," *Journal of the Science of Food and Agriculture*, vol. 80, no. 7, pp. 985–1012, 2000.

[55] D. Treutter, "Managing phenol contents in crop plants by phytochemical farming and breeding—visions and constraints," *International Journal of Molecular Sciences*, vol. 11, no. 3, pp. 807–857, 2010.

[56] L.-P. Choo, J. R. Mansfield, N. Pizzi et al., "Infrared spectra of human central nervous system tissue: diagnosis of alzheimer's disease by multivariate analyses," *Biospectroscopy*, vol. 1, no. 2, pp. 141–148, 1995.

[57] R. Gopalakrishnan and K. Raghu, "Biosynthesis and characterization of gold and silver nanoparticles using milk thistle (Silybum marianum) seed extract," *Journal of Nanoscience*, vol. 2014, Article ID 905404, 8 pages, 2014.

[58] E. Tulukcu, N. Cebi, and O. Sagdic, "Chemical fingerprinting of seeds of some salvia species in Turkey by using GC-MS and FTIR," *Foods*, vol. 8, no. 4, pp. 1–12, 2019.

[59] S. Cai and B. R. Singh, "A distinct utility of the amide III infrared band for secondary structure estimation of aqueous protein solutions using partial least squares methods," *Biochemistry*, vol. 43, no. 9, pp. 2541–2549, 2004.

[60] M. Cocchi, G. Foca, M. Lucisano et al., "Classification of cereal flours by chemometric analysis of MIR spectra," *Journal of Agricultural and Food Chemistry*, vol. 52, no. 5, pp. 1062–1067, 2004.

[61] M. Cocchi, C. Durante, G. Foca, A. Marchetti, L. Tassi, and A. Ulrici, "Durum wheat adulteration detection by NIR spectroscopy multivariate calibration," *Talanta*, vol. 68, no. 5, pp. 1505–1511, 2006.

[62] S. W. Ellepola, M. C. Siu, and C. Y. Ma, "Conformational study of globulin from rice (Oryza sativa) seeds by Fourier-transform infrared spectroscopy," *International Journal of Biological Macromolecules*, vol. 37, no. 1–2, pp. 12–20, 2005.

[63] X. Liu, C. M. G. C. Renard, S. Bureau, and C. Le Bourvellec, "Revisiting the contribution of ATR-FTIR spectroscopy to characterize plant cell wall polysaccharides," *Carbohydrate Polymers*, vol. 262, Article ID 117935, 2021.

[64] M. K. Ahmed, J. K. Daun, and R. Przybylski, "FT-IR based methodology for quantitation of total tocopherols, tocotrienols and plastochromanol-8 in vegetable oils," *Journal of Food Composition and Analysis*, vol. 18, no. 5, pp. 359–364, 2005.

[65] N. Vlachos, Y. Skopelitis, M. Psaroudaki, V. Konstantinidou, A. Chatzilazarou, and E. Tegou, "Applications of Fourier transform-infrared spectroscopy to edible oils," *Analytica Chimica Acta*, vol. 573, no. 574, pp. 459–465, 2006.

[66] N. Fujioka, Y. Morimoto, T. Arai, and M. Kikuchi, "Discrimination between normal and malignant human gastric tissues by Fourier transform infrared spectroscopy," *Cancer Detection and Prevention*, vol. 28, no. 1, pp. 32–36, 2004.

[67] A. Beljebbar, S. Dukic, N. Amharref, S. Bellefqih, and M. Manfait, "Monitoring of biochemical changes through the C6 gliomas progression and invasion by fourier transform infrared (FTIR) imaging," *Analytical Chemistry*, vol. 81, no. 22, pp. 9247–9256, 2009.

[68] R. Manoharan, K. Shafer, L. Perelman et al., "Raman spectroscopy and fluorescence photon migration for breast cancer diagnosis and imaging," *Photochemistry and Photobiology*, vol. 67, no. 1, pp. 15–22, 1998.

[69] M. Schwanninger, J. C. Rodrigues, H. Pereira, and B. Hinterstoisser, "Effects of short-time vibratory ball milling on the shape of FT-IR spectra of wood and cellulose," *Vibrational Spectroscopy*, vol. 36, no. 1, pp. 23–40, 2004.

[70] S. Y. Oh, D. Il Yoo, Y. Shin, and G. Seo, "FTIR analysis of cellulose treated with sodium hydroxide and carbon dioxide," *Carbohydrate Research*, vol. 340, no. 3, pp. 417–428, 2005.

[71] H. Bouafif, A. Koubaa, P. Perré, A. Cloutier, and B. Riedl, "Analysis of among-species variability in wood fiber surface using DRIFTS and XPS: effects on esterification efficiency," *Journal of Wood Chemistry and Technology*, vol. 28, no. 4, pp. 296–315, 2008.

[72] S. Niu, Y. Zhou, H. Yu, C. Lu, and K. Han, "Investigation on thermal degradation properties of oleic acid and its methyl and ethyl esters through TG-FTIR," *Energy Conversion and Management*, vol. 149, pp. 495–504, 2017.

[73] P. de la Mata, A. Dominguez-Vidal, J. M. Bosque-Sendra, A. Ruiz-Medina, L. Cuadros-Rodríguez, and M. J. Ayora-Cañada, "Olive oil assessment in edible oil blends by means of ATR-FTIR and chemometrics," *Food Control*, vol. 23, no. 2, pp. 449–455, 2012.

[74] E. L. Terpugov, O. V. Degtyareva, and V. V. Savransky, "Possibility of light-induced mid-IR emission in situ analysis of plants," *Journal of Russian Laser Research*, vol. 37, no. 5, pp. 507–510, 2016.

[75] S. N. Rabelo, V. P. Ferraz, L. S. Oliveira, and A. S. Franca, "FTIR analysis for quantification of fatty acid methyl esters in biodiesel produced by microwave-assisted transesterification," *International Journal of Environment and Sustainable Development*, vol. 6, no. 12, pp. 964–969, 2015.

[76] L. Cassani, M. Santos, E. Gerbino, M. del Rosario Moreira, and A. Gómez-Zavaglia, "A combined approach of infrared spectroscopy and multivariate analysis for the simultaneous determination of sugars and fructans in strawberry juices during storage," *Journal of Food Science*, vol. 83, no. 3, pp. 631–638, 2018.

[77] A. Yelil Arasi, J. Juliet Latha Jeyakumari, B. Sundaresan, V. Dhanalakshmi, and R. Anbarasan, "The structural properties of Poly(aniline)-Analysis via FTIR spectroscopy," *Spectrochimica Acta Part A: Molecular and Biomolecular Spectroscopy*, vol. 74, no. 5, pp. 1229–1234, 2009.

Research Article

Computer-Aided Classification of New Psychoactive Substances

Alina Bărbulescu [ID],[1] **Lucica Barbeş** [ID],[2] **and Cristian-Ştefan Dumitriu** [ID][3]

[1]*Transylvania University of Braşov, Department of Civil Engineering, 5 Turnului Str., Braşov, Romania*
[2]*Ovidius University of Constanta, Department of Chemistry and Chemical Engineering, 124 Mamaia Bd., Constanta, Romania*
[3]*SC Utilnavorep SA, 55 Aurel Vlaicu Av., Constanţa 90055, Romania*

Correspondence should be addressed to Lucica Barbeş; lucille.barbes2009@gmail.com

The appearance on the free market of synthetic cannabinoids raised the researchers' interest in establishing their molecular similarity by QSAR analysis. A rigorous criterion for classifying drugs is their chemical structure. Therefore, this article presents the structural similarity of two groups of drugs: benzoylindoles and phenylacetylindoles. Statistical analysis and clustering of the molecules are performed based on their numerical characteristics extracted using Cheminformatics methods. Their similarities/ dissimilarities are emphasized using the dendrograms and heat map. The highest discrepancies are found in the phenylacetylindoles group.

1. Introduction

The consumption of psychoactive substances is among the principal causes of young people's mortality and health issues. A significant proportion of adults consumed some drugs at a certain period in their lives or presented with drug addiction. Synthetic cannabinoids are found in "herbal smoking mixes" and mixtures with other psychoactive substances such as sedatives/hypnotics, hallucinogens, and stimulants [1]. Manufactured in clandestine laboratories and widely sold, the class of new psychoactive substances known as different spices poses a growing threat to public health, such as Spice, Spice Gold, and Silver. In some countries, acute poisonings of users' groups [2–4] have been recorded. Synthetic cannabinoids have been missold as THC (Δ9-tetrahydrocannabinol) or CBD (cannabidiol) and are packed in tablets containing powder or utilized in devices as liquids [5].

Another recent development is the popularity of "vaping" among young people, synthetic cannabinoids being discovered in cartridges filled with liquid for use in e-cigarettes [6].

Psychoactive drugs increase the dopamine available in the brain (called the reward circuit) with participation in pleasure modulation. Synthetic cannabinoids (SCs) are much stronger and more toxic than users can often think. Their increasing prevalence has led to severe health problems among young people and adults. Consumption of these new psychoactive substances poses a health risk and generates severe issues in adapting to reality, education, work, family life, incidents, and road accidents [7, 8]. Research has been performed on the cannabinoids detected in different products to determine how cannabinoids affect the human body [9]. They also aim to analyze the possibilities of using these substances to treat certain neurodegenerative diseases, drug addiction, emotional disorders, or cancer [10]. However, separating the psychoactive effects and the medicinal properties of these drugs is challenging [11].

In about 8–10 years, researchers have tried different dynamic simulation models on rapid identification and establishing the relationships of addiction between the chemical structure and effects on consumers to detect possible ways for curing addiction and overdose [12]. Functionally similar to THC (the cannabis active principle), SCs bind to the same receptors in the human body [6].

The group of synthetic cannabinoids or synthetic cannabimimetic is the largest monitored by the EU Early Warning System. In December 2016, 169 synthetic cannabinoids were reported to the EMCDDA and increased to 190

substances reported in 2018 [8]. About 280 synthetic cannabinoids were known at the end of 2019 [6].

SCs fall into different structural groups [13, 14], such as aminoalkylindoles (which include naphthoylindoles, phenylacetylindoles, naphthylmethylindoles, and benzoylindoles), classical cannabinoids, nonclassical cannabinoids, hybrid cannabinoids, eicosanoids, benzimidazole, indazole-based SCs, and others (naphthoylpyrroles, naphthylmethylindenes, carboxamide-type synthetic cannabinoids, etc.) [15, 16]. The first three groups are presented in Figure 1.

In the investigation of the various chemical synthesis compounds or any chemical synthesis preparation, the chemical analyst establishes the relationships between physicochemical parameters and biological (pharmacological) properties, the degree of structural superposability of the chemical products, using filters based on computational structure and quantitative relationship models of structure-activity (QSARs models) [11].

The search for similarity using molecular fingerprints are among the most common approaches in identifying active chemical compounds proposed for analysis in this study. Many structural descriptors or 2D and 3D ownership are encoded in different representations of fingerprints. All fingerprints eventually transform molecular likeness analysis into a paired comparison of template compound patterns and the entire database [17].

Several fingerprint types are known, each representing a difference in the molecule. Artificial intelligence techniques have been employed in the last period for data analysis in various domains [18–21]. Cheminformatics is a tool used to analyze statistical data based on the digital footprint, which is the dynamic field of modern design for pharmaceuticals, in particular. Cheminformatics plays an essential role in accumulating, grouping, examining chemical data, and finding new entities based on which new chemical structures can build active molecules [22].

Swandana et al. [23] showed that the pharmacokinetic parameters could be predicted using the in silico method. The authors emphasize some software (admetSAR, Chemicalize, Molinspiration, QikProp, SwissADME, and pkCSM software) to predict oral-systemic drugs' pharmacokinetics characteristics. Other scientists [24, 25] emphasized different computational methods utilized for discovering drugs and their limitations.

Finding similarities of different molecules has been of interest since the 90s [26] that can be easily done using the new capabilities of the new software. The rcdk, ChemmineR, and rpubchem packages of *R* are powerful tools in the field of cheminformatics [27–32]. Their utilization helps the cheminformatics-oriented *R* user to organize chemical information efficiently. Guha et al. [27] showed that one of the main tasks is to include further coverage of the CDK API by developing the CDK itself, such as extending the 3D builder model. The authors noted that the CDK API could be accessed directly via rJava, so the functions provided by the rcdk package make cheminformatics functionality readily available for the end-users.

In this study, we used the *R* software capacity to characterize 14 new cannabinoids from the benzoylindoles and phenylacetylindoles groups and determine the similarities among their molecules. Clustering techniques are applied for grouping the studied molecules based on the determined characteristics to cross-validate similar attributes in the same group of drugs.

2. Materials and Methods

The structures subject to the study have been downloaded as .sdf files from PubChem [33]. They belong to the class aminoalkylindoles, subclasses benzoylindoles, and phenylacetylindoles.

The *R* software has been used for performing the study. For this aim, the following libraries have been installed: ChemmineR, chemometrics, cluster, factoextra, fingerprint, fmcsR, ggplot2, gridExtra, iqspr, NbClust, rcdk, rJava, rgl, and vegan. They are necessary for drawing the structures, finding the characteristics of the chemical structures, or determining the appurtenance of the chemical structures to some clusters.

The stages of this study are presented in Figure 2. They are

(i) Import the molecule from ChemPub, as SDF files, and visualize them

(ii) Visualize the molecule structure and molecular formula (MF), and determine the molar weight filter (MW), the types and numbers of atoms, and the functional groups together with the corresponding frequencies

(iii) Compute different descriptors utilizing the library ChemmineOB:

(i) HBA1: number of hydrogen bond acceptors 1
(ii) HBA2: number of hydrogen bond acceptors 2
(iii) HBD: number of hydrogen bond donors
(iv) logP: logarithmic of partition coefficients (log P)
(v) MR: molar refractivity
(vi) TPSA: topological polar surface area

The hydrogen bonds are among the most significant interactions between the solute and solvent. In binding the ligands, the hydrogen bonds have important contributions to the substrates, antagonists, and agonist recognition [34]. The octanol/water partition coefficient is used to characterize the lipophilicity of the compounds and is defined by the ratio $[solute]_{octanol}/[solute]_{water}$. Generally, the logarithm of this ratio, logP, is reported [35].

The molar refractivity (MR) measures the steric factor, which is the volume covered by an atom or a group of atoms. It is correlated to the London dispersive forces acting during the drug-receptor interaction [36].

The hydrophilic interaction and the hydrogen bond formation are reflected by the polar surface (PSA) [37], computed by eliminating the area of nonpolar hydrogen, carbon, and halogen atoms from the molecular surface. Determined by the method of Ertl et al. [38], it is referred to
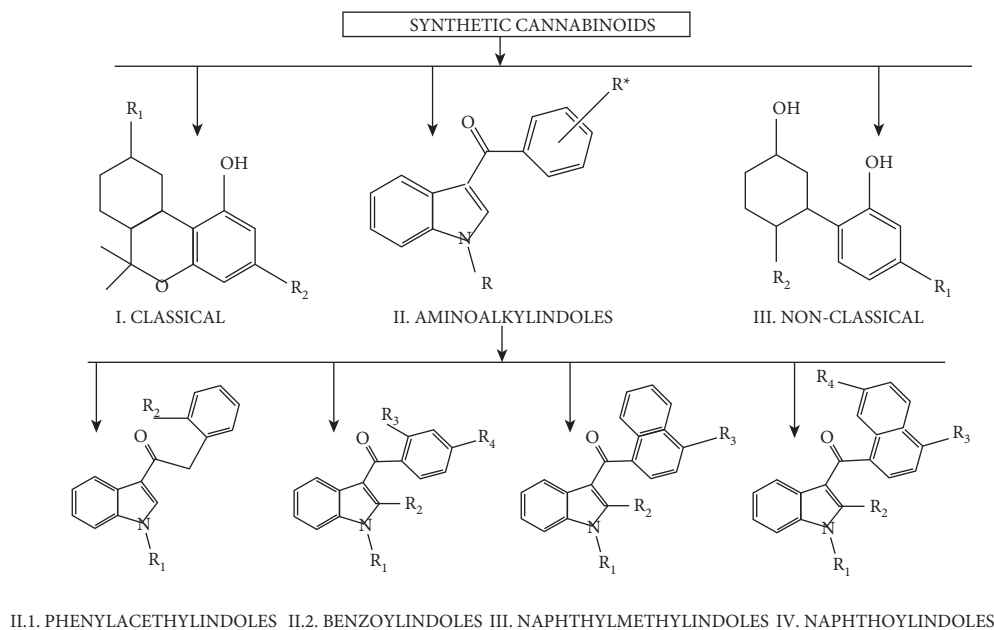
Figure 1: Synthetic cannabinoids.

as topological PSA (TPSA) [39]. According to the available literature, Turner and Agatonovic-Kustrin [40] showed that most drugs have a molar weight lower than 500 and PSA less than 120 Å.

(i) Search the atom pair similarity by cmp.similarity command from ChemmineR. For this aim, the Tanimoto index was utilized [41] due to its performance [26]. For dichotomous variables, it is computed by

$$SS_{A,B} = \frac{c}{(a + b - c)}. \tag{1}$$

The following relationship exists between the distance and similarity metrics:

$$similarity = \frac{1}{(1 + distance)}. \tag{2}$$

(ii) Determine the intermolecular distances, using the fmcs function from the fmscR library and the compound similarities.

(iii) Clustering the molecules' sets: for this aim, the binning clustering (using cmp.function that implements the Tanimoto and Tversky methods) [41, 42], the Jarvis–Patrick algorithm [43], the k-means, and the hierarchical clustering (with the NbClust package) have been utilized [44]. Comparisons are provided.

3. Results and Discussion

The structures of the molecules from the benzoylindoles group (Group 1) are represented in Figure 3, and those from the phenylacetylindoles (Group 2) are represented in

Figure 4, together with the identification number from PubChem.

A similar representation, but showing the number of atoms, is presented in Figure 5, for the molecule 9889172. It contains an automatic numbering added by *R* software when extracting the information from PubChem: the atoms are numbered consecutively (from 1 to the total number of atoms), based on the following order: elements in the seventh group, from the highest to the lowest atomic number, elements in the sixth group, from the highest to the lowest atomic number, and so on, from left to right in the Mendeleev table.

Table 1 contains the molecules formula, the types and numbers of atoms in each molecule from both groups, the molecular weight filters (MW), the number of rings, and the number of aromatic rings retrieved using ChemmineR. The molar weight filters vary in a larger range in the first group by comparison to the second one.

All but the first molecule do not contain F; all the molecules in Group 2 do not contain I. Only one molecule in each group contains Cl. The number of N and O is one or two. The number of C and H atoms is lower in the first group than the second one.

The analysis shows that no molecule contains groups RNH2, R2NH, ROPO3, ROH, RCHO, RCOOH, RCOOR, RCCH, and RCN, but all contain rings, most of them aromatic.

Table 2 contains the most important descriptors that characterize the molecules. The values of HBA1 are lower for the first group, HBD is absent for both groups, logP is in the range of 3.4594–5.8860 for Group 1 and 4.4975–6.0457 for Group 2 (showing higher hydrophilicity for the second group compared to the first one). TPSA varies in larger limits for Group 1 than for Group 2. The higher the TPSA is, the higher the drug transport is. In the studied case, the molecule with CID = 56463 has the highest TPSA.

FIGURE 2: The flowchart.

For example, in Table 4, the query molecule has CID 9889172, and the target molecule in row three has CID 117587582. For both, the query and target sizes are equal (24 atoms, the number of hydrogen atoms is not counted), the Tanimoto coefficient is 0.92, and the overlap coefficient is 0.9583. The higher the Tanimoto and the overlap coefficients are, the higher the similarity of the structures is. The highest dissimilarity is that between molecule CID 56463 and the other molecules in Group 1.

The similarity coefficients in Group 2 are higher than in the first group, as shown in Table 5. Hence, the compounds in the second group have more similar structural characteristics than those in the first group.

The computed similarity coefficients between the pairs of atoms in different molecules from Group 1 and those from Group 2 are shown in Table 6.

The similarities of atom pairs from 9889172 (Group 1) with those from 44397500 and 1161723 (Group 2) are higher than those from 57507905 and 56463 (Group 1). There are high similarities of atoms pairs from 57507911 (Group 1), on the one hand, and 44397540 and 11616723 (Group 2), on the other hand (higher than those with other molecules from Group 1). Similarities above 0.60, which are significant, are noticed for other pairs of molecules belonging to different groups.

A similar result has been obtained using the Tanimoto coefficient for molecules' similarities. Table 7 displays the Tanimoto coefficients and their ranked similarities (from 1 to 7) for pairs of molecules: one from the first group and another from the second group. Blank means a similarity rank over 8. There is only one molecule not listed in Table 7(ID 53394099, Group 2), whose similarity with all the molecules in Group 1 is very low.

Based on the structural characteristics, the molecules' clustering has been performed. The results for Group 1 are presented in the following. The binning clustering, with cutoffs (lower similarity bounds) of 0.3, 0.6, and 0.9 resulted in 1, 2, or 7 clusters, respectively (for both groups). The Jarvis–Patrick algorithm provided 2 clusters when considering four neighbors, and a single cluster when considering 5 and 6 neighbors. The optimal number of clusters (3) in the k-means algorithm has been selected by the elbow method.

Running the k-means algorithm resulted in three clusters with the sizes 1, 3, and 3 and between the sum of squares/total sum of squares = 77.0%. The first clusters contain the first three molecules; the second one, the next three molecules; and the last cluster contains molecule CID 56463.

For the second group, the algorithms binning and Jarvis–Patrick algorithms provided a single cluster.

The heat map and the dendrogram resulted from the hierarchical clustering are presented in Figure 6 for Group 1 and in Figure 7 for Group 2.

In the heat maps, the darker the color is, the lower the distance between the compounds is, so the higher the similarity is. Hence, the pair of compounds whose corresponding squares are dark green are the most similar. A very low similarity is noticed for the pairs of compounds situated in the bottom right-hand side of both heat maps.

The similarity among the pairs of atoms in different molecules is given in Table 3.

Most similarity coefficients are above 0.5, the best ones corresponding to the pair of CIDs (57507911, 57507905), (988917, 0.8462) in Group 1 and (44397540, 11616723), (44397500, 11616723) in Group 2.

The compounds' similarity has been studied using the fmcs function. The output shows the size of the query molecule and that of the target molecule (Query_Size and Target_Size, respectively), the Tanimoto coefficient, and the overlap coefficient, measuring the structures' superposition degree.

FIGURE 3: The structures of the molecules from the benzoylindoles group.
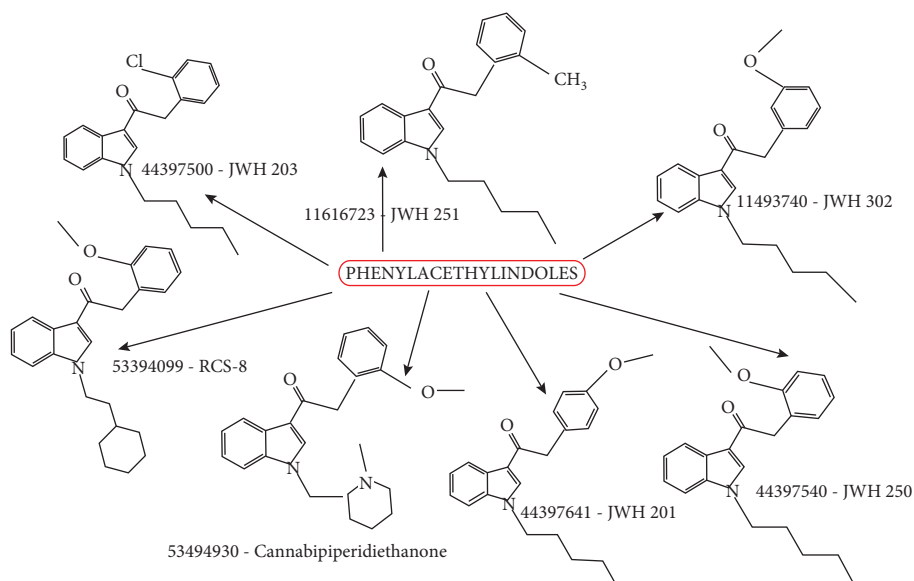
FIGURE 4: The structures of the molecules from the phenylacetylindoles group.

The dendrograms (right-hand side of Figures 6 and 7) confirm the similarity strength. The higher the branch between two compounds is, the lower the similarity is.

In Figure 6, the highest similarity is found between the groups of molecules (117587582 and 9889172) and (79507911 and 56841530). They both have a Tanimoto coefficient of 0.900 and an overlap coefficient of 0.9583 (listed in Table 4 for the first pair, not listed for the second one for the lack of space). From the viewpoint of similarity intensity, the second place is occupied by the pairs of molecules (10226340, 117587582) and (10226340, 9889172), with a Tanimoto coefficient of 0.8519 and the same overlap coefficient.

In Figure 7, the most similar molecules are in the pairs (44397500, 11616723), (44397641, 44397500), and (44397641, 11616723), which is in concordance with the results from

Table 6, because the second and third pairs have the same Tanimoto coefficient (0.8846) and the overlap coefficient 0.8846. The Tanimoto coefficient of the pair (11616723, 44397500) is 0.9152, and the overlap coefficient is 0.9011. They are not listed in the tables to avoid repeating similar information.

Analyzing Figures 6 and 7, remark that the molecules in Group 2 have the distance between them, measured on the dendrograms, lower than those from Group 1, confirming the previous findings related to the molecules' similarity.

The same procedures have been utilized, putting together all the 14 molecules. The heat map and the dendrogram are shown in Figure 8.

The highest similarities are found for the triple (44397500, 44397540, 11616723) from Group 2 and the pairs (957507905, 56481530) and (117587582, 9889172) from the first group.
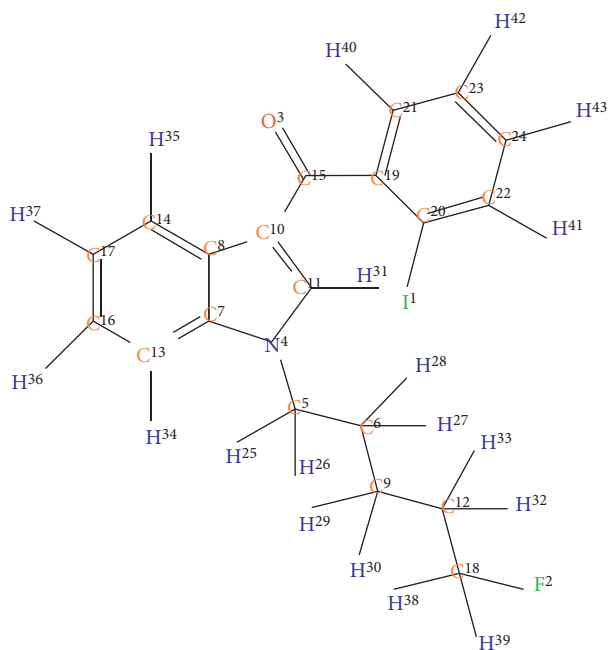
Figure 5: The structure of the molecule 9889172.

Table 1: The cod identification (CID), molecular formula (MF), molar weight filter (MW), types, and the numbers of atoms, rings, and aromatic rings in the molecules.

	CID	Formula	MW	C	F	H	I	N	O	Cl	Rings	Aromatic
	9889172	C20H19FINO	435.2738	20	1	19	1	1	1	0	3	3
	117587582	C20H19ClINO	451.7284	20	0	19	1	1	1	1	3	3
	10226340	C22H23IN2O	458.3353	22	0	23	1	2	1	0	4	3
Group 1	56841530	C21H23NO2	321.4128	21	0	23	0	1	2	0	3	3
	57507911	C21H23NO2	321.4128	21	0	23	0	1	2	0	3	3
	57507905	C20H21NO2	307.3862	20	0	21	0	1	2	0	3	3
	56463	C23H26N2O3	378.4641	23	0	26	0	2	3	0	4	3
	44397641	C22H25NO2	335.4394	22	0	25	0	1	2	0	3	3
	44397500	C21H22ClNO	339.8585	21	0	22	0	1	1	1	3	3
	44397540	C22H25NO2	335.4394	22	0	25	0	1	2	0	3	3
Group 2	53494930	C24H28N2O2	376.4913	24	0	28	0	2	2	0	4	3
	11616723	C22H25NO	319.4400	22	0	25	0	1	1	0	3	3
	11493740	C22H25NO2	335.4394	22	0	25	0	1	2	0	3	3
	53394099	C25H29NO2	375.5033	25	0	29	0	1	2	0	4	3

Table 2: Molecules' descriptors.

	CID	HBA1	HBA2	HBD	logP	MR	TPSA
	9889172	20	2	0	5.6167	105.0705	22.00
	117587582	20	2	0	5.8860	109.8155	22.00
	10226340	25	3	0	4.8991	119.3305	25.24
Group 1	56841530	25	3	0	5.0711	98.7945	31.23
	57507911	25	3	0	5.0711	98.7945	31.23
	57507905	23	3	0	4.6810	93.9875	31.23
	56463	30	4	0	3.4594	114.3495	43.70
	44397641	27	3	0	5.2655	103.6015	31.23
	44397500	23	2	0	5.9103	102.1195	22.00
	44397540	27	3	0	5.2655	103.6015	31.23
Group 2	53494930	31	4	0	4.4975	117.9125	34.47
	11616723	26	2	0	5.5653	102.0755	22.00
	11493740	27	3	0	5.2655	103.6015	31.23
	53394099	31	3	0	6.0457	115.9085	31.23

TABLE 3: Tanimoto coefficients for the atoms similarity.

	CID	9889172	117587582	10226340	57507911	56841530	57507905	56463
	9889172	1.0000	0.8462	0.6788	0.6140	0.5376	0.4901	0.4469
	117587582		1.0000	0.6788	0.5376	0.6140	0.4901	0.4469
	10226340			1.0000	0.5139	0.5774	0.4859	0.5054
Group 1	57507911				1.0000	0.7250	0.8497	0.5425
	56841530					1.0000	0.6635	0.5069
	57507905						1.0000	0.4953
	56463							1.0000
	CID	44397641	44397500	44397540	53494930	11616723	11493740	53394099
	44397641	1.0000	0.6609	0.7249	0.5777	0.7000	0.7654	0.5455
	44397500		1.0000	0.7840	0.5731	0.8467	0.6802	0.5545
	44397540			1.0000	0.6873	0.8526	0.7654	0.6545
Group 2	53494930				1.0000	0.6158	0.5888	0.6882
	11616723					1.0000	0.7357	0.5769
	11493740						1.0000	0.5490
	53394099							1.0000

TABLE 4: Similarity measures for the molecule CID 9889172 and the molecules in Group 1.

CID	Query_Size	Target_Size	Tanimoto_Coefficient	Overlap_Coefficient
9889172	24	24	1.0000	1.0000
117587582	24	24	0.9200	0.9583
10226340	24	26	0.8519	0.9583
57507911	24	24	0.8469	0.9167
56841530	24	24	0.8469	0.9167
57507905	24	23	0.8077	0.9130
56463	24	28	0.5758	0.7917

TABLE 5: Similarity measures for the molecule CID 44397641 and the molecules in Group 2.

CID	Query_Size	Target_Size	Tanimoto_Coefficient	Overlap_Coefficient
44397641	25	25	1.0000	1.0000
44397500	25	24	0.8846	0.9583
44397540	25	25	0.8519	0.9200
53494930	25	28	0.7667	0.9200
11616723	25	24	0.8846	0.9583
11493740	25	25	0.8519	0.9200
53394099	25	28	0.7667	0.9200

TABLE 6: Pair-atoms similarities for molecules from different groups.

CID	44397641	44397500	44397540	53494930	11616723	11493740	53394099
9889172	0.4883	0.5248	0.4922	0.4566	0.5248	0.4884	0.4598
117587582	0.4883	0.5462	0.4922	0.4566	0.5248	0.4884	0.4598
10226340	0.4706	0.4913	0.4810	0.6087	0.5062	0.4741	0.4894
57507911	0.6364	0.5817	0.6842	0.5646	0.6677	0.6600	0.5000
56841530	0.6649	0.5249	0.6134	0.5139	0.5726	0.7194	0.4696
57507905	0.6029	0.4901	0.5937	0.4847	0.5333	0.6361	0.4244
56463	0.4803	0.3915	0.4456	0.4595	0.42173	0.4934	0.4766

TABLE 7: Tanimoto coefficients for the atoms similarity in different groups of molecules.

CID	44397641	44397500	44397540	53494930	11616723	11493740
9889172		0.5262 (6)			0.5262 (7)	
117587582					0.5262 (7)	
10226340				0.6096 (4)	0.5075 (7)	
57507911		0.6374 (7)	0.6851 (3)			0.6609 (6)
56841530	0.6657 (5)		0.6145 (6)			0.7202 (4)
57507905	0.6040 (5)		0.5948 (6)		0.5347 (7)	0.6371 (4)
56463	0.4815 (7)					0.4945 (6)
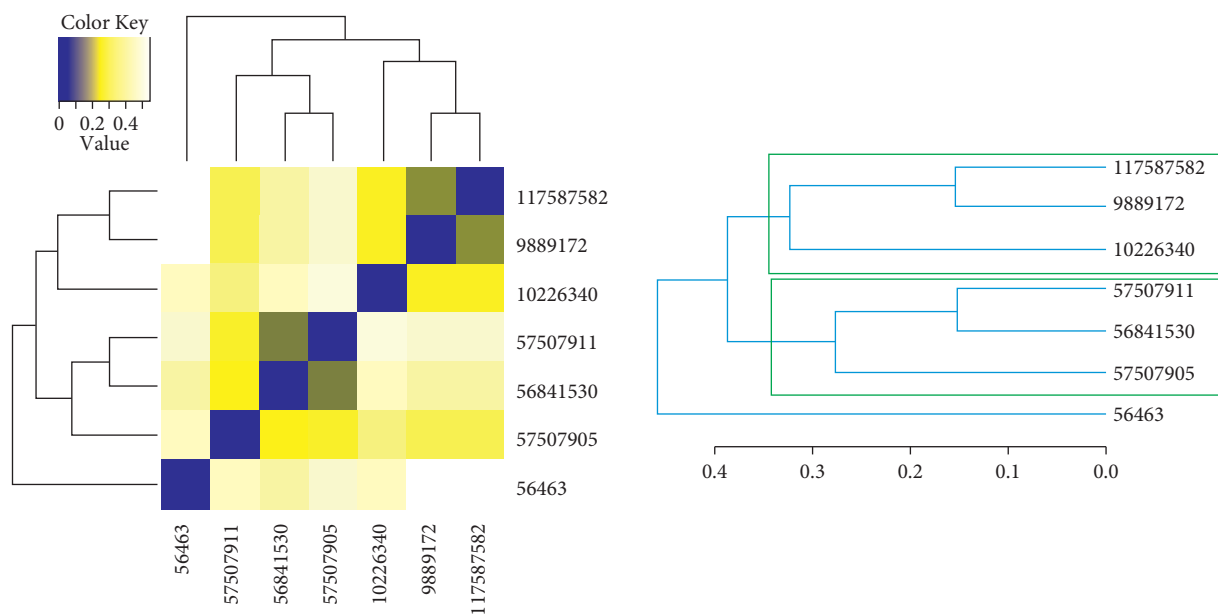
FIGURE 6: The heat map and dendrogram for Group 1.
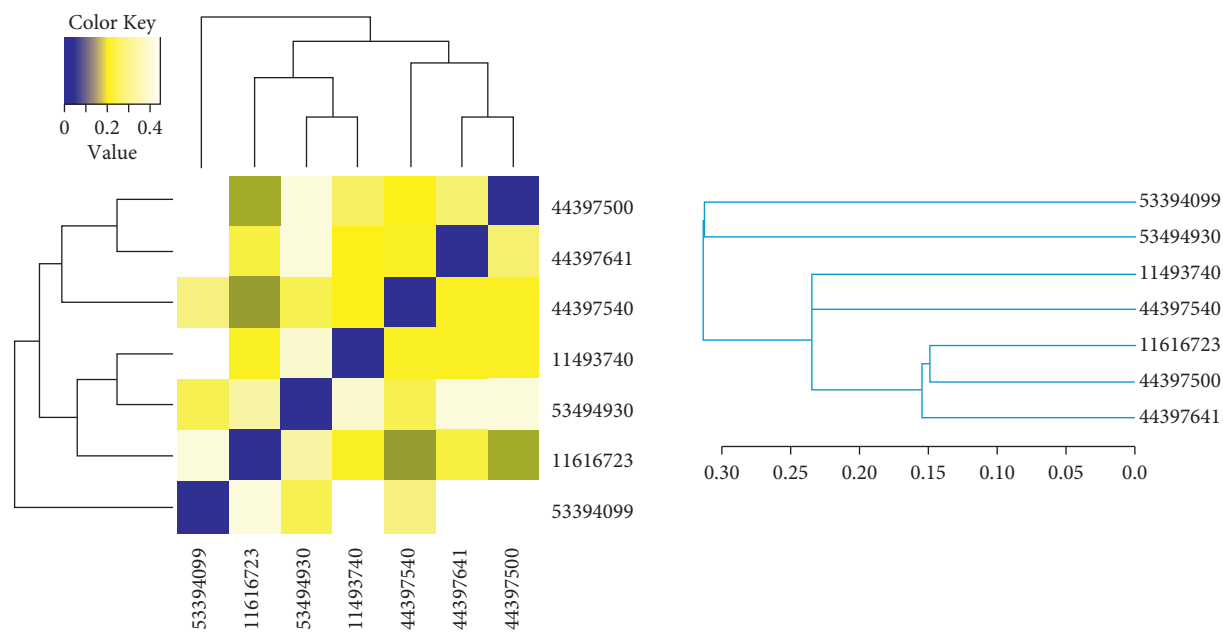
FIGURE 7: The heat map and dendrogram for Group 2.

The clusters determined by the k-means algorithm on the 14 molecules are shown in Figure 9.

The first cluster contains all the molecules in Group 2, a result consistent with the previous findings. The first group is divided into two clusters: the first one containing the first three molecules and the second one, the rest. The result is consistent with the dendrogram in Figure 6. Cluster 2 (Figure 9) contains the same elements as the top subtree in Figure 7.
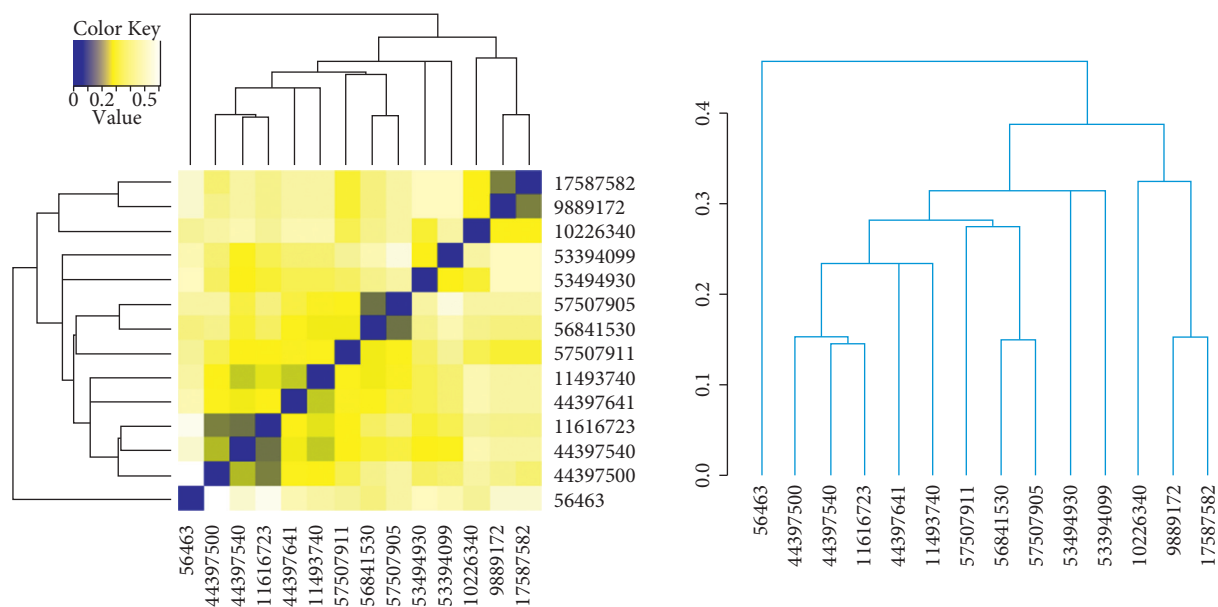
FIGURE 8: The heat map and dendrogram for Groups 1 and 2.
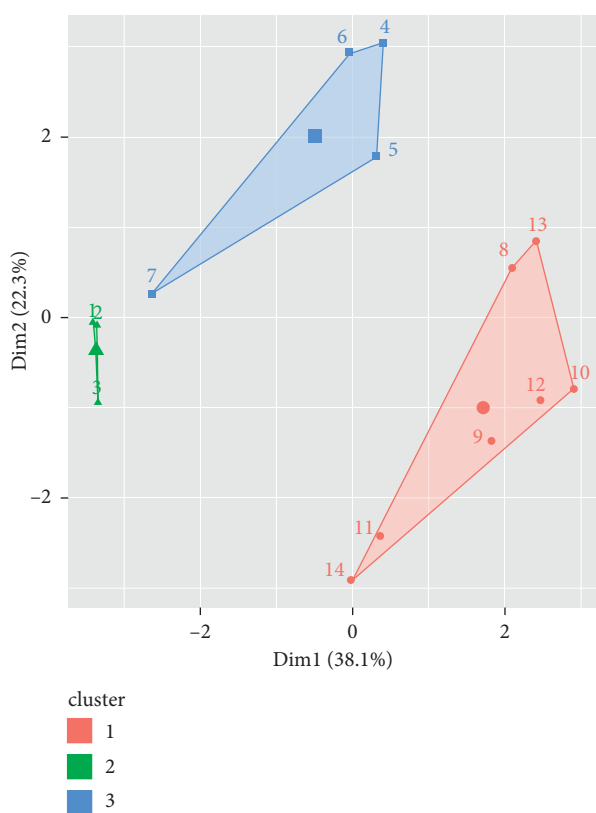
FIGURE 9: The clusters.

4. Conclusions

Cheminformatics is a study field that offers many facilities in collecting, organizing, and studying chemical information [45]. Its contribution is essential to drug design [46, 47]. In this view, our article focused on some applications of Cheminformatics to analyze the benzoylindoles and phenylacetylindoles groups of drugs. The structures and molecules functional groups have been emphasized using the facilities provided by rcdk and ChemmineR packages. Structural similarities of different molecules have been determined using the Tanimoto index and clustering techniques. A higher similarity in the second group compared to the first one is observed. Further practical studies should confirm the hypothesis of the similar actions and effects of these drugs and the possible cure using the same inhibitors.

Data Availability

Data can be freely downloaded from https://pubchem.ncbi.nlm.nih.gov/ by introducing the compound name in the search window.

Conflicts of Interest

The authors declare that they have no conflicts of interest.

References

[1] S. O'Mahony Carey, "Psychoactive Substances. A Guide to Ethnobotanical Plants and Herbs, Synthetic Chemicals, Compounds and Products", http://lab.bnn.go.id/nps_alert_system/publikasi%20web/Psychoactive%20plant/Psychoactive_plant.pdf.

[2] J. van Amsterdam, D. Nutt, and W. van den Brink, "Generic legislation of new psychoactive drugs," *Journal of Psychopharmacology*, vol. 27, no. 3, pp. 317–324, 2013.

[3] C. Vlădescu, S. G. Scîntee, V. Olsavszky, C. Hernández-Quevedo, and A. Sagan, "Romania: health system review," *Health Systems in Transition*, vol. 18, no. 4, pp. 1–170, 2016.

[4] L. Elliott, C. K. Haddock, S. Campos, and E. Benoit, "Polysubstance use patterns and novel synthetics: a cluster analysis from three U.S. cities," *PLoS One*, vol. 14, no. 12, Article ID e0225273, 2019.

[5] A. Hardon, "Chemical breath," *Critical Studies in Risk and Uncertainty*, vol. 6, pp. 81–111, 2021.

[6] A. Shafi, A. J. Berry, H. Sumnall, D. M. Wood, and D. K. Tracy, "New psychoactive substances: a review and updates," *Therapeutic advances in psychopharmacology*, vol. 10, Article ID 2045125320967197, 2020.

[7] EMCDDA 2016, European Monitoring Center for Drugs and Drugs Addiction, "Perspectives on Drugs Health Responses to New Psychoactive Substances", https://www.emcdda.europa.eu/system/files/publications/2933/NPS%20health%20responses_POD2016.pdf.

[8] EMCDDA 2017, European monitoring center for drugs and drugs addiction, "perspectives on drugs synthetic cannabinoids in europe" https://www.emcdda.europa.eu/system/files/publications/2753/POD_Synthetic%20cannabinoids_0.pdf.

[9] L. Ernst, N. Langer, A. Bockelmann, E. Salkhordeh, and T. Beuerle, "Identification and quantification of synthetic cannabinoids in 'spice-like' herbal mixtures: update of the German situation in summer 2018," *Forensic Science International*, vol. 294, pp. 96–102, 2019.

[10] A. D. Lesiak and J. R. Shepard, "Recent advances in forensic drug analysis by DART-MS," *Bioanalysis*, vol. 6, no. 6, pp. 819–842, 2014.

[11] S. Mignani, J. Rodrigues, H. Tomas et al., "Present drug-likeness filters in medicinal chemistry during the hit and lead optimization process: how far can they be simplified?" *Drug Discovery Today*, vol. 23, no. 3, pp. 605–615, 2018.

[12] P. J. Rogers, "Food and drug addictions: similarities and differences," *Pharmacology Biochemistry and Behavior*, vol. 153, pp. 182–190, 2017.

[13] F. Zapata, J. M. Matey, G. Montalvo, and C. García-Ruiz, "Chemical classification of new psychoactive substances (NPS)," *Microchemical Journal*, vol. 163, Article ID 105877, 2021.

[14] V. L. Alves, J. L. Gonçalves, J. Aguiar, H. M. Teixeira, and J. S. Câmara, "The synthetic cannabinoids phenomenon: from structure to toxicological properties. A review," *Critical Reviews in Toxicology*, vol. 50, no. 5, pp. 359–382, 2020.

[15] K. Soltaninejad, "Clinical and forensic toxicological aspects of synthetic cannabinoids: a review and update," *Asia Pacific Journal of Medical Toxicology*, vol. 9, no. 3, pp. 108–118, 2020.

[16] A. J. Potts, C. Cano, S. H. L. Thomas, and S. L. Hill, "Synthetic cannabinoid receptor agonists: classification and nomenclature," *Clinical Toxicology*, vol. 58, no. 2, pp. 82–98, 2020.

[17] J. W. Godden, F. L. Stahura, and J. Bajorath, "Anatomy of fingerprint search calculations on structurally diverse sets of active compounds," *Journal of Chemical Information and Modeling*, vol. 45, no. 6, pp. 1812–1819, 2005.

[18] F. L. Dragomir, "Modeling resource in E-commerce," in *Proceedings of the 10th International Conference on Knowledge Management: Projects*, Systems and Technologies, Bucharest, Romania, November 2017.

[19] F. L. Dragomir, "Models of digital markets," in *Proceedings of the 10th International Conference on Knowledge Management: Projects*, Systems and Technologies, Bucharest, Romania, November 2017.

[20] F. L. Dragomir, "Approaches to modeling consultancy systems by recommendation," in *Proceedings of the 10th International Conference on Knowledge Management: Projects*, pp. 38–41, Systems and Technologies, November 2017.

[21] F. L. Dragomir and G. Alexandrescu, "Operational Research–Theoretical Bases," *Sitech, Craiova, Romania*, 2017, in Romanian.

[22] A. Voicu, N. Duteanu, M. Voicu, D. Vlad, and V. Dumitrascu, "The rcdk and cluster R packages applied to drug candidate selection," *Journal of Cheminformatics*, vol. 12, p. 3, 2020.

[23] R. Iswandana, P. Aisyah, and R. R. Syahdi, "Prediction analysis of pharmacokinetic parameters of several oral systemic drugs using insilico method," *International Journal of Applied Pharmaceutics*, vol. 12, no. 1, pp. 260–263, 2020.

[24] S. P. Leelananda and S. Lindert, "Computational methods in drug discovery," *Beilstein Journal of Organic Chemistry*, vol. 12, pp. 2694–2718, 2016.

[25] G. Sliwoski, S. Kothiwale, J. Meiler, and E. W. Lowe Jr., "Computational methods in drug discovery," *Pharmacological Reviews*, vol. 66, no. 1, pp. 334–395, 2014.

[26] P. Willett, "Similarity searching using 2D structural fingerprints," *Methods in Molecular Biology (Clifton, N.J.)*, vol. 672, pp. 133–158, 2011.

[27] R. Guha, K. Gilbert, G. Fox, M. Pierce, D. Wild, and H. Yuan, "Advances in cheminformatics methodologies and infrastructure to support the data mining of large, heterogeneous chemical datasets," *Current Computer-Aided Drug Design*, vol. 6, no. 1, pp. 50–67, 2010.

[28] Y. Cao, A. Charisi, L.-C. Cheng, T. Jiang, and T. Girke, "ChemmineR: a compound mining framework for R," *Bioinformatics*, vol. 24, no. 15, pp. 1733-1734, 2008.

[29] Y. Wang, T. W. H. Backman, K. Horan, and T. Girke, "fmcsR: mismatch tolerant maximum common substructure searching in R," *Bioinformatics*, vol. 29, no. 21, pp. 2792–2794, 2013.

[30] R. Guha, "Chemical informatics functionality in R," *Journal of Statistical Software*, vol. 18, no. 5, pp. 1–16, 2007.

[31] R. Guha and M. R. Cherto, "Integrating the CDK with R," *Chemical informatics functionality in R*, vol. 1–17, 2017, http://cran.nexr.com/web/packages/rcdk/vignettes/rcdk.pdf.

[32] S. Mente and M. Kuhn, "The use of the R language for medicinal chemistry applications," *Current Topics in Medicinal Chemistry*, vol. 12, no. 18, p. 1957, 2012.

[33] PubChem. Available at: https://pubchem.ncbi.nlm.nih.gov.

[34] H. Kubinyi, "Hydrogen bonding: the last mystery in drug design?," in *Pharmacokinetic Optimization in Drug Research: Biological, Physicochemical, and Computational Strategies*, B. Testa, H. van de Waterbeemd, G. Folkers, and R. Guy, Eds., pp. 513–521, Verlag Helvetica Chimica Acta, Zürich, Switzerland, 2001.

[35] G. Caron, M. Vallaro, and G. Ermondi, "Log P as a tool in intramolecular hydrogen bond considerations," *Drug Discovery Today: Technologies*, vol. 27, pp. 65–70, 2018.

[36] G. L. Patrick, *An Introduction to Médicinal Chemistry*, Oxford University Press, Oxford, UK, 1995.

[37] S. A. Cuesta, J. R. Mora, and E. A. Márquez, "In silico screening of the DrugBank database to search for possible drugs against SARS-CoV-2," *Molecules*, vol. 26, no. 1100, 2021.

[38] P. Ertl, B. Rohde, and P. Selzer, "Fast calculation of molecular polar surface area as a sum of fragment-based contributions and its application to the prediction of drug transport properties," *Journal of Medicinal Chemistry*, vol. 43, no. 20, pp. 3714–3717, 2000.

[39] G. Vistoli and A. Pedretti, "Molecular fields to assess recognition forces and property spaces," *Comprehensive Medicinal Chemistry II*, vol. 5, pp. 577–602, 2007.

[40] J. V. Turner and S. Agatonovic-Kustrin, "In silico prediction of oral bioavailability," *Comprehensive Medicinal Chemistry II*, vol. 5, pp. 699–724, 2007.

[41] D. Bajusz, A. Rácz, and K. Héberger, "Why is Tanimoto index an appropriate choice for fingerprint-based similarity calculations?" *Journal of Cheminformatics*, vol. 7, no. 1, 2015.

[42] A. Tversky, "Features of similarity," *Psychological Review*, vol. 84, no. 4, pp. 327–352, 1977.

[43] F. Murtagh and P. Contreras, "Algorithms for hierarchical clustering: an overview," *Wiley Interdisciplinary Reviews. Data Minining Knowledge Discovery*, vol. 2, no. 1, pp. 86–97, 2021.

[44] R. A. Jarvis and E. A. Patrick, "Clustering using a similarity measure based on shared near neighbors," *IEEE Transactions on Computers*, vol. C-22, no. 11, pp. 1025–1034, 1973.

[45] M. Karthikeyan and R. Vyas, "Machine learning methods in chemoinformatics for drug discovery," in *Practical Chemoinformatics*, M. Karthikeyan and R. Vyas, Eds., Springer, New Delhi, India, pp. 133–194, 2014.

[46] J. A. DiMasi, R. W. Hansen, and H. G. Grabowski, "The price of innovation: new estimates of drug development costs," *Journal of Health Economics*, vol. 22, no. 2, pp. 151–185, 2003.

[47] M. Hassan Baig, K. Ahmad, S. Roy et al., "Computer aided drug design: success and limitations," *Current Pharmaceutical Design*, vol. 22, no. 5, pp. 572–581, 2016.

Research Article

Chemo-Profiling of Illicit Amphetamine Tablets Seized from Jazan, Saudi Arabia, Using Gas Chromatography-Mass Spectrometry and Chemometric Techniques

Hassan A. Alhazmi [1,2] **Waquar Ahsan** [2] **Mohammed Al Bratty** [2] **Asaad Khalid** [1] **Shahnaz Sultana** [3] **Asim Najmi** [2] **Hafiz A. Makeen** [4] **Ibraheem M. Attafi** [5] **Farid M. Abualsail** [5] **Mohammed A. Arishy** [5] and **Ibrahim A. Khardali** [5]

¹*Substance Abuse and Toxicology Research Centre, Jazan University, P. Box No. 114, Jazan, Saudi Arabia*
²*Department of Pharmaceutical Chemistry, College of Pharmacy, Jazan University, P. Box No. 114, Jazan, Saudi Arabia*
³*Department of Pharmacognosy, College of Pharmacy, Jazan University, P. Box No. 114, Jazan, Saudi Arabia*
⁴*Department of Clinical Pharmacy, College of Pharmacy, Jazan University, P. Box No. 114, Jazan, Saudi Arabia*
⁵*Poison Control and Medical Forensic Chemistry Center, General Directorate of Health Affairs, Jazan, Saudi Arabia*

Correspondence should be addressed to Waquar Ahsan; wmohammad@jazanu.edu.sa

A number of illegal drug tablets with unknown constituents are supplied to countries around the world, most of which are habit forming. Amphetamine constitutes the majority of illegal tablets supplied to Saudi Arabia. In this study, we investigated illicit amphetamine tablets seized from Jazan region located in the southwest of Saudi Arabia to identify the insidious additives present in them and their health-related risks. Tablets were analyzed for the presence of amphetamine and other additives using gas chromatography-mass spectroscopy (GC-MS) technique. Amphetamine was detected in good to high area % values in all analyzed tablets in the range of 16.29–41.23%. Interestingly, a number of other additives were also detected with amphetamine in most of the tested samples including caffeine, lidocaine, diphenhydramine, and 8-chlorotheophylline in considerable area %. Caffeine may have been added to enhance the psychotic effect of amphetamine, whereas lidocaine was added to prevent the cardiovascular side effects of amphetamine. Diphenhydramine was probably added to prevent other undesirable side effects of amphetamine such as insomnia and tremors. Chemometric hierarchical cluster analysis was carried out to make samples clusters which have similar characteristics. It resulted into a dendrogram tree showing eight clusters signifying different sources of tablet samples. Owing to the toxic effects of amphetamine and other psychoactive constituents in the tested tablets, the illegal trafficking of these tablets should be prevented by all means and public awareness should be increased.

1. Introduction

Amphetamine is the psychostimulant drug that had been indicated clinically for the treatment of attention-deficit hyperactivity disorder (ADHD). However, it is no longer used clinically due to its addictive and other adverse effects. Nevertheless, amphetamine and its congeners are still produced and used illegally for their transient euphoric effects leading to mood elevation and increased physical and mental performance [1, 2]. These drugs are known to show dose-dependent adverse effects on humans such as confusion, hallucinations, tremors, hypertension, and arrhythmias. Amphetamine tablets are generally supplied under the common brand name "captagon" containing the active ingredient "fenethylline hydrochloride," which is the theophylline derivative of amphetamine and has similar effects to those of amphetamine. Captagon tablets are believed to be originated from European countries and are widely

consumed in Middle Eastern countries including Saudi Arabia, Kuwait, Jordan, and Qatar [3]. News regarding seizure of captagon tablets are very frequent in these countries. Instead of religious and legal prohibitions in Middle Eastern countries including Saudi Arabia, the use of narcotic substances is prevalent [4]. It was estimated in 2019 that around 7-8% of Saudis are drug users and 70% among them are of age 12–22 years [5, 6]. Also, the accuracy of this data is not clear and the United Nations Office on Drugs and Crime (UNODC) suggests that this data may be underestimated owing to the higher number of seizures in these areas. The social stigma and fear of disclosure associated with the use of these substances further decrease the numbers. It was also estimated that more than 50% of the total global interception of amphetamine-type stimulants (ATS) is reported from the Arabian Peninsula [7].

A number of cases of amphetamine tablet seizures have been reported worldwide earlier and were analyzed for their content using various analytical techniques. Results revealed that amphetamine was present in varied quantities in different tablets, from trace amounts to even more than one-third of the total weight of the tablets. Previously, analysis of several seized captagon tablets from Saudi Arabia showed presence of amphetamine in trace quantities in almost half of the tablets; however, the other half showed very high concentration of more than 38% [8]. Similarly, another seizure from Iraq by the Drug Enforcement Administration (DEA) showed that the tablets contained varying concentrations of amphetamine (7–20 mg) along with several other additives. These included caffeine (30–65 mg), theophylline (14–39 mg), and acetaminophen (9–21 mg) [9]. Similar results were obtained when German Bundeskriminalamt (BKA) carried out the analysis of seized tablets in 2013 and reported the presence of amphetamine (8–14%) along with other additives including caffeine (12–35%), theophylline (10–14%), and acetaminophen (6–20%) [10].

A number of tablets of unknown constituents were detained from three major cities of Jazan, Saudi Arabia, which were suspected to be containing amphetamine. Earlier, they were subjected to the LC-MS/MS analysis by our research group at the Poison Control and Medical Forensic Chemistry Center, Jazan, to determine the concentration of amphetamine and methamphetamine in these tablets. The amounts of amphetamine in the tested tablets were calculated to be between 9.07 and 14.77 mg, which were considerably high [11]. In continuation to the analysis of these tablets for the determination of unknown constituents, we intended to perform the GC-MS analysis of these tablets which could give information of all constituents present in the tablets. Previously, we successfully employed techniques such as GC-MS and ICP-MS to perform analysis of various other substances of abuse and determined a number of constituents [12–15] in their samples. Analysis of amphetamine tablets seized in Jazan province is very important keeping in consideration the fact that Jazan province is situated at the southwest of Saudi Arabia and shares borders with Yemen where the use of amphetamine is common. The similarities in constituents would give an insight about the place of origin of these tablets. No previous study has been reported to investigate the constituents of seized amphetamine tablets in this region.

2. Materials and Methods

2.1. Chemicals and Reagents. The standard amphetamine and the internal standard (IS) amphetamine-D5 vials (1 mg/mL) were procured from Lipomed AG (Cambridge, USA). All other chemicals and solvents including isopropyl alcohol, ammonium hydroxide, dichloromethane, methanol, hexane, ethyl acetate, acetonitrile, and acetic acid were purchased from Sigma-Aldrich (Steinheim, Germany). All the solvents used were of HPLC grade. Extrapure Deionized (DI) water was prepared in our lab using Millipore purification system.

2.2. Sample Collection. Sample tablets were seized and collected by local police raid from Ahad Al-Masariha, Al-Darb, and Jazan cities of Jazan province and sent to the Poison Control and Medical Forensic Chemistry Center, General Directorate of Health Affairs, Jazan, for further analysis. For the determination of chemical constituents, randomly 10 tablets seized from each city were selected. Coding of samples was performed according to the city from where they were collected: A1-A10 (Ahad Al-Masariha), D1-D10 (Al-Darb), and G1-G10 (Jazan/Gizan city). All these thirty tablets were analyzed separately using the developed GC-MS method at the Poison Control Center.

2.3. Preparation of Solutions. Amphetamine standard solution (1 mg/mL) was further diluted appropriately using methanol to obtain the solutions of concentrations 5, 10, 15, 20, and 25 μg/mL which were used to construct the calibration curve. The IS amphetamine-D5 solution was added to each calibration standard keeping the IS concentration at 10 μg/mL. Three quality-control (QC) solutions of concentrations of 5 (low; LQC), 10 (medium; MQC), and 20 μg/mL (high; HQC) were also prepared using the standard stock solution of amphetamine. An aliquot of 2 mL from each calibration standard was placed into the GC-vial and 2 μL was injected to the system and the analysis was performed in triplicate.

2.4. Sample Preparation. Half tablet from each sample was crushed into fine powder and dissolved in 3 mL methanol and sonicated using WUC.D10H digital ultrasonicator (Acinterlab, Fl, USA) for 15 min at room temperature [16]. Samples were then filtered to the GC-vial using 0.45 μm Millex-LCR PTFE syringe filter (Merck Millipore, MA, USA) and the analyses were performed in triplicate. Samples were prepared fresh before each analysis.

2.5. Method Validation. The SPE method for sample preparation as well as the proposed GC method was validated according to the ICH guidelines Q2B. The intraday and interday precisions were determined by calculating the % relative standard deviation (% RSD) of peak areas of amphetamine standard and measuring the retention times of

the three replicate injections. Accuracy of the experiment was determined by calculating the % recovery of the amphetamine. The quality control samples (5, 10, and 20 μg/mL) were analyzed to get the data for precision and accuracy. All the quality control samples were analyzed on the same day to get the intraday precision and accuracy data, whereas the samples were analyzed for three consecutive days to get the interday data.

Linearity of the proposed method was also evaluated using the ICH protocol by analyzing the above prepared calibration standards. The prepared standard solutions of five concentrations were injected in increasing concentrations and the chromatograms were recorded. The corresponding peak area values were calculated and the calibration curve was plotted between the peak area ratio of amphetamine standard and amphetamine-D5 internal standard against amphetamine concentration and the intercept and slope values were obtained from the plot. For the determination of sensitivity of the method, the limit of detection (LOD) and limit of quantification (LOQ) values were calculated from the standard deviation and slope of the curve.

2.6. GC-MS Analysis of Tablets.

Shimadzu Gas Chromatograph (Shimadzu, Japan) was used for GC-MS analysis for all the samples and solutions. The GC instrument was equipped with a TR-5MS capillary column (30 m × 0.25 mm) having a 0.25 μm film thickness. The carrier gas helium (He) was used at a flow rate of 1.2 mL/min throughout the process. Instrument was heated to 70°C initially, followed by ramping at a rate of 15°C per min to 300°C, and held for 30 min. Fragments were detected using Shimadzu QP2010 Ultra MS detector coupled to the chromatograph instrument with electron-ionization (EI) system and working at an ionization energy of 70 eV. The temperature of the ion source was kept at 230°C. The mass spectrometric analysis was performed by obtaining a full mass spectrum over a range of m/z 100–550 and m/z 136 and 141 were used for monitoring amphetamine and amphetamine-D5, respectively. All the analyses were carried out in triplicate.

2.7. Identification of Constituents.

The constituents present in the samples were identified by using authentic standards (Sigma Aldrich, Steinheim, Germany) present in our laboratory and by comparing their retention indices. The major components present in the tablets were identified using the authentic standards of amphetamine, lidocaine, and caffeine present in our laboratory. The retention indices and the fragmentation pattern which were in close agreement to reference standards were used for identification. For other constituents, the fragmentation patterns were compared and identified using built-in NIST08 and Wiley 9 libraries stored in the software database. The area % values (±SD) were used for quantification of the constituents.

2.8. Chemometric Analysis.

Owing to the significant variations in the constituents of tablets, most abundant constituents were selected and subjected to multivariate chemometric analysis in order to determine the relation, if any, among the constituents. Hierarchical Cluster Analysis (HCA) was performed and dendrogram trees were obtained using NCSS software 2020 version. The area % values of different constituents were considered as variables and were expressing columns, whereas the samples constituted 30 rows. The HCA analysis was run to obtain significant groups of samples or clusters which have similar characteristics and which might have the same source of origin.

3. Results and Discussion

3.1. Method Validation

3.1.1. Linearity, LOD, and LOQ.

The calibration curve was plotted by analyzing five increasing concentrations of amphetamine standard solutions and the linearity was observed by calculating the correlation coefficient (R^2) value of the plot. The method showed a good linearity over the tested range as the R^2 value was calculated to be 0.997. The equation for linear regression was attained to be $y = 0.182x - 0.5443$. The LOD and LOQ values were calculated to be 0.44 μg/mL and 0.975 μg/mL, respectively, which showed good sensitivity of the method.

3.1.2. Precision and Accuracy.

The precision and accuracy of the GC method were determined by calculating the % relative standard deviations (% RSDs) in case of intra- and interday analysis and it was calculated to be <2% for both peak area and the retention time of the analyte which were within the prescribed limits given in the ICH guidelines. Percent recoveries were also calculated for the intra- and interday samples and were found to be in the range of 100 ± 2% which were also within the acceptable limits of the ICH guidelines. The precision and accuracy data are given in Table 1.

3.1.3. Specificity.

To determine the specificity of the method, methanol as blank was injected to the sample and analyzed using the method and the chromatogram obtained was compared to the chromatograms of calibration standards. No interferences were observed at the retention times of analytes and IS showing the good specificity of the method.

3.2. GC-MS Analysis.

Using the developed GC-MS method, various constituents present in all tablet samples were separated within 30 min runtime. The area % values of all the constituents were calculated and the values more than 1% were reported. A total of 59 compounds were identified using the technique, which were present in one or more samples with area % more than 1. The names and area % values of all the components present in 30 samples are summarized in Table 1S (Supplementary file). The major constituents which were common in most of the samples are shown in Table 2 and the structures thereof are depicted in Figure 1 along with their area % values. Figures 2(a)–2(c) represent the total ion chromatograms for representative samples from each city.

TABLE 1: Results of precision and accuracy experiments for intra- and interday analysis of the three quality control samples using the proposed GC method.

	Concentrations of samples (μg/mL)	% RSD of peak area[*]	% RSD of retention time[*]	% recovery $\pm$ SD[*]
Intraday analysis	5.0 (LQC)	0.75	0.92	99.4
	10.0 (MQC)	0.63	0.54	100.2
	20.0 (HQC)	0.94	0.88	98.5
Interday analysis	5.0 (LQC)	0.36	0.63	98.2
	10.0 (MQC)	0.57	0.49	98.6
	20.0 (HQC)	0.77	0.53	100.5

[*]$n = 3$; LQC: low quality control, MQC: medium quality control, and HQC: high quality control.

The tablet samples from Ahad Al-Masariha, Al-Darb, and Jazan showed considerable variations in their contents. Amphetamine was the only constituent that was detected at retention time (RT) of 4.78 min in all samples but in different area % values ranging from 16.29 to 41.23% in all tablet samples. This variation was also observed in different samples from the same city. Another amphetamine derivative, N-formyl amphetamine, was also present at RT of 8.15 min in few samples from each city in the range of 1.54–2.9%, which might be present as an impurity that has been introduced during the manufacture of amphetamine or as a degradation product of amphetamine during storage. Another important constituent that was present in most of the samples was methyl diphenyl methyl ether at RT of 8.57 min in the range of 3.47–28.63% of the total constituents present.

Interestingly, several unusual compounds were also detected such as caffeine (9.3–25.71%, RT = 10.88 min) and lidocaine (12.98–26.1%, RT = 11.03 min) in good to significant amounts. Additionally, most of the samples showed presence of dimenhydrinate at RT 10.96 min, which is a combination of diphenhydramine and 8-chlorotheophylline as 2.05–13.05% of the total constituents. N,N′-di(phenyl isopropyl) formamide and di(phenyl isopropyl) amine were another two constituents which were present in considerable amounts with their area % values ranging from 1.4 to 3.5% and from 1.4 to 21.5% with RT of 13.72 min and 11.13 min, respectively. A number of long chain aliphatic alcohols were also detected in most of the samples including 2-octyldodecanol (1.9–8.65%), 2-hexyldodecanol (1.6–9.98%), and n-nonadecanol (1.04–2.51%).

Few compounds were found to be specifically present in tablets collected from certain cities and were not common in all. For instance, 13-docosenamide was present at RT of 16.26 min in samples obtained from Al-Darb (2 out of 10) and Jazan (8 out of 10) cities only in the area % values ranging from 1.99 to 2.93% but was absent in all the tested tablets from Ahad Al-Masariha city. Similarly, Cycloeicosane was also present in Al-Darb tablet samples (1.87–2.63%) as well as tablets from Jazan (1.51–2.11%) at RT of 11.47 min but not in Ahad Al-Masariha samples. Another constituent, heptacosane, was exclusively present at RT of 16.27 min in 5 out of 10 tested tablets from Al-Darb city in a considerable area % values of 1.47–2.8%, whereas it was absent in all samples from Ahad Al-Masariha and Jazan cities. All of the rest detected constituents either were present in very few samples or were present in very less area

% values. These were considered insignificant and may have arisen due to impurities from any of the ingredient at the time of manufacturing the tablets.

The illicit usage and peddling of amphetamine and related substances have been a cause of concern for most of the countries in the Middle Eastern and European regions. Seizure of illegal captagon tablets is common in this region and a number of cases have already been surfaced from many countries including Saudi Arabia, Yemen, Turkey, Iraq, Jordan, Serbia, and so forth and the number keeps counting. When subjected to forensic analysis, amphetamine was found to be the major constituent of these tablets with several other additives [17–23]. The amphetamine content in these studies was found to be very high and varied considerably among the samples. It was as low as 16% in some tablets and as high as 41% in others and tablets from all the cities showed the same variation. This indicated that there was not any fixed protocol used in the manufacture of these tablets and amphetamine was added to tablets randomly irrespective of its weight. Similar results were found previously in analyses of illegal captagon tablets in Saudi Arabia and Iraq, which revealed 2–38% amphetamine content in all tablets [24]. Comparatively higher amount of amphetamine present in the tested tablets reveals the toxicity it can cause as amphetamine at this dose can cause a number of untoward reactions and dependence. High doses of amphetamine lead to impairment of cognitive functions and augmentation of nerve damage along with the induction of rapid muscles breakdown [25, 26].

The findings of this study were similar to the findings reported in an earlier study in which the presence of nonpsychoactive substances such as caffeine, quinine, ephedrine, paracetamol, theophylline, and chloroquine in 12–16% of the seized tablets from Saudi Arabia [27] was reported. Addition of theophylline derivatives such as 8-chlorotheophylline to the tablets suggested that the manufacturer wanted to produce an effect similar to captagon tablets containing fenethylline [27], which is a theophylline derivative of amphetamine used in captagon tablets. Theophylline is a drug used to treat chronic obstructive pulmonary diseases (COPD) and asthma and is a known bronchodilator having positive inotropic and chronotropic effects. The theophylline derivatives are also known to stimulate the central nervous system similar to caffeine and these two substances must have been added to the tablets to increase the psychostimulant effects of amphetamine [27].

TABLE 2: Major constituents found in samples collected from different cities showing their area % values.

City	Compounds	Amphetamine	N-Formylamphetamine	Methyl diphenylmethyl ether	Caffeine	Lidocaine	3-Eicosene	2-Octyl-1-dodecanol	N,N-Di-(-phenylisopropyl)formamide	1-Dodecanol,2-hexyl	Di-(-phenylisopropyl)amine	Dimenhydrinate	Cycloeicosane
	1	38.96	2.63	3.78	14.21	20.16	2.5	4.76					
	2	36.46	2.68	3.47	13.85	21.14		4.95					
	3	31.93		28.63	13					1.88			
	4	25.3	2.7	8.4	9.3	23.6		4.8	1.93	3.8			
Ahad Al-Masariha	5	33.36		8.99	10.91	18.45	2.54	2.91		2.3	1.4		
	6	17.55		23.01	14.23		2.55	3.4	2.03	2.85	1.77	7.23	
	7	41.23		6.6	15.6		4.1	3.2	3.1	8.2	1.91	5.2	
	8	23.18		20.12	21.27			2.32	1.7	4.07	1.4	4.88	
	9	40.43		9.2	15.25	14.67		2.49		2.13	1.58		
	10	32.03			18.35	8.3	8.36	2.35	1.88	9.98	21.31		
	1	30.31		25.81	10.18			1.9	1.75					1.95
	2	37.2			14.66	20		2.76		2.29				1.98
	3	31.66	1.54		13.52	26.1		2.51		2.25				1.995
	4	34.4	2.5	3.45	14.53	21.49		2.43		2.48				1.87
Al-Darb	5	36.71		22.8				3.58		2.58		2.5		2.71
	6	27.19		27.3	10.89			5.26		3.05		3.98		
	7	16.29		15.81	18.9			8.65	1.8	2.37	2.17	12.62	
	8	20.8		28.01				4.2	1.4	2.5				2.63
	9	31.3	1.7	4.9	19.99			8.4	3.5	6.4	1.9	12.1	
	10	35.5		10.14	17.04			4.1	2.6	8.02	3.2	10.11	
	1	39.2			10.82	17.33						7.1	
	2	18.4		15.52	14.51				3.1		18.4	10.11	
	3	32.9		18.33	17.04	18.37		5.9				6.21	
	4	17.3	2.4	22.89	12.26	12.98		3.8	2.8	2.3	21.5	2.05		2.11
Jazan	5	36.4		26.43	20.43			7.4	2.4		17.3	3.07		2.9
	6	33.54		21.41	25.71			6.88	2.8		18.4	13.05	
	7	38.31		19.05	22.31				2.5	2.05	12.18	3.66		1.69
	8	24.22		17.37	10.6				1.6				
	9	22.31	2.1	18.09	13.45			2.31	1.4	1.6	16.4	3.65	
	10	26.35	2.9		17.28	16.52			1.9	5.89				1.51

Amphetamine (16.29-41.23%)

N-Formylamphetamine (1.54-2.9%)

Caffeine (9.3-25.71%)

Lidocaine (12.98-26.1%)

8-Chlorotheophylline
(2.05-13.05%)

Diphenhydramine
(2.05-13.05%)

N,N-di (-phenylisopropyl) formamide
(1.4-3.5%)

di- (-phenylisopropyl) amine
(1.4-21.5%)

Methyl diphenyl ether
(3.47-28.63%)

3-Eicosene (2.5-8.36%)

Cycloeicosane (1.51-2.9%)

2-Octyl-dodecan-1-ol
(1.9-8.65%)

2-Hexyl-dodecan-1-ol
(1.6-9.98%)
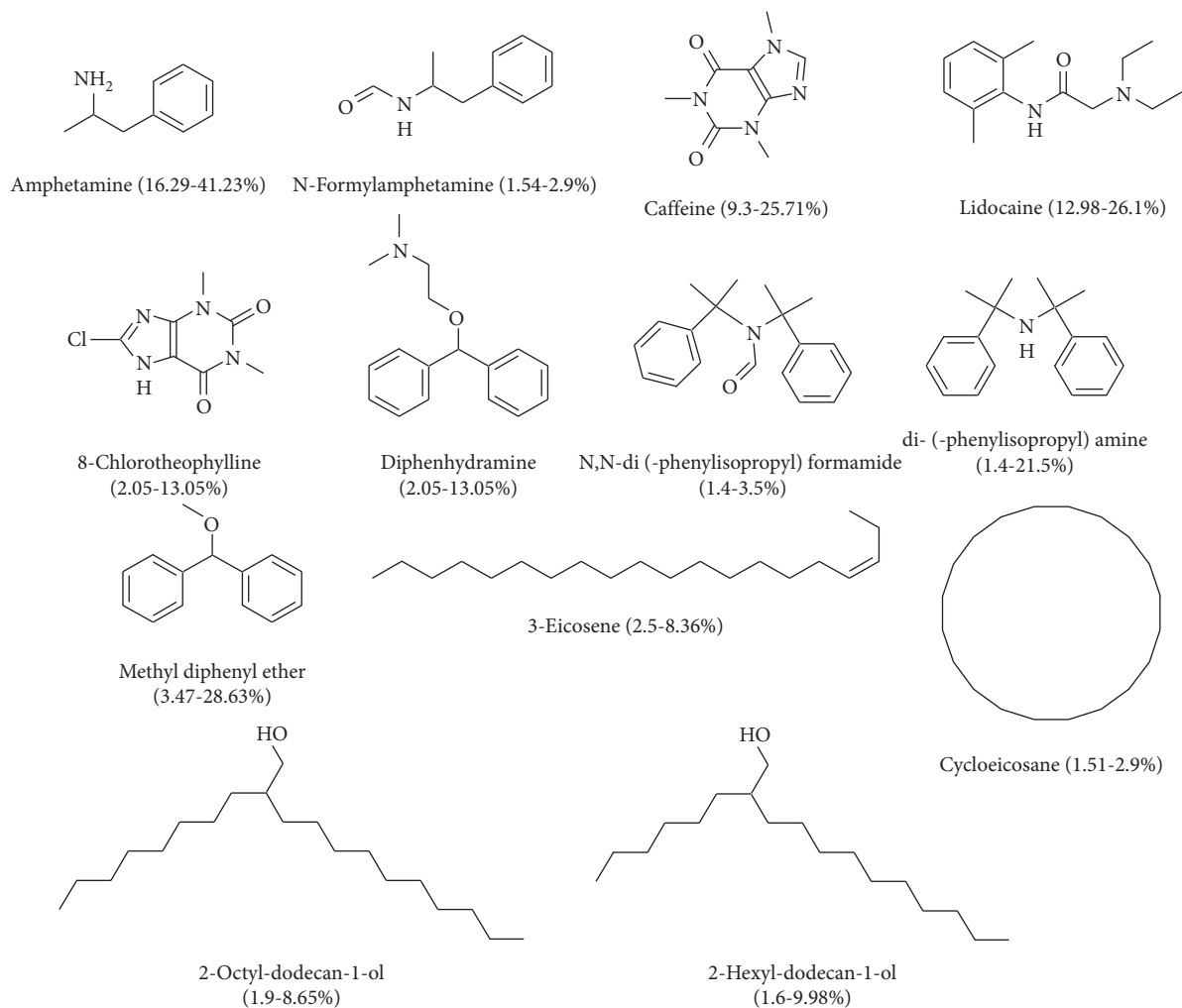
Figure 1: Structures of major constituents present in tablet samples showing their area % values.
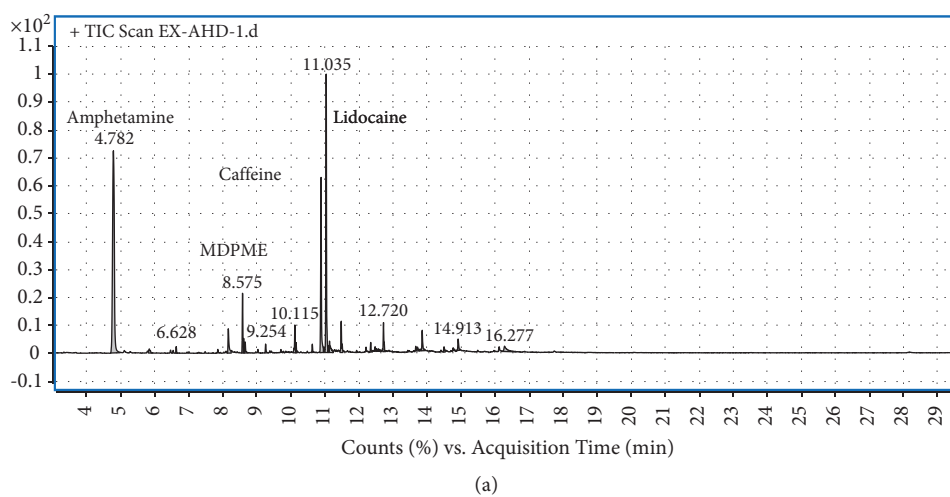
Figure 2: Continued.

(b)

(c)
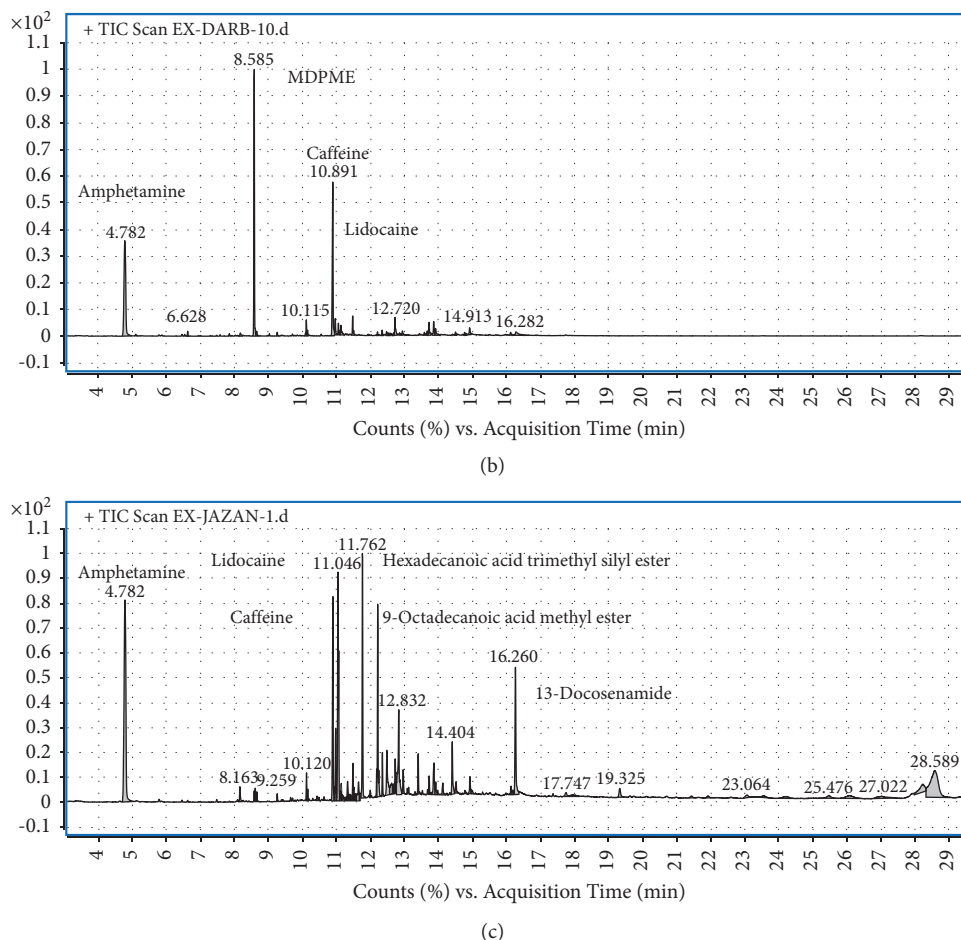
FIGURE 2: Total ion chromatograms (TIC) obtained for representative samples from each city. (a) TIC of A1, (b) TIC of D1, and (c) TIC of G1.

In a similar study, Alabdalla analyzed the counterfeit tablets of captagon seized from Jordan [17] using the GC-MS technique and detected amphetamine with several other additives including caffeine and quinine with the absence of fenethylline. Other seizures from Turkey [22] and Serbia [20] and subsequent analysis of tablets using GC-MS and FT-IR techniques revealed the presence of amphetamine along with other additives such as theophylline, caffeine, quinine, acetaminophen, ephedrine, lactose, diphenhydramine, and several other compounds, with absence of fenethylline. It suggested the similar trend of adding other compounds with amphetamine as in our study; most of the additives were the same and these additives are added to the amphetamine to enhance psychoactivity and, therefore, acceptability of the tablets.

The addition of diphenhydramine to the tablets was also important as diphenhydramine is a potent antihistaminic agent that is used therapeutically to treat allergic symptoms, common cold, and motion sickness. Additionally, it is also shown to have implications in neurotransmission affecting behavior including norepinephrine, dopamine, serotonin, opioid, and acetylcholine systems. It has also been investigated to have antianxiety, sedation, and antidepressant activities [28], which probably may have been the reason for its inclusion to the tablet. Finally, lidocaine was added for its

nerve blocking activity leading to prevention of cardiovascular system side effects of amphetamines such as ventricular tachycardia and bleeding.

3.3. *Hierarchical Cluster Analysis (HCA).* Hierarchical Cluster Analysis (HCA) is one of the most common multivariate chemometric analyses used to determine the correlation between the constituents of different samples. It is employed to determine the hierarchy of clusters which are presented graphically as dendrogram or a tree. Samples are divided into pairs and the distances between these pairs are measured. These distances are the representative of dissimilarities between the sets. The variables are attached with each other in a hierarchical fashion in the dendrograms and the closest samples are considered to be most similar; however, the farthest is the most different [29]. Samples categorized in one cluster have unique and similar characteristics or, in other words, they are least dissimilar with each other and are separated by lesser distances. At each step, the two clusters that were most similar were joined into a single new cluster and once they get fused, objects were never separated. The two axes of dendrograms are the distance or the dissimilarities as the horizontal axis, whereas the samples and clusters are placed on the vertical axis.

Dendrogram of Sample_no.
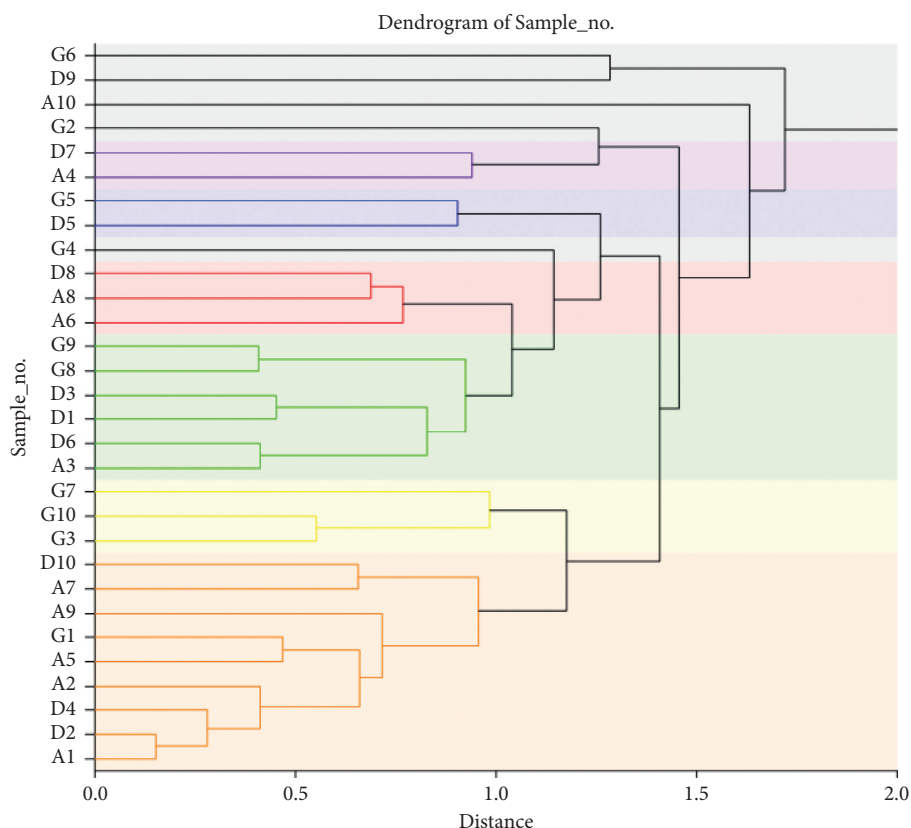
FIGURE 3: Dendrogram tree obtained for amphetamine tablet samples using average linkage (between groups) showing six clusters (colored lines) and distances between the samples.

When two clusters are fused, this is shown in the dendrogram, as the splitting of horizontal line to two horizontal lines and the horizontal position of the split signifies the dissimilarity (distance) between the two clusters.

All the 30 samples were classified into different clusters depending upon the constituents present in them which were considered as variables. Results are depicted as a dendrogram tree (Figure 3) which showed the presence of six distinct clusters of samples. If two samples were separated by a distance less than one, it was considered as significant and the lesser the distance was, the more was the similarity between the samples. The first cluster comprised three samples A6, A8, and D8, which showed similar characteristics as far as the constituents present in them are concerned. The second cluster consisted of two samples, D5 and G5, from Al-Darb and Jazan cities, respectively. The third cluster was having six samples, A3, D1, D3, D6, G8, and G9, consisting of samples from all three samples. The fourth cluster was again having two samples only, A4 and D7, from Ahad Al-Masariha and Al-Darb, respectively. The fifth cluster was the largest one having nine samples A1, A2, A5, A7, A9, D2, D4, D10, and G1 from all three cities. The sixth cluster comprised samples from Jazan city only showing presence of G3, G7, and G10 samples. The rest of all the samples G6, D9, A10, G2, and G4 were separated by distances more than 1.0 and were not significant, meaning that their characteristics are different from others and are linked to each other but not significantly.

Figure 3 shows dendrogram tree of the samples having all the samples connected to each other using colored lines. The black lines show distance more than 1 and hence, nonsignificant relations. Samples of fifth cluster showed most significant characteristics and are separated by orange lines and few samples are connected with a very short distance showing very close similarities between them. It was followed by samples from third cluster separated by green lines, sixth cluster separated by yellow lines, first cluster separated by red lines, second cluster separated by blue lines, and fourth cluster separated by violet line. Together they are connected at larger distances with nonsignificant black lines. The samples within the same cluster signify that they may have originated from the single source and together there may be six sources of samples tested in this study.

4. Conclusions

Using GC-MS technique, we were able to identify and quantify the constituents present in seized amphetamine tablets form three major cities of Jazan region, Saudi Arabia. A total of 30 samples were subjected to analysis using a simple and faster GC-MS method and all the constituents were separated at different retention times. All the tablet samples showed amphetamine as the major constituent present in the range of 16.29–41.23% of the total constituents. Interestingly, other psychoactive and nonpsychoactive additives were also identified including caffeine, lidocaine, diphenhydramine, and 8-chlorotheophylline,

which may have been added to enhance the effects of amphetamine and to increase the dependence. Several other organic compounds were also detected which altogether increase the toxicity of these tablets. Users as well as the government authorities should be informed and educated regarding the harmful constituents of these tablets which could help in stopping the illegal trafficking and use of these tablets on priority basis.

Data Availability

Data related to the study are available from the authors and can be produced upon request.

Conflicts of Interest

The authors declare that they have no conflicts of interest.

Acknowledgments

Supplementary Materials

Table 1S: GC-MS analyses of amphetamine tablets collected from different cities of Jazan province. Ten tablets of amphetamine were analyzed in triplicate from three different cities, Ahad Al-Masariha, Al-Darb, and Jazan. (*Supplementary Materials*)

References

[1] S. M. Stahl, "Amphetamine (D, L)," *Prescriber's Guide: Stahl's Essential Psychopharmacology*pp. 45–51, Cambridge University Press, Cambridge, UK, 6th edition, 2017.

[2] Evekeo Prescribing Information (EPI) (2016) Arbor Pharmaceuticals LLC, 2019, https://www.evekeo.com/assets/evekeo-pi.pdf/.

[3] European Monitoring Centre for Drugs and Drug Addiction, *Captagon: Understanding Today's Illicit Market, EMCDDA Papers*, Publications Office of the European Union, Luxembourg, Europe, 2018.

[4] M. Bassiony, "Substance use disorders in Saudi Arabia: review article," *Journal of Substance Use*, vol. 18, no. 6, pp. 450–466, 2013.

[5] N. Saquib, A. M. Rajab, J. Saquib, and A. AlMazrou, "Substance use disorders in Saudi Arabia: a scoping review," *Substance Abuse Treatment, Prevention, and Policy*, vol. 15, no. 41, p. 41, 2020.

[6] H. M. Al-Musa and S. D. S. Al-Montashri, "Substance abuse among male secondary school students in Abha city, Saudi Arabia: prevalence and associated factors," *Biomedical Research*, vol. 27, pp. 1364–1373, 2016.

[7] United Nations Office on Drugs and Crime (UNODC), *Global Synthetic Drugs Assessment, Amphetamine-type Stimulants and New Psychoactive Substances*, United Nations Office on Drugs and Crime, New York, NY, USA, 2014, https://www.unodc.org/documents/scientific/2014_Global_Synthetic_Drugs_Assessment_web.pdf.

[8] M. Al-Mazroua, "Analysis of captagon tablets in Saudi Arabia, presentation to the ministry of health of Saudi Arabia," 2019, https://www.moh.gov.sa/en/Sectors/PCCs/DMM/PCC_Information/Publications/Analysis%20of%20Captagon%20Tablets%20in%20Saudi%20Arabia.pdf.

[9] Drug Enforcement Administration (DEA), "Captagon mimic tablets (containing d,l-amphetamine, caffeine, theophylline, and other components) in Al Anbar Province, Iraq," *Microgram Bull*, vol. 42, no. 3, pp. 28-29, 2009.

[10] German Bundeskriminalamt (BKA), *Captagon, Presentation, BKA (Germany)*, pp. 18-19, EMPACT Synthetic Drugs Meeting, Prague, Czech Republic, 2016.

[11] H. A. Alhazmi, W. Ahsan, M. Al Bratty et al., "Analysis of amphetamine and methamphetamine contents in seized tablets from Jazan, Saudi Arabia by liquid chromatography-mass spectroscopy (LC-MS/MS) and chemometric techniques," *Saudi Pharmaceutical Journal*, vol. 28, no. 6, pp. 703–709, 2020.

[12] A. Khalid, H. A. Alhazmi, A. N. Abdalla et al., "GC-MS analysis and cytotoxicity evaluation of shammah (smokeless tobacco) samples of Jazan region of Saudi Arabia as promoter of cancer cell proliferation," *Journal of Chemistry*, vol. 2019, Article ID 3254836, 8 pages, 2019.

[13] H. A. Alhazmi, A. Khalid, S. Sultana et al., "Determination of phytocomponents of twenty-one varieties of smokeless tobacco using gas chromatography-mass spectroscopy (GC-MS)," *South African Journal of Chemistry*, vol. 72, no. 1, pp. 47–54, 2019.

[14] M. Al Bratty, W. Ahsan, H. A. Alhazmi, I. M. Attafi, I. A. Khardali, and S. I. Abdelwahab, "Determination of trace metal concentrations in different parts of the khat varieties (Catha edulis) using inductively coupled plasma-mass spectroscopy technique and their human exposure assessment," *Pharmacognosy Magazine*, vol. 15, pp. 449–458, 2019.

[15] H. Alhazmi, W. Ahsan, I. Attafi et al., "Elemental profiling of smokeless tobacco samples using inductively coupled plasma-mass spectrometry, their chemometric analysis and assessment of health hazards," *Pharmacognosy Magazine*, vol. 14, no. 58, pp. 587–596, 2018.

[16] Customs Laboratories European Network, "Recording of mass spectra of organic substances such as new psychoactive substances or designer drugs with a mass selective detector after gas-chromatographic separation, ILIADe code 403," 2021, https://ec.europa.eu/taxation_customs/sites/taxation/files/iliade_403_gcms_drugs.pdf.

[17] M. A. Alabdalla, "Chemical characterization of counterfeit captagon tablets seized in Jordan," *Forensic Science International*, vol. 152, pp. 185–8, Article ID 185, 2005.

[18] N. Al-Gharably and A. R. Al-Obaid, "The characterization of counterfeit captagon tablets," *Journal of the Forensic Science Society*, vol. 34, no. 3, pp. 165–167, 1993.

[19] D. Dimova and N. Dinkof, "Psychotropic substances of the amfetamine type used by drug addicts in Bulgaria. Synthesis and medical forms," *Analytical Methods of Identification, Scientific and Technical Notes, SCITEC/10*, United Nations Office on Drugs and Crime, Sofia, Bulgaria, 1994.

[20] M. Nevescanin, S. Banovic-Stevic, S. Petrovic, and V. Vajs, "Analysis of amphetamines illegally produced in Serbia," *Journal of the Serbian Chemical Society*, vol. 73, no. 7, pp. 691–701, 2008.

[21] United Nations Office on Drugs and Crime (UNODC), *World Drug Report 2009*, United Nations Office on Drugs and Crime, New York, NY, USA, 2009.

[22] Turkish Monitoring Centre for Drugs and Drug addiction (TUBIM), *National Report (2012 Data) to the EMCDDA by the Reitox National Focal Point*, Turkish Monitoring Centre for Drugs and Drug addiction, Ankara, Turkey, 2013.

[23] S. Demirkiran, C. Zeren, A. Çelikel, and M. M. Arslan, "The captagon tablets captured in Hatay between 2011-2012," *Turkish Journal of Forensic Medicine*, vol. 28, no. 1, pp. 17–23, 2014.

[24] European Academy of Forensic Science, "Istanbul Üniversitesi, & European Academy of Forensic Science," *Proceedings of the 3rd European Academy of Forensic Science Meeting*, Istanbul, Turkey, Elsevier, 2003.

[25] M. Carvalho, H. Carmo, V. M. Costa et al., "Toxicity of amphetamines: an update," *Archives of Toxicology*, vol. 86, no. 8, pp. 1167–1231, 2012.

[26] S. Berman, J. O'Neill, S. Fears, G. Bartzokis, and E. D. London, "Abuse of amphetamines and structural abnormalities in the brain," *Annals of the New York Academy of Sciences*, vol. 1141, no. 1, pp. 195–220, 2008.

[27] Drug enforcement administration (DEA) (2003) fenethylline and the middle east: a brief summary, DEA-03046.

[28] É. Lessard, M.-A. Yessine, B. A. Hamelin et al., "Diphenhydramine alters the disposition of venlafaxine through inhibition of CYP2D6 activity in humans," *Journal of Clinical Psychopharmacology*, vol. 21, no. 2, pp. 175–184, 2001.

[29] P. M. Mather, *Computational Methods of Multivariate Analysis in Physical Geography*, John Wiley & Sons, London, UK, 1976.

Research Article

Optimized Extraction Method for Kleeb Bua Daeng Formula with the Aid of the Experimental Design

Nittaya Ngamkhae,[1] **Orawan Monthakantirat,**[2] **Yaowared Chulikhit,**[2]
Chantana Boonyarat,[2] **Charinya Khamphukdee,**[2] **Juthamart Maneenat** ⓘ**,**[1]
Pakakrong Kwankhao,[3] **Supaporn Pitiporn,**[3] **and Supawadee Daodee** ⓘ[2]

[1]*Graduate School of Pharmaceutical Sciences, Khon Kaen University, Khon Kaen 40002, Thailand*
[2]*Division of Pharmaceutical Chemistry, Faculty of Pharmaceutical Sciences, Khon Kaen University, Khon Kaen 40002, Thailand*
[3]*Department of Pharmacy, Chao Phya Abhaibhubejhr Hospital, Ministry of Public Health, Tha Ngam,*
 Prachinburi 25000, Thailand

Correspondence should be addressed to Supawadee Daodee; csupawad@kku.ac.th

Kleeb Bua Daeng formula is one of the popular remedies sold in Chao Phya Abhaibhubejhr Hospital, Thailand. This formula contains *Piper nigrum* L., *Nelumbo nucifera* Gaertn., and *Centella asiatica* L. as active components. Owing to getting the highest content of its phytochemical compounds, the conditions of solvent extraction for this formula were optimized. The type of solvent, number of extraction times, and ratio between the material and solvent were varied in this study using the Box–Behnken design. The important phytochemical constituents (total phenolics, flavonoids, carotenoids, and anthocyanins) were also determined. From the result of this study, it was found that the highest content of each total active compound was obtained from different conditions such as the optimal extraction condition of phenolic content was obtained using methanol as solvent, one time of extraction, and the ratio of powder and solvent was 1 : 6. Thus, the variation of solvent extraction condition could affect the phytochemical content. Further studies about the herbal formula involving the extraction process should concern the variation of extraction conditions to get the highest content of the active compound.

1. Introduction

Kleeb Bua Daeng formula (KBD) is one of the Thai traditional herbal formula products by Chao Phya Abhaibhubejhr Hospital, Prachinburi Province, Thailand. Three main components are *Piper nigrum* L. fruit, *Nelumbo nucifera* Gaertn. petal, and *Centella asiatica* L. leaf. This product was claimed to help insomnia improvement and support memory. Black pepper (*Piper nigrum* L.) is a medicinal plant in family *Piperaceae*. Pharmacological activities of *Piper nigrum* fruit were reviewed such as anticancer, antidepressant, anti-inflammatory, analgesic, antioxidant, and antimicrobial [1–5]. The bioactive compounds such as polyphenols, piperine, and essential oils were also reported [1, 6]. *Nelumbo nucifera* Gaertn. (NN) is an aquatic plant in

family *Nelumbonaceae*. Various parts of this plant has been reported and used for the anti-inflammatory, antioxidant, neuroprotective, anticancer, and antibacterial activities [7–12]. The bioactive compounds found in the petal part were flavonoids (e.g., quercetin) and anthocyanins (e.g., cyanidin-3-O-glucoside) [13–17]. *Centella asiatica* L. (CA) also known as Kotu Gola is medicinal plant in family *Apiaceae* commonly used in the treatment of wound healing and as an anti-inflammatory, antioxidant, and neuroprotective agent [18–21]. The active constituents found in the aerial part are asiaticoside, polyphenols, flavonoids, and carotenoids [22, 23]. Many techniques can be used for the extraction of the active component in herbal remedy or herbal plant such as solvent extraction, ultrasound-assisted extraction, microwave-assisted extraction, and supercritical

fluid extraction. One of the important basic and versatile techniques used for a long time is the solvent extraction method. The principle of solvent extraction is to separate compounds based on their relative solubility in two immiscible solvents, usually one polar and one nonpolar. The advantages of this technique are that it is considered widely, simple, low cost, and requires uncomplicated utensil and equipment [24]. Many factors or variables for solvent extraction should be optimized in which the extraction is an important process for herbal product development to obtain high content of active phytochemical compounds. KBD formula, one of the popular products by Chao Phya Abhaibhubejhr Hospital, is the interesting product in the list of product development which needs to find a new formula from the extract.

Experimental design is one of the methods to study the various factors' or parameters' effect on the results of the study. The response surface methodology (RSM) is one of the effective statistical analysis techniques which comprises several statistical designs such as the Box–Behnken Design (BBD), Central Composite Design (CCD), Optimal Design, and other statistical procedures. Among these designs, the BBD-based statistical modeling represents a simplified design to cover three levels of experimental factors with a smaller number of experiments [25]. BBD was developed in 1960 by Box and Behnken. This design can be applied to use in the issues having three or more factors, and each has three levels [26]. BBD is easy to perform experiments and interpret in comparison to other models. RSM is an effective statistical tool optimizing complex processes and widely used for optimizing the extraction [27]. This method could evaluate the interactions among various factors, as well as simultaneously estimating the effects of several process variables and their interactions with response variables [28]. Optimization by the response surface design is one of the chemometric approaches which endorse the optimal condition of the method. From the study of Dhawan in 2018 [29], a definitive screening design and response surface methodology were used in order to maximize the extraction yield of an Indian coal by optimization of acid pretreatment conditions [29].

Thus, in this study, optimization of the variable factor for solvent extraction of KBD formula using the response surface methodology (RSM) with Box–Behnken design (BBD), which is an effective statistical method to find optimum processing parameters, was studied in order to maximize the extraction yield and total active contents. The best extraction condition in this study could give the highest active compound which could be used for the product development in the future.

2. Materials and Methods

2.1. Materials and Equipment.
Thai Traditional herbal formula used in this study is the KBD Formula, which contains 3 herbs: *Centella asiatica* L. leaf (voucher specimen ABH17), *Nelumbo nucifera* Gaertn. petal (voucher specimen ABH15), and *Piper nigrum* L. fruit (voucher specimen ABH18), and their voucher specimens were deposited at the Chao Phya Abhaibhubejhr Hospital Foundation Under the Royal Patronage of H.R.H. Princess Bejraratanarajsuda, Prachinburi Province, Thailand. Folin–Ciocalteu phenol reagent, β-carotene, sodium acetate, and quercetin were purchased from Sigma-Aldrich (Germany), ethanol, methanol, and ethyl acetate were purchased from VWR Chemicals BDH (France), and gallic acid, hexane, and hydrochloric acid were purchased from Merck (Germany). Sodium carbonate (Loba chemie, India), aluminum chloride (Ajax Finechem, Australia), potassium chloride (QRëC, New Zealand), acetone (RCI Labscan, Thailand), and ultrapure water were also used in this study. A rotary vacuum evaporator (Buchi, Germany), a freeze dryer (Labconco, USA), and an incubator microplate reader (PerkinElmer, Inc, USA) were used.

2.2. Experimental Design.
Seventeen laboratory experiments at three levels (−1, 0, +1) and three factors of BBD with RSM were used to evaluate the optimal conditions of the extraction process. The experimental design of this study was performed using Design-Expert software (Free Trial Version 12, Stat-Ease Inc., Minneapolis, USA). All experiments were performed in triplicate. The factors and their levels are shown in Table 1 . Parameters or factors for this study were the type of solvent, number of extraction times, and material-to-solvent ratio.

The type of solvent is one of the most important parameters for extraction study as an active compound could be dissolved in different types of solvent depending on its solubility which ultimately affects the percentage of extraction yield and total active content. Different types of solvent mean different polarities which effects the extraction yield and the active compound content dissolved in each solvent. The number of extraction times was the other parameter which was concerned to improve the efficiency of extraction as the aspect of countercurrent extraction. Another important parameter that was optimized was the material-to-solvent ratio. This parameter was kept from 1 : 3 to 1 : 9. Even though excessive solvent seems to get the high extraction yield, it becomes more economical. Based on the responses of the screening design, three-level continuous factors were developed.

The experimental design was determined using Design-Expert software (Free Trial Version 12, Stat-Ease Inc., USA).

2.3. Extraction Process.
Seventeen experimental sets were used to extract KBD powder material. The KBD powder (5 g) was taken in a 100 ml round-bottom flask and extracted along with each set of variable factors. After that, the extract solutions were filtered, evaporated with a rotary evaporator at 40°C, and freeze-dried for 24 hr. Percentage yield of crude extract was calculated for each set of experiment. The extracts were kept at −20°C prior to analysis.

2.4. Determination of Percentage Extraction Yield.
The percentage extraction yield of KBD Formula was calculated by the following equation:

TABLE 1: Box–Behnken design for the optimization of extraction conditions.

Factor	Symbol	Levels		
		−1	0	1
Type of solvent	A	Ethyl acetate	Ethanol	Methanol
Number of extraction times (times)	B	1	2	4
Material-to-solvent ratio (g/ml)	C	1 : 3	1 : 6	1 : 9

$$\text{Extraction yield}\,(\%) = \frac{W_c}{W_s}\,x100, \qquad (1)$$

where W_c is the mass of KBD crude extract and W_s is the mass of the sample.

2.5. Phytochemical Analysis.

Total phenolic content in KBD formula was determined using the Folin–Ciocalteu method as described by Singleton and Rossi in 1965 [30]. Briefly, $20\,\mu l$ of the extract solution (1 mg of extract dissolved in $1{,}000\,\mu l$ of ethanol) was added into $100\,\mu l$ of Folin–Ciocalteu reagent (10%) and $80\,\mu l$ of sodium carbonate (7%). After 30 minutes of incubation in the dark, the absorbance was measured at 760 nm by using a microplate reader. Total phenolic content was expressed as milligram gallic acid equivalents per gram of extract (mg GAE/g extract).

Total flavonoid content in the KBD Formula was determined using the aluminum chloride colorimetric method [31]. Briefly, $20\,\mu l$ of the extract solution was added to $15\,\mu l$ of aluminum chloride, $20\,\mu l$ of sodium acetate (10%), and $145\,\mu l$ distilled water. After 15 minutes of incubation in the dark, the absorbance was measured at 430 nm by using a microplate reader. Total flavonoid content was expressed as milligram quercetin equivalents per gram of extract (mg QE/g extract).

Total carotenoid content was also determined in the KBD Formula. Briefly, $100\,\mu l$ of the extract solution (pretreatment by extraction with ethanol, acetone, and hexane) was added into a 96-well plate, and the absorbance was measured at 450 nm by using a microplate reader [32]. Total carotenoid content was expressed as milligram β-carotene equivalents per gram of extract (mg β-carotene/g extract).

Total anthocyanin content in the KBD formula was determined using the pH differential method as described and modified from the work of Lee et al. [33]. Briefly, $20\,\mu l$ of extracts was diluted with $100\,\mu l$ of 0.025 M potassium chloride solution at pH 1. Similarly, the extracts were diluted with $100\,\mu l$ of 0.4 M sodium acetate at pH 4.5. The absorbance of these solutions was measured at 535 and 700 nm by using a microplate reader. Total anthocyanin content was expressed as milligram cyanidin-3-glucoside equivalents per gram of extract (mg C3G/g extract).

3. Results and Discussion

3.1. Fitting the Model.

BBD with the response surface method (RSM) was used to optimize solvent extraction factors. The results from analysis of variance (ANOVA) are shown in Table 2. The analysis of variance method was used to analyze the results in order to obtain an adequate elution model. The coefficient of determination (R^2) showed a good relationship for all variable factors (Figure 1). This figure also represented the observed response values compared with that of the predicted values depicting a good fit. The model showed high F-value which implied this model was significant and P value was less than 0.05 indicating the model term was also significant. R^2 and adjusted R^2 values were higher than 0.75 for extraction yield, TPC, TFC, TCC, and TAC, respectively. Generally, higher R^2 could better predict the results from the equation and R^2 should have at least 0.75 [34, 35]. The effect from all variable factors (type of solvent, number of extraction times, and ratio between material and solvent) on the response results was described as a quadratic model in which there was the corelationship between each factor. Comparative results between the predicted value and experimental value which verified the good strength of model fitting are shown in Table 3.

3.2. Effect of Extraction Factors on Percentage Extraction Yield.

Before using the data to integrate for the relationship of factors, we had to conduct model adequate checking by three categories which were an independence test, normality test, and variance stability test, as shown in Figure 2. From the figure, it can be seen that the experimental data were accurate and suitable to be used for the analysis of coefficient of determination and the analysis of variance.

The appropriate quadratic model for extraction yield showed a significant linear and quadratic effect shown by the following equation:

$$Y = +6.36 + 4.65A + 1.38B + 1.72C + 1.53AB + 1.49AC$$
$$- 0.33BC + 2.16A^2 - 0.78B^2 - 0.56C^2, \qquad (2)$$

where Y is the percentage extraction yield (%), A is the type of solvent, B is the number of extraction times, C is the material-to-solvent ratio, A, B, and C are linear terms of factors; AB, AC, and BC are interaction terms of factors; and A^2, B^2, and C^2 are quadratic terms of factors. Most of the terms had a significant effect on response with P value less than 0.05 (percentage extraction yield) except BC and C^2. From the high values of R^2 and adjusted R^2 (Table 2), it could be concluded that the suggested models fit the obtained experimental data adequately. Large F-value of this model implied the model was significant.

The result showed the extraction yield was found between 2.15–16.14%. The response surface method was used to explain the relationship between these three variable factors. The interaction effect between the type of solvent and number of extraction times (AB) and the interaction

TABLE 2: The results from response surface model of percentage extraction yield, TPC, TFC, TCC, and TAC by analysis of variance (ANOVA).

Response	Model	F-value	P value	R^2	Adjusted R^2
Percentage extraction yield	Quadratic	92.87	<0.0001*	0.9917	0.9810
Total phenolic content	Quadratic	30.14	<0.0001*	0.9748	0.9425
Total flavonoid content	Quadratic	20.18	0.0003*	0.9629	0.9152
Total carotenoid content	Quadratic	6.22	0.0124*	0.8889	0.7460
Total anthocyanin content	Quadratic	144.87	<0.0001*	0.9947	0.9878

Level of significance: *significant at $P < 0.05$.
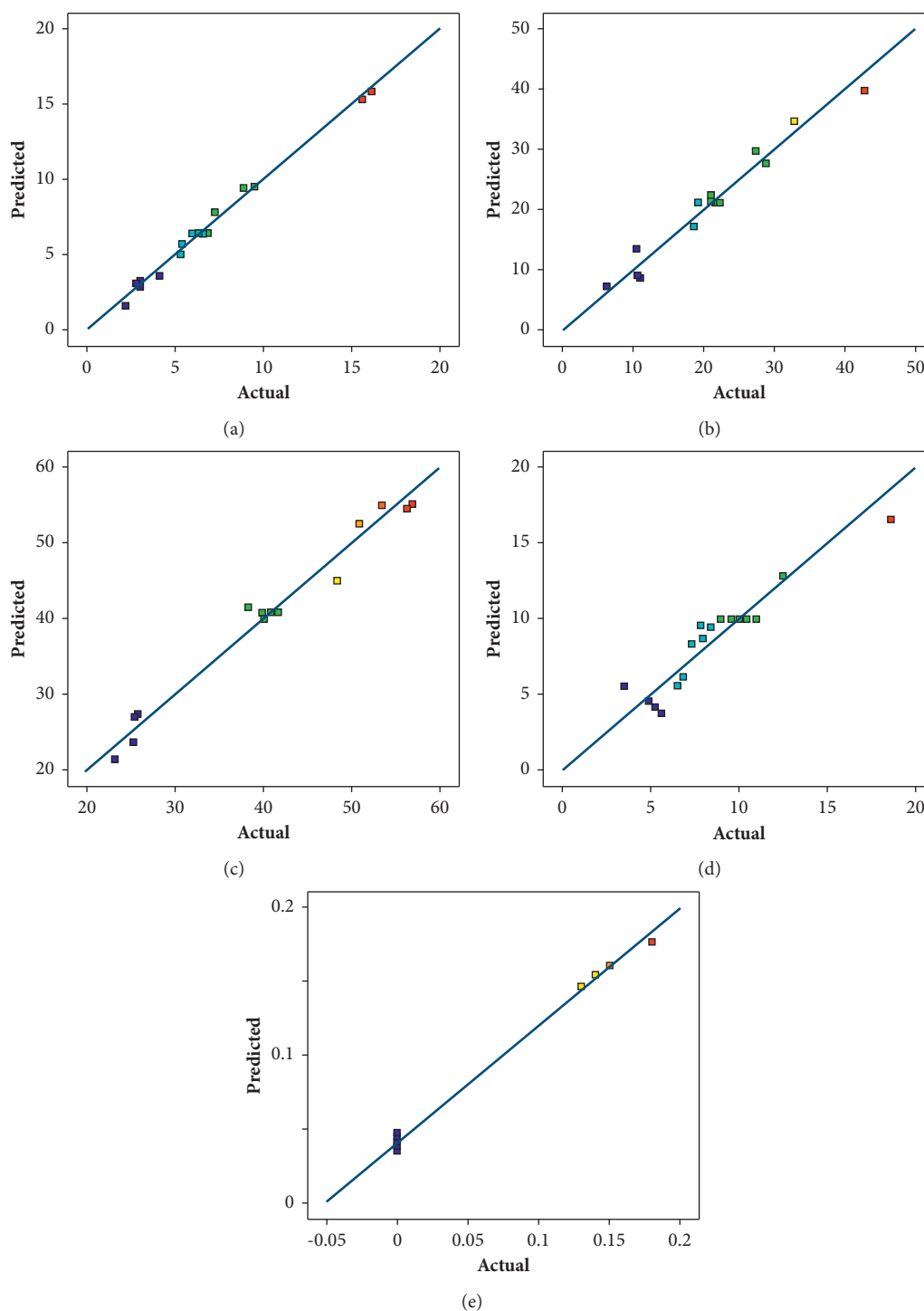
FIGURE 1: Plot of the relationship between the predicted value from the model and the observed or experimental value from the experiment in each response (I = percentage extraction yield, II = total flavonoid content, III = total phenolic content, IV = total carotenoid content, and V = total anthocyanin content).

TABLE 3: Box–Behnken design matrix for percentage extraction yield, TPC, TFC, TCC, and TAC from Kleeb Bua Daeng formula by the solvent extraction method.

Run order	Extraction variables			Response										
	A^* (solvent)	B^{**} (number of extraction times)	C^{***} (material-to-solvent ratio)	Percentage extraction yield (%)		TPC (mg GAE/g extract)		TFC (mg QE/g extract)		TCC (mg β-carotene/g extract)		TAC (mg cyanidin-3-glucoside/g extract)	
				Experimental	Predicted	Experimental	Predicted	Experimental	Predicted	Experimental	Predicted	Experimental	Predicted
1	−1	0	−1	2.77	3.08	25.26	23.68	28.77	27.76	8.43	9.47	0.00	0.00
2	0	0	0	6.84	6.36	41.89	40.86	19.21	21.20	8.97	10.00	0.00	0.00
3	0	1	1	7.24	7.80	48.39	45.11	21.00	21.63	6.57	5.57	0.00	0.00
4	0	1	−1	5.31	5.01	40.09	40.01	18.59	17.23	5.56	3.83	0.00	0.01
5	0	−1	1	5.39	5.69	40.13	40.21	20.99	22.35	7.84	9.57	0.00	−0.01
6	0	0	0	6.00	6.36	39.87	40.86	22.23	21.20	9.56	10.00	0.00	0.00
7	0	−1	−1	2.15	1.59	38.28	41.56	21.62	20.99	7.32	8.32	0.00	0.00
8	−1	1	0	2.95	2.94	25.73	27.39	27.36	29.73	7.99	8.68	0.00	0.00
9	1	1	0	15.57	15.31	50.93	52.63	10.63	8.99	3.52	5.56	0.18	0.17
10	1	−1	0	9.48	9.49	56.90	55.24	10.99	8.62	6.83	6.14	0.13	0.13
11	1	0	−1	8.86	9.42	56.29	54.67	10.52	13.52	4.89	4.58	0.15	0.15
12	1	0	1	16.14	15.83	53.51	55.09	6.26	7.27	5.23	4.19	0.14	0.14
13	−1	−1	0	2.98	3.24	23.14	21.44	32.96	34.60	18.64	16.60	0.00	0.01
14	0	0	0	6.41	6.36	39.94	40.86	21.67	21.20	10.06	10.00	0.00	0.00
15	0	0	0	6.29	6.36	40.99	40.86	21.03	21.20	10.97	10.00	0.00	0.00
16	0	0	0	6.28	6.36	41.59	40.86	21.88	21.20	10.44	10.00	0.00	0.00
17	−1	0	1	4.11	3.55	25.41	27.03	42.76	39.76	12.55	12.86	0.00	0.00

*Type of solvent: (−1) ethyl acetate, (0) ethanol, (1) methanol, ** number of extraction times (times): (−1) 1, (0) 2, (1) 4, *** material/solvent ratio (g/ml): (−1) 1 : 3, (0) 1 : 6, (1) 1 : 9.
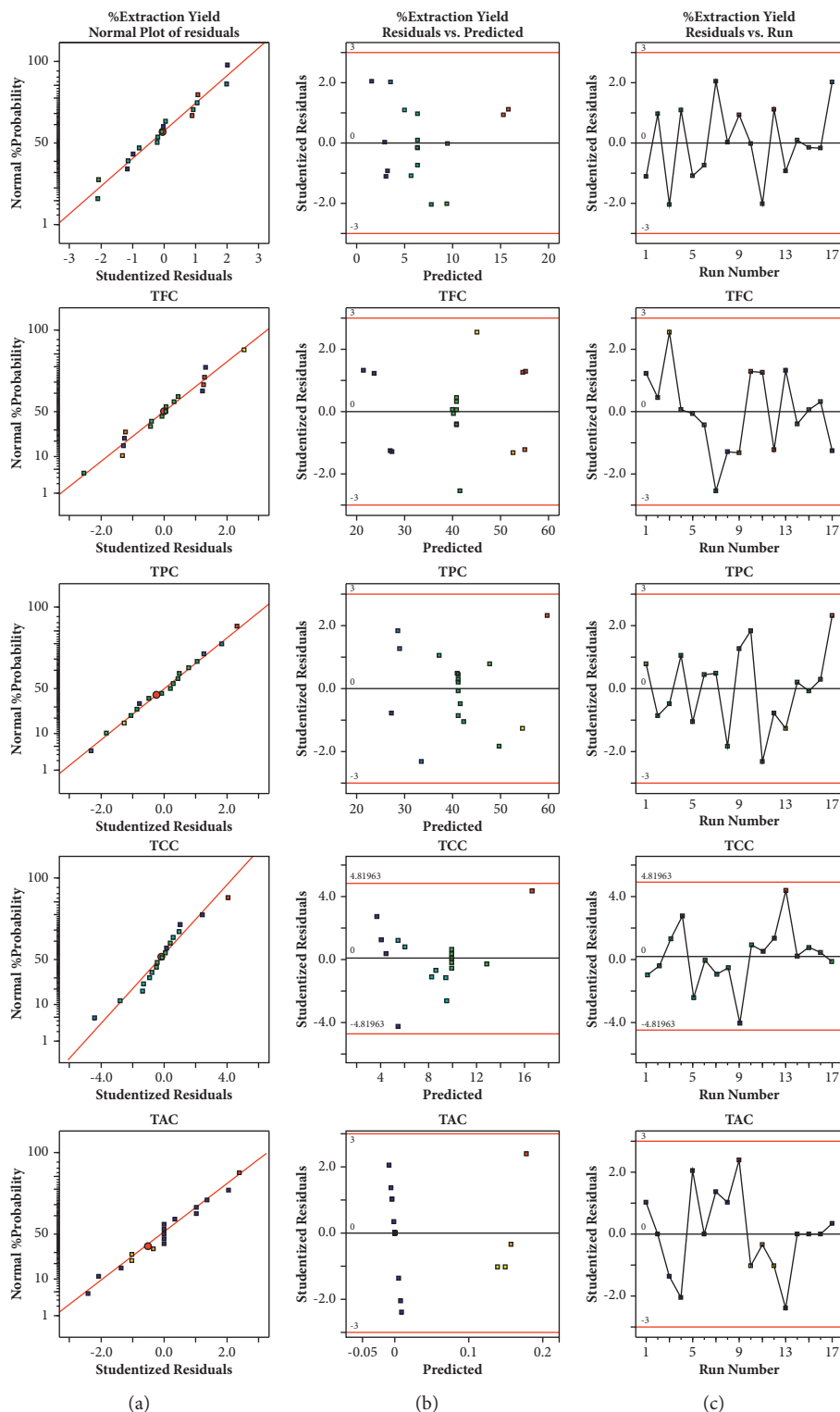
FIGURE 2: Diagnostic plot for model adequate checking of percentage extraction yield (%), TPC, TFC, TCC, and TAC: (a) normal % probability against internally studentized residuals, (b) internally studentized residuals against predicted, and (c) internally studentized residuals against run number.

effect between type of solvent and material-to-solvent ratio (AC) on the extraction yield were demonstrated and showed significance at $P < 0.05$ but not for the interaction effect between the number of extraction times and material-to-solvent ratio (BC). Thus, the response (percentage extraction yield) was not affected by the interaction between the number of extraction times and material-to-solvent ratio.

The results of this study also showed the highest the extraction yield (16.14%) of the 12th run on the condition (methanol, 2 times the number of extraction times, and 1 : 9 g/ml of material-to-solvent ratio) presented in Table 3. The type of solvent showed the most enhancing effect to the extraction yield. The extraction yield increased with the increase in the polarity of solvent used. The solubility of some substances in methanol might be higher than in ethanol and ethyl acetate [36]. Increasing material-to-solvent ratio gave higher diffusion coefficient [37]. The number of extraction times affected the efficiency of extraction which might be explained as the principle of countercurrent extraction [38]. Even though the highest extraction yield was performed by methanol as a solvent, the better use for preparing the extract as the herbal product composition should provide the lowest toxicity. Thus, ethanol is the most effective and appropriate solvent for using in this herbal product formulation even though it may not show the highest efficiency for some phytochemical compounds such as anthocyanins.

3.3. Effect of Extraction Factors on Total Phenolic Content (TPC).
The quadratic model for total phenolic content showed a significant linear and quadratic effect. The second-order polynomial equation (3) is

$$Y = +40.86 + 14.76A + 0.84B + 0.94C - 2.14AB - 0.73AC$$
$$+ 1.61BC - 1.64A^2 - 0.038B^2 + 0.90C^2,$$
$$(3)$$

where Y is the total phenolic content and the other terms (A, B, C, AB, AC, BC, A^2, B^2, and C^2) were also described above. The results of the statistical significance of every regression coefficient are presented in Table 2. The model P value of <0.05 for total phenolic content was revealed. In a similar manner, model adequate checking of total phenolic content was also performed as shown in Figures 2(a)–2(c).

Total phenolic content was found between 23.14–56.90 mg GAE/g extract. The results from the response surface method demonstrated no interaction effect between the type of solvent and number of extraction times (AB), type of solvent and material-to-solvent ratio (AC), and number of extraction times and material-to-solvent ratio (BC) on the total phenolic content which were not significant at $P > 0.05$. Thus, these results indicated no interaction effect between these factors to the response (total phenolic content).

The results of this study showed the highest total phenolic content (56.90 mg GAE/g extract) at the 10th run on the condition (methanol, 1 time the number of extraction times, and 1 : 6 g/ml of material-to-solvent ratio) presented in Table 3. The type of solvent enhanced and performed the most effect to the amount total phenolic content. The total phenolic content was higher in polar solvents. In this study, the total phenolic content depends on the type of solvent used, polarity index, and the solubility. The solubility of polyphenols depends on the hydroxyl groups, molecular size, and length of the hydrocarbon [39], as increasing material-to-solvent ratio gave higher diffusion coefficient [37]. Moreover, the number of extraction times was increasing affecting the total phenolic content.

3.4. Effect of Extraction Factors on Total Flavonoid Content (TFC).
The quadratic model for total flavonoids content showed significant linear and quadratic effect. The second-order polynomial equation (4) is

$$Y = +21.20 - 11.68A - 1.12B + 1.44C + 1.31AB - 4.56AC$$
$$+ 0.76BC + 0.40A^2 - 1.12B^2 + 0.47C^2,$$
$$(4)$$

where Y is the total flavonoid content and the other terms were described above. The results of the statistical significance of every regression coefficient are presented in Table 2. The model showed P value of <0.05 for total flavonoids content which revealed the influencing effect of all variable factors on total flavonoid content. Figures 2(a)–2(c) show the data normality and model adequate checking.

Total flavonoid content was found between 6.26–42.76 mg QE/g extract and demonstrated the interaction effect between each factor. Only a significant interaction effect between the type of solvent and material-to-solvent ratio (AC) was observed with P value <0.05 while the others (BC and AB) were not. Moreover, the type of solvent showed the most effective factor to the flavonoid content as shown by the highest coefficient of this factor from the fitting equation (equation (4)).

The results of this study showed the highest the total flavonoid content (42.76 mg QE/g extract) of the 17th run on the condition (ethyl acetate, 2 times the number of extraction times, and 1 : 9 g/ml of material-to-solvent ratio) presented in Table 3. The type of solvent enhances the amount of total flavonoid content which means the medium polarity of solvent is likely to dissolve the flavonoid compound from this sample. Polar solvents are used to obtain flavonoid glycosides, whereas nonpolar solvents extracted mostly their aglycones. Flavonoids have a diversity of chemical structures constituted of 15 carbon atoms in their basic skeletons with a C6–C3–C6. The chemical structure diversity of flavonoids is particularly obtained from glycosylation, methoxylation, prenylation, and hydroxylation that usually took place with some specific positions [40]. This result showed the flavonoid content in this sample could be extracted by ethyl acetate, ethanol, and methanol because of the mix type of flavonoid in our sample, and the results would be different for the other types of herbal sample. Among the examples of solvents for the extraction of herbal tea from *Viscum album* L., ethanol, methanol, and acetone were among the best solvents for extracting flavonoids from this tea. As increasing material-to-solvent ratio gave higher diffusion coefficient [37], higher volume of solvent can better improve the penetration into the material particle. The number of extraction times was increasing affecting the total flavonoid content.

3.5. Effect of Extraction Factors on Total Carotenoid Content (TCC). The quadratic model for total carotenoid content showed a significant linear and quadratic effect. The second-order polynomial equation (5) is

$$Y = +10.00 - 3.39A - 2.12B + 0.75C + 1.83AB - 0.95AC$$
$$+ 0.12BC + 0.099A^2 - 0.85B^2 - 2.32C^2, \tag{5}$$

where Y is the total carotenoid content and the other terms were described above. The results of statistical significance of every regression coefficient are presented in Table 2. The model showed a P value of 0.0124 for this response which showed a significant effect. Normal percentage of probability against internally studentized residuals, internally studentized residuals against predicted, and internally studentized residuals against run number of total carotenoid content was used to check the distribution of residuals, as shown in Figures 2(a)–2(c).

Total carotenoid content was found between 3.52–18.64 mg β-carotene/g extract. No interaction effect between these factors (AB, AC, and BC) was found. However, the type of solvent and number of extraction times (AB) showed the highest effect as performed by the highest coefficient of this term in equation (5).

The results of this study showed the highest total carotenoid content (18.64 mg β-carotene/g extract) of the 13th run on the condition (ethyl acetate, 1 times the number of extraction times, and 1 : 6 g/ml of material-to-solvent ratio) presented in Table 3. The type of solvent enhances the amount of total carotenoid content. The total carotenoid content was higher in ethyl acetate. In general, the nonpolar solvent seems to enhance the solubility of the nonpolar carotenoids (beta-carotene) [41]. Increasing material-to-solvent ratio gave higher diffusion coefficient [37], hence increasing the carotenoid content. The number of extraction times was also increasing the total carotenoid content.

3.6. Effect of Extraction Factors on Total Anthocyanin Content (TAC). The quadratic model for total anthocyanin content showed a significant linear and quadratic effect. The second-order polynomial equation (6) is

$$Y = 0.075A + 0.0063B - 0.0012C + 0.012AB - 0.0025AC$$
$$+ 0.0.075A^2 + 0.0025B^2 - 0.0025C^2, \tag{6}$$

where Y is the total anthocyanin content and the other factors were the terms as described above. The results of the statistical significance of every regression coefficient are presented in Table 2. In the same manner as the other factors, the model showed a P value of <0.0001 for total anthocyanin content which expressed the effect of all factors on anthocyanin content. The normality of data was also checked as shown in Figures 2(a)–2(c).

Total anthocyanin content was found between 0.00–0.18 mg cyanidin-3-glucoside/g extract) and demonstrated the interaction effect between the type of solvent and number of extraction times (AB) which was significant at $P < 0.05$ which revealed the interaction effect between these two factors on response.

The results of this study showed the highest total anthocyanin content (0.18 mg cyanidin-3-glucoside/g extract) of the 9th run on the condition (methanol, 4 times the number of extraction times, and 1 : 6 g/ml of material-to-solvent ratio) presented in Table 3. The type of solvent enhances the amount of total anthocyanin content. The total anthocyanin content was higher in polar solvents. In general, anthocyanins occur naturally as glycosides, so polar solvents are essential for good extraction [42]. Similarly, increasing material-to-solvent ratio and number of extraction times was also increasing the effect on the total anthocyanin content.

4. Conclusions

From our study, the optimal extraction for KBD formula was developed. Many responses as percentage yield and total active content were chosen. The selected variable factors (type of solvent, number of extraction times, and ratio of material to solvent) affected to these responses as from RSM analysis results. A screening of factors based on RSM-BBD analysis revealed the optimal conditions which led to the high level of responses. However, the selection of the optimal condition for each active content to product development should depend on the purpose and use of that formulation. Different types of active compound would express different biological activities. Thus, product development should concern the biological effect and justify the extraction condition to fit the purpose. These results gave the important data to develop a new formula KBD with high percentage yield and the selected active contents. Further study about the optimized extraction method such as ultrasound-assisted extraction or supercritical fluid extraction should be performed to get the better yield of active compound and lead to use the newer technique for saving the time of extraction and less organic solvent as the green extraction technique. Moreover, improving the variable factors from the study for the basic solvent extraction technique might be necessary to get the better suitable variable factors such as changing the type of organic solvent (ethyl acetate, methanol, and ethanol) to the ratio of ethanol and water for the extraction.

Data Availability

The main part of the data is included within the content. Other data can be obtained from the corresponding author upon request.

Conflicts of Interest

The authors declare no conflicts of interest regarding the publication of this paper.

Acknowledgments

References

[1] A. Ahmad, A. Husain, M. Mujeeb, S. A. Khan, H. A. A. Alhadrami, and A. Bhandari, "Quantification of total phenol, flavonoid content and pharmacognostical evaluation including HPTLC fingerprinting for the standardization of *Piper nigrum* L fruits," *Asian Pacific Journal of Tropical Biomedicine*, vol. 5, no. 2, pp. 101–107, 2015.

[2] Y. Deng, S. Sriwiriyajan, A. Tedasen, P. Hiransai, and P. Graidist, "Anti-cancer effects of *Piper nigrum* via inducing multiple molecular signaling in vivo and in vitro," *Journal of Ethnopharmacology*, vol. 188, pp. 87–95, 2016.

[3] L. Hritcu, J. A. Noumedem, O. Cioanca, M. Hancianu, P. Postu, and M. Mihasan, "Anxiolytic and antidepressant profile of the methanolic extract of *Piper nigrum* fruits in beta-amyloid (1–42) rat model of Alzheimer's disease," *Behavioral and Brain Functions: BBF*, vol. 11, no. 1, p. 13, 2015.

[4] Z. Zarai, E. Boujelbene, N. Ben Salem, Y. Gargouri, and A. Sayari, "Antioxidant and antimicrobial activities of various solvent extracts, piperine and piperic acid from *Piper nigrum*," *Lebensmittel-Wissenschaft und-Technologie-Food Science and Technology*, vol. 50, no. 2, pp. 634–641, 2013.

[5] F. Tasleem, I. Azhar, S. N. Ali, S. Perveen, and Z. A. Mahmood, "Analgesic and anti-inflammatory activities of *Piper nigrum* L," *Asian Pacific Journal of Tropical Medicine*, vol. 7, no. S1, pp. S461–S468, 2014.

[6] F. Zhu, R. Mojel, and G. Li, "Physicochemical properties of black pepper (*Piper nigrum*) starch," *Carbohydrate Polymers*, vol. 181, pp. 986–993, 2018.

[7] S. H. Liu, T. H. Lu, C. C. Su et al., "Lotus leaf (*Nelumbo nucifera*) and its active constituents prevent inflammatory responses in macrophages via JNK/NF-κB signaling pathway," *American Journal of Chinese Medicine*, vol. 42, no. 4, pp. 869–889, 2014.

[8] D.-J. Shin, J. Choe, K.-E. Hwang, C.-J. Kim, and C. Jo, "Antioxidant effects of lotus (*Nelumbo nucifera*) root and leaf extracts and their application on pork patties as inhibitors of lipid oxidation, alone and in combination," *International Journal of Food Properties*, vol. 22, no. 1, pp. 383–394, 2019.

[9] E. S. Kim, J. B. Weon, B. R. Yun et al., "Cognitive enhancing and neuroprotective effect of the embryo of the *Nelumbo nucifera* seed," *Evidence-Based Complementary & Alternative Medicines*, vol. 2014, Article ID 869831, 9 pages, 2014.

[10] T. Prabsattroo, J. Wattanathorn, P. Somsapt, and O. Sritragool, "Positive modulation of pink *Nelumbo nucifera* flowers on memory impairment, brain damage, and biochemical profiles in restraint rats," *Oxidative Medicine & Cellular Longivity*, vol. 2016, Article ID 5789857, 11 pages, 2016.

[11] X. Zhao, X. Feng, C. Wang, D. Peng, K. Zhu, and J.-L. Song, "Anticancer activity of *Nelumbo nucifera* stamen extract in human colon cancer HCT-116 cells in vitro," *Oncology Letters*, vol. 13, no. 3, pp. 1470–1478, 2016.

[12] D. Brindha and D. Arthi, "Antimicrobial activity of white and pink *Nelumbo nucifera* gaertn flowers," *Asian Journal of Pharmaceutical Research and Health Care*, vol. 2, pp. 147–155, 2010.

[13] S. Chen, L. Fang, H. Xi et al., "Simultaneous qualitative assessment and quantitative analysis of flavonoids in various tissues of lotus (*Nelumbo nucifera*) using high performance liquid chromatography coupled with triple quad mass spectrometry," *Analytica Chimica Acta*, vol. 724, pp. 127–135, 2012.

[14] S. Chen, Y. Xiang, J. Deng, Y. Liu, and S. Li, "Simultaneous analysis of anthocyanin and non-anthocyanin flavonoid in various tissues of different lotus (*Nelumbo*) cultivars by HPLC-DAD-ESI-MS (n)," *PLoS One*, vol. 8, no. 4, Article ID e62291, 2013.

[15] J. Deng, S. Chen, X. Yin et al., "Systematic qualitative and quantitative assessment of anthocyanins, flavones and flavonols in the petals of 108 lotus (*Nelumbo nucifera*) cultivars," *Food Chemistry*, vol. 139, no. 1–4, pp. 307–312, 2013.

[16] S. S. Li, J. Wu, L. G. Chen et al., "Biogenesis of C-glycosyl flavones and profiling of flavonoid glycosides in Lotus (*Nelumbo nucifera*)," *PLoS One*, vol. 9, no. 10, Article ID e108860, 2014.

[17] R.-Z. Yang, X.-L. Wei, F.-F. Gao et al., "Simultaneous analysis of anthocyanins and flavonols in petals of lotus (*Nelumbo*) cultivars by high-performance liquid chromatography-photodiode array detection/electrospray ionization mass spectrometry," *Journal of Chromatography A*, vol. 1216, no. 1, pp. 106–112, 2009.

[18] H. A. Azis, M. Taher, A. S. Ahmed et al., "In vitro and In vivo wound healing studies of methanolic fraction of *Centella asiatica* extract," *South African Journal of Botany*, vol. 108, pp. 163–174, 2017.

[19] J. H. Park, J. Y. Choi, D. J. Son et al., "Anti-inflammatory effect of titrated extract of *Centella asiatica* in phthalic anhydride-induced allergic dermatitis animal model," *International Journal of Molecular Sciences*, vol. 18, no. 4, pp. 1–14, 2017.

[20] A. Kumar, S. Dogra, and A. Prakash, "Neuroprotective effects of *Centella asiatica* against intracerebroventricular colchicine-induced cognitive impairment and oxidative stress," *International Journal of Alzheimer's Disease*, vol. 2009, Article ID 972178, 2009.

[21] F. Pittella, R. Dutra, D. Junior, M. T. Lopes, and N. Barbosa, "Antioxidant and cytotoxic activities of *Centella asiatica* (L) urb," *International Journal of Molecular Sciences*, vol. 10, no. 9, pp. 3713–3721, 2009.

[22] B. Brinkhaus, M. Lindner, D. Schuppan, and E. G. Hahn, "Chemical, pharmacological and clinical profile of the East Asian medical plant *Centella aslatica*," *Phytomedicine*, vol. 7, no. 5, pp. 427–448, 2000.

[23] K. D. P. P. Gunathilake, K. K. D. S. Ranaweera, and H. P. V. Rupasinghe, "Response surface optimization for recovery of polyphenols and carotenoids from leaves of *Centella asiatica* using an ethanol-based solvent system," *Food Sciences and Nutrition*, vol. 7, no. 2, pp. 528–536, 2019.

[24] N. N. Azwanida, "A review on the extraction methods use in medicinal plants, principle, strength and limitation," *Medicinal & Aromatic Plants*, vol. 4, no. 3, pp. 196–201, 2015.

[25] Q. Zhao, J. F. Kennedy, X. Wang et al., "Optimization of ultrasonic circulating extraction of polysaccharides from Asparagus officinalis using response surface methodology," *International Journal of Biological Macromolecules*, vol. 49, no. 2, pp. 181–187, 2011.

[26] G. E. Box and D. W. Behnken, "Some new three level designs for the study of quantitative variables," *Technometrics*, vol. 2, no. 4, pp. 455–475, 1960.

[27] A. Pandey, T. Belwal, K. C. Sekar, I. D. Bhatt, and R. S. Rawal, "Optimization of ultrasonic-assisted extraction (UAE) of phenolics and antioxidant compounds from rhizomes of *Rheum moorcroftianum* using response surface methodology (RSM)," *Industrial Crops and Products*, vol. 119, pp. 218–225, 2018.

[28] J. Prakash Maran, S. Manikandan, K. Thirugnanasambandham, C. Vigna Nivetha, and R. Dinesh, "Box-behnken design based

statistical modeling for ultrasound-assisted extraction of corn silk polysaccharide," *Carbohydrate Polymers*, vol. 92, no. 1, pp. 604–611, 2013.

[29] H. Dhawan, S. Upadhyayula, and D. K. Sharma, "Design of experiments to optimize the extraction parameters of a power grade Indian coal," *International Journal of Coal Science & Technology*, vol. 5, no. 4, pp. 417–429, 2018.

[30] V. L. Singleton and J. A. Rossi, "Colorimetry of total phenolics with phosphomolybdic-phosphotungstic acid reagents," *American Journal of Enology and Viticulture*, vol. 16, pp. 144–158, 1965.

[31] C. Chang, M. Yang, H. Wen, and J. Chern, "Estimation of total flavonoid content in propolis by two complementary colorimetric methods," *Journal of Food and Drug Analysis*, vol. 10, pp. 178–182, 2002.

[32] M. A. Ashraf, M. J. Maah, and I. Yusoff, "Estimation of antioxidant phytochemicals in four different varieties of durian (*Durio zibethinus* murray) fruit," *Middle-East Journal of Scientific Research*, vol. 6, pp. 465–471, 2010.

[33] J. Lee, R. W. Durst, and R. E. Wrolstad, "Determination of total monomeric anthocyanin pigment content of fruit juices, beverages, natural colorants, and wines by the pH differential method: collaborative study," *Journal of AOAC International*, vol. 88, no. 5, pp. 1269–1278, 2005.

[34] P. D. Haaland, *Biotechnology Experimental Design*, Marcel Dekker, Inc., Newyork, NY, USA, 1989.

[35] R. Hu, *Food Product Design: A Computer-Aided Statistical Approach*, Technomic Publishing Co., Ltd, Lancaster, PA, USA, 1999.

[36] Q. D. Do, A. E. Angkawijaya, P. L. Huynh, F. E. Soetaredjo, S. Ismadji, and Y.-H. Ju, "Effect of extraction solvent on total phenol content, total flavonoid content, and antioxidant activity of Limnophila aromatica," *Journal of Food and Drug Analysis*, vol. 22, no. 3, pp. 296–302, 2014.

[37] T. Belwal, P. Dhyani, I. D. Bhatt, R. S. Rawal, and V. Pande, "Optimization extraction conditions for improving phenolic content and antioxidant activity in *Berberis asiatica* fruits using response surface methodology (RSM)," *Food Chemistry*, vol. 207, pp. 115–124, 2016.

[38] S. Hartland, *Counter-Current Extraction-An Introduction to the Design and Operation of Counter-current Extractors*, Perkamon Press Ltd, London, UK, 1970.

[39] R. Abarca-Vargas, C. F. Peña Malacara, and V. L. Petricevich, "Characterization of chemical compounds with antioxidant and cytotoxic activities in bougainvillea x buttiana holttum and standl, (Var. rose) extracts," *Antioxidants*, vol. 5, no. 4, Article ID 5040045, 2016.

[40] M. D. Awouafack, P. Tane, and H. Morita, *Isolation and Structure Characterization of Flavonoids, Flavonoids - from Biosynthesis to Human Health*, Intech Open, London, UK, 2017.

[41] R. K. Saini and Y.-S. Keum, "Carotenoid extraction methods: a review of recent developments," *Food Chemistry*, vol. 240, pp. 90–103, 2018.

[42] S. Oancea, M. Stoia, and D. Coman, "Effects of extraction conditions on bioactive anthocyanin content of *Vaccinium corymbosum* in the perspective of food applications," *Procedia Engineering*, vol. 42, pp. 489–495, 2012.

Research Article

Optimization of Spectrophotometric and Fluorometric Assays Using Alternative Substrates for the High-Throughput Screening of Lipase Activity

Jun-Young Park,[1] **Jisu Ha,**[2] **Yoonseok Choi,**[1] **Pahn-Shick Chang** [iD]**,**[1,3,4,5] **and Kyung-Min Park** [iD][2,5]

[1]*Department of Agricultural Biotechnology, Seoul National University, Seoul 08826, Republic of Korea*
[2]*Department of Food Science and Biotechnology, Wonkwang University, Iksan 54538, Republic of Korea*
[3]*Research Institute of Agriculture and Life Sciences, Seoul National University, Seoul 08826, Republic of Korea*
[4]*Center for Food and Bioconvergence, Seoul National University, Seoul 08826, Republic of Korea*
[5]*Center for Agricultural Microorganism and Enzyme, Seoul National University, Seoul 08826, Republic of Korea*

Correspondence should be addressed to Pahn-Shick Chang; pschang@snu.ac.kr and Kyung-Min Park; kmpark79@wku.ac.kr

The effects of reaction conditions on the spectrophotometric and fluorometric assays using alternative substrates (p-nitrophenyl palmitate and 4-methylumbelliferyl oleate) were investigated to optimize them for the high-throughput screening of lipase activity from agricultural products. Four model lipases from *Chromobacterium viscosum*, *Pseudomonas fluorescens*, *Sus scrofa* pancreas, and wheat germ (*Triticum aestivum*) were allowed to hydrolyze the alternative substrates at different substrate concentrations (1–5 mM), operating pH (5.0–8.0), and operating temperatures (25–55°C). The results show that both the spectrophotometric and fluorometric assays worked well at the standard reaction conditions (pH 7.0 and 30°C) for finding a typical lipase, although pH conditions should be considered to detect the catalytic activity of lipases, which are applicable to more acidic or alkaline pH circumstances. To validate the optimized conditions, the high-throughput screening of lipase activity was conducted using 17 domestic agricultural products. A pileus of *Pleurotus eryngii* showed the highest activity in both the spectrophotometric (633.42 μU/mg) and fluorometric (101.77 μU/mg) assays. The results of this research provide practical information for the high-throughput screening of lipases using alternative substrates on microplates.

1. Introduction

Lipases (i.e., triacylglycerol hydrolase, EC 3.1.1.3) are carboxylic ester hydrolases found in diverse organisms, including animals, plants, fungi, and bacteria that can catalyze the hydrolysis of triacylglycerols into diacylglycerols, monoacylglycerol, and free fatty acids [1]. These enzymes are highly soluble in aqueous phases, similar to other enzymes; however, their substrates are highly water-insoluble acylglycerol species, and consequently, lipases can efficiently catalyze hydrolysis at the interface between water and oil droplets [2]. Most lipases from eukaryotes precisely control the accessibility of their active site to their substrates by opening and closing their lid structure at oil/water interface [3, 4]. Furthermore, lipases typically exhibit unique selectivities on their substrates, such as typoselectivity, regioselectivity, and stereoselectivity [5, 6], though a few lipases show promiscuous behavior toward their substrates [7]. Because of those attractive properties, lipases are being studied in the fields of selective hydrolysis for flavor/texture improvement [8, 9], esterification for the synthesis of structured lipids or functional compounds [10, 11], and other catalytic reactions. These versatile enzymes have been discovered and developed from various sources to have

individual characteristics and stabilities suitable for the food, chemical, detergent, cosmetic, leather, diagnosis, and pharmaceutical industries [12]. Therefore, it is important to pursue the discovery of novel lipases with unique properties from natural sources.

The first requirement for the discovery of lipases is to establish a high-throughput methodology to rapidly and precisely determine their catalytic activity. Numerous methodologies are available for the detection of lipase activity [13]. Among them, chemical methodologies (e.g., titrimetric, spectroscopic, and chromatographic assays) that measure the appearance of hydrolytic reaction products are commonly used [14]. Ironically, using original acylglycerol species as substrates for lipase reactions is a hindrance to high-throughput screening because most of the relevant methodologies are complicated or laborious due to their high lipophilicity and analytical difficulty of their products. Those reactions have to be conducted in a complex phase such as an emulsion or reverse micelle to adequately disperse the lipophilic substrates in the aqueous phase, which demands a number of ingredients to prepare a reaction medium [15, 16]. Those methods also require further steps and a long time to analyze the free fatty acids that are the reaction products. For that reason, previous studies have developed artificial alternative substrates such as p-nitrophenyl fatty acid esters, 4-methylumbelliferyl fatty acid esters, or other functionalized fatty acid derivatives [17, 18], which are relatively soluble in the aqueous phase. The products liberated from the alternative substrates during lipase-catalyzed hydrolysis contain specific compounds that can be detected by spectrophotometry or fluorometry, which allows the reaction progress to be analyzed conveniently on microplates and is thus appropriate for high-throughput screening. Unfortunately, however, studies to find novel lipases have been conducted sporadically, and the detailed screening conditions (e.g., buffer, pH, temperature, and enzyme-substrate ratio) are highly inconsistent. These methodologies need to be optimized according to the type of substrate and lipase to validate whether they can be reliably reproduced with lipases from a variety of natural sources.

In this study, to establish an optimized enzymatic platform for the high-throughput screening of lipase from agricultural sources, we constructed spectrophotometric and fluorometric assays based on two alternative substrates (p-nitrophenyl palmitate (p-NPP) [19] and 4-methylumbelliferyl oleate (4-MUO) [20]) and investigated the effects of major reaction conditions (pH and temperature) on both assays using four commercial lipases from different origins (lipase from *Chromobacterium viscosum* (CVL), lipase from *Pseudomonas fluorescens* (PFL), lipase from porcine (*Sus scrofa*) pancreas (PPL), and lipase from wheat germ (*Triticum aestivum*) (WGL)). The reactions were tested on 96-well microplates at different pH, temperature, enzyme concentration, and substrate concentration conditions, and their discrepancy was investigated. The lipase reactions using p-NPP and 4-MUO as substrates were monitored by spectrophotometric and fluorometric methodologies to detect p-nitrophenol and 4-methylumbelliferone, respectively. Furthermore, we validated the optimized conditions

by applying them to high-throughput screening for lipase activity in crude protein extracts from domestic agricultural sources. The following results would provide practical information about high-throughput screening for lipases using alternative substrates on microplates.

2. Materials and Methods

2.1. Materials. The alternative substrates, p-NPP ($\geq$98%) and 4-MUO ($\geq$95%), were purchased from Sigma-Aldrich Co. (St. Louis, MO, USA). The reaction products, p-nitrophenol ($\geq$99%) and 4-methylumbelliferone ($\geq$98%), and commercial lipases, CVL ($\geq$2,500 U/mg), PFL ($\geq$20 U/mg), PPL (100–650 U/mg), and WGL (5–15 U/mg, triacetin), were also purchased from Sigma-Aldrich Co. One unit is defined as the amount of enzyme that will release 1.0 μmol of fatty acids from the substrate per min at each condition given in the manufacturer's instructions. All other chemicals were of analytical reagent grade and were used after filtration through a membrane filter (0.45 μm). The 17 domestic agricultural products (cereals, vegetables, mushrooms, nuts, and seeds) were purchased from local markets. The Costar® 96-well microplates (black wall, clear bottom) used for the fluorometric analyses were purchased from Corning Co. (Corning, NY, USA). The JetBiofil® 96-well microplates (clear wall and clear bottom) used for the spectrophotometric analyses were purchased from Guangzhou Jet Biofiltration Co. (Guangzhou, China).

2.2. Enzyme and Substrate Sample Preparation. Four lipase stock solutions (CVL, PFL, PPL, and WGL) were prepared by dissolving 10 mg of the solid enzyme directly into 1 mL of 50 mM Tris-HCl buffer at room temperature. The PPL stock solution was subsequently centrifuged at 5,000 ×g for 10 min to remove a large amount of insoluble material before the enzyme assay [21]. All the lipase stock solutions were stored at 4°C until use. The substrate stock solutions (p-NPP and 4-MUO) were prepared as previously described [21, 22] with slight modifications. In brief, the p-NPP stock solution (5.00 mM) was prepared by dissolving 62.29 mg of p-NPP into 33 mL of distilled water with 330.0 mg of Triton X-100 and 11.0 mg of sodium dodecyl sulfate. The solution was heated at 65°C for 20 min with magnetic stirring, cooled to room temperature, and stored at 4°C until use. The 4-MUO stock solution (50 mM) was prepared by dissolving 25 mg of 4-MUO into 1.1348 mL of dimethyl sulfoxide (DMSO) with vortexing. The 4-MUO stock solution was stored at −18°C until use. All the substrate stock solutions were dissolved in 50 mM Tris-HCl buffer to give the specific concentration needed for each experiment.

2.3. Lipase Activity Assay Using p-NPP as a Substrate. The lipase assay using p-NPP as a substrate was established based on the spectrophotometric methodology as previously described [22] with slight modifications. Substrate solution (0.1 mL) at a specific concentration was added to a 96-well microplate and preincubated in a microplate reader (SpectraMax iD3 multimode microplate reader, Molecular

Devices, San Jose, CA, USA) for 5 min. Then, lipase-catalyzed hydrolysis was initiated by adding the enzyme solution (0.1 mL) to the substrate solution. The absorbance of each well at 410 nm ($\varepsilon = 18.3\,\text{mM}^{-1}\,\text{cm}^{-1}$) was monitored over the reaction time to quantitate the amount of p-nitrophenol liberated from the p-NPP during the hydrolysis. A calibration curve of p-nitrophenol concentration versus the absorption unit (AU) was plotted using a p-nitrophenol standard compound (Supplementary Figure S1). One unit of lipase catalytic activity was defined as the amount of enzyme liberating 1 μmol of p-nitrophenol per minute. Hyperbolic nonlinear regression curve fitting for the production of p-nitrophenol against the reaction time was performed using SigmaPlot software (ver. 12.5, Systat Software Co., San Jose, CA, USA). The final concentration of the liberated p-nitrophenol was determined from each reaction curve, and the differences between initial concentration and final concentration of the product were converted into the values of the average rate of change (i.e., U/mL per 60 min) as follows:

$$\text{Catalytic activity} \, (\mu\text{mol/min/mL}) = \frac{[P]_f - [P]_i}{t}, \quad (1)$$

where $[P]_i$ and $[P]_f$ are the initial and final concentrations of p-nitrophenol in each well, respectively, and t is the reaction time (in this case, 60 min).

2.4. Lipase Activity Assay Using 4-MUO as a Substrate.
The lipase assay using 4-MUO as a substrate was established based on the fluorometric methodology as previously described [21] with slight modifications. Substrate solution (0.1 mL) at a specific concentration was added to a 96-well microplate and preincubated in a microplate reader for 5 min. Then, lipase-catalyzed hydrolysis was initiated by adding the enzyme solution (0.1 mL) to the substrate solution. The fluorescence of 4-methylumbelliferone liberated during hydrolysis was detected at an excitation wavelength of 320 nm and an emission wavelength of 455 nm over the reaction time. The fluorescence data were acquired in bottom-reading mode and PMT low measurement. The excitation and emission slit widths were set at 9 and 15 nm, respectively. A calibration curve of 4-methylumbelliferone concentration versus the relative fluorescence unit (RFU) was plotted using 4-methylumbelliferone standard compound (Supplementary Figure S2). One unit of catalytic activity of lipase was defined as the amount of enzyme liberating 1 μmol of 4-methylumbelliferone per minute. Hyperbolic nonlinear regression curve fitting of the production of 4-methylumbelliferone against the reaction time was conducted as aforementioned. The final concentration of the liberated 4-methylumbelliferone was determined from each reaction curve, and the differences between initial concentration and final concentration of the product were converted into the values of the average rate of change as follows:

$$\text{Catalytic activity} \, (\mu\text{mol/min/mL}) = \frac{[M]_f - [M]_i}{t}, \quad (2)$$

where $[M]_i$ and $[M]_f$ are the initial and final concentrations of 4-methylumbelliferone in each well, respectively, and t is the reaction time (in this case, 60 min).

2.5. Crude Protein Extraction and Lipase Activity Screening.
Crude protein extraction from the domestic agricultural products was conducted using a Pierce™ Plant Total Protein Extraction Kit (Thermo Fisher Scientific Co., Rockford, IL, USA) according to the manufacturer's instructions with slight modifications. In brief, a 100 mg sample of each domestic agricultural product was prepared and placed in the filter. For plant leaves, the samples were folded into a small size and punched with a pipette tip about 60 times. For seeds and stems, the samples were cut into small pieces and minced about 60 times using a plastic rod. One hundred microliters of native lysis buffer were added to the filter, and the samples were ground using a plastic rod with twisting force about 60 times. Then, the filter was covered and incubated on ice for 5 min before centrifugation at 16,000 ×g for 5 min. The supernatant containing the total proteins was used for the lipase activity screening, and the spectrophotometric and fluorometric assays were conducted as aforementioned.

2.6. Statistical Analysis.
All the reactions were conducted in triplicate under the same conditions. Statistical analyses were performed using SPSS software (ver. 25.0, IBM Co., Armonk, NY, USA). The data were subjected to one-way analysis of variance (ANOVA), and statistical significance between data groups was validated using Duncan's multiple range test ($p < 0.05$).

3. Results and Discussion

3.1. Optimization of the Lipase Assay Using p-NPP as an Alternative Substrate

3.1.1. Effects of Substrate Concentration on the Lipase Assay Using p-NPP.
Lipase activity is highly affected by physicochemical conditions such as the enzyme-substrate molar ratio, pH, temperature, ionic strength, and additives [23]. Lipases could exhibit different catalytic activity and especially substrate specificity depending on to the reaction conditions. Hence, in this study, we investigated the effects of three major reaction conditions (substrate concentration, pH, and temperature) and scrutinized the practical results of spectrophotometric and fluorometric lipase assays conducted using alternative substrates. The substrate molar concentration is the most critical parameter in determining the initial velocity and kinetics of an enzyme reaction. At a specific enzyme concentration, the reaction rate is relatively slow in the range of low substrate concentration, whereas it gradually increases with the substrate concentration until substrate saturation point is reached [24]. Thus, high-throughput screening for catalytic activity should consider whether the target substrate added to the reaction medium is enough to react with the target enzyme. To investigate the effects of substrate concentration, we conducted lipase-

catalyzed hydrolysis of p-NPP at different initial concentrations (1.0–5.0 mM) using otherwise standard conditions (pH 7.0 and 30°C) for 60 min (Figure 1). The reaction progress curves of all lipases showed constant linearity at the early stage of progress (data not shown), and the final concentrations of the liberated p-nitrophenol were determined from the nonlinear regression curves of p-nitrophenol concentrations versus reaction time. As the substrate concentration increased, the catalytic activity of the lipases increased gradually, peaked at 2.0-3.0 mM p-NPP, and then decreased slightly. Among them, WGL showed the highest catalytic activity (1.38 ± 0.10 U/mL, $p = 0.000$–0.002) at 3 mM substrate condition. Except PFL (0.55 ± 0.02 U/mL at 2 mM p-NPP), other lipases similarly showed the optimal reaction at 3 mM substrate condition. The detailed catalytic characteristics of the model lipases differ from one other; however, our results indicate that the present range of p-NPP concentration is enough to find various lipases with adequate catalytic activity in a small-scale reaction on microplates. Notably, there was a reduction of lipase activity at higher substrate concentrations, a phenomenon called substrate inhibition that is generally observed in lipase-catalyzed hydrolysis. Excessive amounts of substrate compared with enzyme cause unintended competition with itself in a form of competitive inhibition [25]. Furthermore, the water solubility of p-NPP is relatively low due to its fatty acid moiety, so surfactants such as Triton X-100 and sodium dodecyl sulfate had to be used to completely solubilize p-NPP in the aqueous phase (3.2.), although these molecules could have a negative effect on enzyme protein. Therefore, the high-throughput methodology using p-NPP as an alternative substrate basically considers whether the substrate concentration is appropriate to mitigate the negative effect on the lipase activity and consequently detect any level of lipase activity efficiently.

3.1.2. Effects of Operating pH on the Lipase Assay Using p-NPP.

The pH value of the reaction medium (i.e., operating pH) is also important to screen the lipase activity from natural sources. The degree of acidity or basicity can affect the catalytic activity of enzymes by altering the ionization state of an enzyme's active site, even worse, causing an irreversible change in the protein structure by disrupting internal ionic bonds [26]. In other words, enzymes only work in a particular pH range typically showing a bell-shaped plot of the pH value versus catalytic activity. Until now, lipases with various optimum pH from acidic to basic have been discovered and developed to serve industrial purpose. Hence, a high-throughput methodology to detect lipase activity should be uninterrupted by any pH value. To investigate the effects of operating pH on the lipase-catalyzed hydrolysis of p-NPP, reactions were conducted in a typical pH range (5.0–8.0) at 30°C for 60 min (Figure 2), and final concentrations of liberated p-nitrophenol were compared. All the lipases except WGL showed the highest catalytic activity (CVL, 1.32 ± 0.16 U/mL; PFL, 0.50 ± 0.02 U/mL; PPL, 0.37 ± 0.01 U/mL) at pH 7.0 than at mild acidic pH 5.0-6.0, and WGL showed a constant activity at pH 6.0–8.0
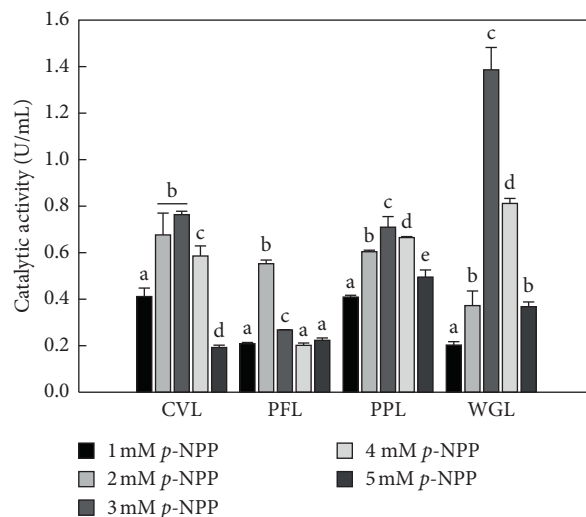

Figure 1: Effects of substrate (p-nitrophenyl palmitate, p-NPP) concentration on the catalytic activity of lipases. The substrate concentration was in the range of 1–5 mM. Error bars indicate the standard error of the mean. Superscripts (a–e) above the bars denote significant differences in catalytic activity ($p < 0.05$, Duncan's multiple range test on ANOVA). CVL, *Chromobacterium viscosum* lipase (0.01 mg/mL); PFL, *Pseudomonas fluorescens* lipase (0.001 mg/mL); PPL, porcine (*Sus scrofa*) pancreatic lipase (10 mg/mL); WGL, wheat germ (*Triticum aestivum*) lipase (1 mg/mL).
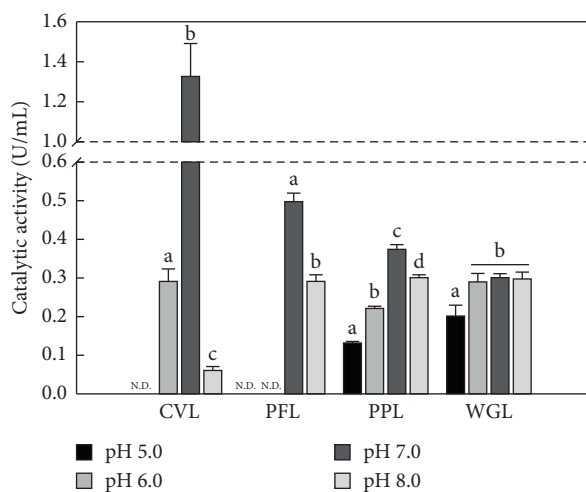
Figure 2: Effects of operating pH on the catalytic activity of lipases against p-nitrophenyl palmitate as a substrate. The operating pH was in the range of 5.0–8.0. Error bars indicate the standard error of the mean. Superscripts (a–d) above the bars denote significant differences in catalytic activity ($p < 0.05$, Duncan's multiple range test on ANOVA). CVL, *Chromobacterium viscosum* lipase (0.01 mg/mL); PFL, *Pseudomonas fluorescens* lipase (0.001 mg/mL); PPL, porcine (*Sus scrofa*) pancreatic lipase (10 mg/mL); WGL, wheat germ (*Triticum aestivum*) lipase (1 mg/mL); N.D, not detected.

($p = 0.908$–0.978). In fact, the optimum pH of the four lipases was already known to be from neutral to slightly alkaline [27–30], and our results confirm that p-NPP can be used as the alternative substrate to detect the lipase activity at appropriate pH conditions. However, notably, the

dissociation constant (pKa) of *p*-nitrophenol is 7.0–7.5 in aqueous solution at room temperature, and it gradually changes from yellow to colorless as the pH decreases to 5.4 [31, 32], which means the liberated products are difficult to detect in acidic conditions. Therefore, operating pH in the range of 7.0–8.0 is proper to screen typical lipase activity by using *p*-NPP, and it is also applicable to any alkaline pH to find the desired lipase with high activity or stability in strong alkaline environment.

3.1.3. Effects of Operating Temperature on the Lipase Assay Using p-NPP.

Chemical reactions happen at specific rates at given conditions of substrate concentration and reaction temperature (i.e., operating temperature), and those reaction rates depend on the operating temperature according to the Arrhenius equation [24]. The hydrolysis of ester bonds catalyzed by lipase is also significantly affected by the operating temperature, and lipase assays therefore need the proper temperature to trigger and sustain a catalytic reaction. Furthermore, an enzyme can easily be inactivated at a high temperature because enzymes are protein macromolecules susceptible to thermal damage. Thus, a high-throughput methodology for detecting enzymes should maintain an appropriate operating temperature. To investigate the effects of operating temperature on the lipase-catalyzed hydrolysis of *p*-NPP, we conducted reactions in a typical temperature range for lipase reactions (25–55°C) at pH 7.0 for 60 min (Figure 3) and compared the final concentrations of liberated *p*-nitrophenol. The lipase activity at certain levels was successfully detected in all reaction conditions, and the highest catalytic activity occurred at 30–40°C, which is near the optimum temperatures of four lipases (30–50°C) [27–30]. Among them, CVL showed the highest catalytic activity (2.48 ± 0.15 U/mL, $p = 0.000$) at 30°C. Therefore, operating temperatures in the range of 30–40°C are appropriate when screening for typical lipase activity using *p*-NPP without any interruption of catalytic activity, though a broad range of operating temperatures is also applied to find lipases specialized to specific temperature ranges from the small-scale reaction on microplates. Additionally, *p*-NPP is a highly stable compound at moderately high temperatures, which implies that a high-throughput methodology using *p*-NPP as the substrate could be applicable for finding thermostable lipases with high activity or stability at higher than usual temperatures.

3.2. Optimization of the Lipase Assay Using 4-MUO as an Alternative Substrate

3.2.1. Effects of Substrate Concentration on the Lipase Assay Using 4-MUO.

Crude protein extracts of natural sources generally contain large amounts of chemical compounds such as phytochemicals, fatty acids, inorganic materials, and other proteins [33]. Compounds with noticeable color or fluorescence can interfere with the detection of catalytic activity of the target enzymes in the crude protein extract by directly inhibiting those enzymes or indirectly confusing the reaction outcomes. For that reason, more than a single

Figure 3: Effects of operating temperature on the catalytic activity of lipases against *p*-nitrophenyl palmitate as a substrate. The operating temperature was in the range of 25–55°C. Error bars indicate the standard error of the mean. Superscripts (a–f) above the bars denote significant differences in catalytic activity ($p < 0.05$, Duncan's multiple range test on ANOVA). CVL, *Chromobacterium viscosum* lipase (0.01 mg/mL); PFL, *Pseudomonas fluorescens* lipase (0.001 mg/mL); PPL, porcine (*Sus scrofa*) pancreatic lipase (10 mg/mL); WGL, wheat germ (*Triticum aestivum*) lipase (1 mg/mL).
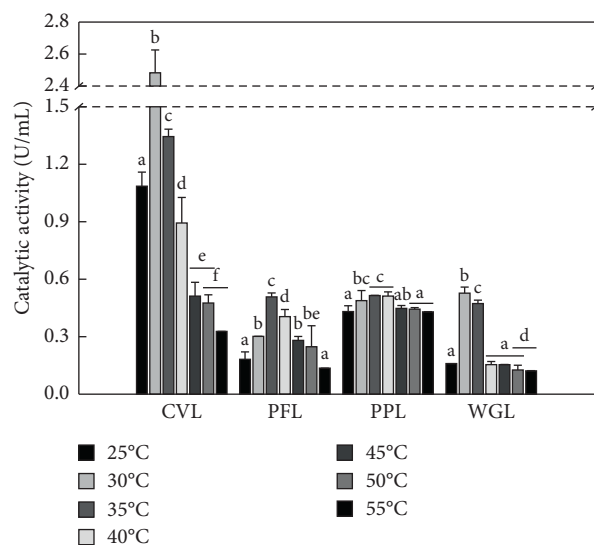
substrate should be used for high-throughput screening to discover novel lipases from natural sources. In this study, we also investigated the use of 4-MUO as an alternative substrate for high-throughput screening for lipase activity and optimized this fluorometric methodology, which detects light emissions (i.e., fluorescence) from the products absorbing excitation light at a specific wavelength. Upon lipase-catalyzed hydrolysis of the ester bond, 4-MUO produces 4-methylumbelliferone, which emits fluorescence at 445–455 nm wavelength when it is excited by light at 320–390 nm wavelength [20, 34].

First of all, to investigate the effects of substrate on the reaction, we tested lipase-catalyzed hydrolysis of 4-MUO at different initial concentrations (1.0–5.0 mM) using standard conditions (pH 7.0 and 30°C) for 60 min (Figure 4). The reaction progress curves of all lipases showed constant linearity at the early stage of progress (data not shown), and the final concentrations of the products were determined from each nonlinear regression curve of 4-methylumbelliferone concentration versus reaction time. The catalytic activity of PPL gradually increased, peaked (0.31 ± 0.01 U/mL) at 3.0 mM 4-MUO, and decreased as the substrate concentration continued to increase, as shown in the *p*-NPP reaction. In the case of PFL and CVL, a slight tendency towards reduction in catalytic activity (*i.e.*, substrate inhibition) was shown, whereas WGL showed a slight tendency to increase in catalytic activity. Notably, the molar concentrations of PFL and CVL used for the reaction with 4-MUO as a substrate were relatively lower than those used for the reaction with *p*-NPP. We found that the catalytic activity of PFL and CVL was consistently higher than that of PPL
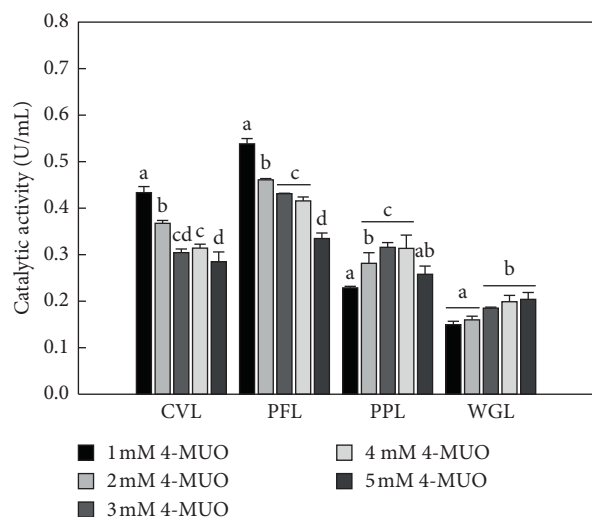
FIGURE 4: Effects of substrate (4-methylumbelliferyl oleate, 4-MUO) concentration on the catalytic activity of lipases. The substrate concentration was in the range of 1–5 mM. Error bars indicate the standard error of the mean. Superscripts (a–d) above the bars denote significant differences in catalytic activity ($p < 0.05$, Duncan's multiple range test on ANOVA). CVL, *Chromobacterium viscosum* lipase (0.1 μg/mL); PFL, *Pseudomonas fluorescens* lipase (0.1 μg/mL); PPL, porcine (*Sus scrofa*) pancreatic lipase (10 mg/mL); WGL, wheat germ (*Triticum aestivum*) lipase (1 mg/mL).
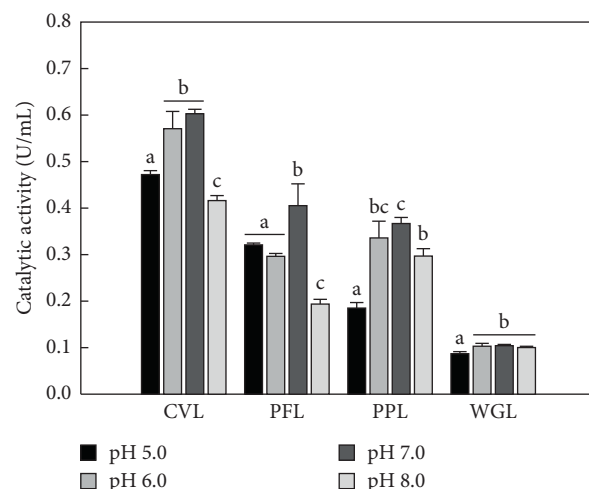

FIGURE 5: Effects of operating pH on the catalytic activity of lipases against 4-methylumbelliferyl oleate as a substrate. The operating pH was in the range of 5.0–8.0. Error bars indicate the standard error of the mean. Superscripts (a–c) above the bars denote significant differences in catalytic activity ($p < 0.05$, Duncan's multiple range test on ANOVA). CVL, *Chromobacterium viscosum* lipase (0.1 μg/mL); PFL, *Pseudomonas fluorescens* lipase (0.1 μg/mL); PPL, porcine (*Sus scrofa*) pancreatic lipase (10 mg/mL); WGL, wheat germ (*Triticum aestivum*) lipase (1 mg/mL).

and WGL at the same enzyme concentrations (data not shown). In the fluorometric assay, an excessive amount of liberated fluorophore could generate a fluorescence value exceeding the sensitivity of the photomultiplier tube- (PMT-) based microplate reader. Therefore, a high-throughput methodology using 4-MUO as an alternative substrate should ensure that the substrate and enzyme concentrations are appropriate to detect any level of lipase activity precisely. Additionally, the presence of organic solvent DMSO for dissolving 4-MUO efficiently could have negatively affected the catalytic activity of the lipase; however, the actual amount of DMSO in the aqueous reaction medium (<50% (v/v)) was not sufficient to lower the catalytic activity of lipase [35].

3.2.2. Effects of Operating pH on the Lipase Assay Using 4-MUO.

The effects of the operating pH on the lipase-catalyzed hydrolysis of 4-MUO were investigated in a typical pH range (5.0–8.0) at 30°C for 60 min (Figure 5). All the lipases except WGL showed the highest catalytic activity (CVL, 0.60 ± 0.01 U/mL; PFL, 0.41 ± 0.05 U/mL; PPL, 0.37 ± 0.01 U/mL) at pH 7.0, exhibiting typical bell-shaped plots of pH value versus catalytic activity. Those results correspond with those from the spectrophotometric assay, indicating that the catalytic characteristics of each lipase with regard to operating pH conditions were expressed in the fluorometric assay without any external interference. Furthermore, 4-methylumbelliferone, which is the fluorescent product of the lipase-catalyzed hydrolysis of 4-MUO, is highly stable at acidic or alkaline pH circumstances, and lipase activity was

successfully detected in all reaction conditions. These results indicated that a high-throughput methodology using 4-MUO as an alternative substrate could detect lipase activity in a broad range of pH conditions, in contrast to the spectrophotometric assay. On the other hand, a previous report on 4-methylumbelliferone showed that its maximum excitation and emission wavelengths (λ_{max}) could be affected by changes in pH and the addition of organic solvents [20, 36]. This point should be especially considered when using 4-MUO as an alternative substrate for high-throughput screening of lipase activity; however, no critical change occurs in the fluorescence until the pH conditions become extreme. Therefore, an operating pH in the range of 7.0–8.0 is appropriate for screening typical lipase activity using 4-MUO, and the excitation and emission conditions should be adjusted to detect the catalytic activity of lipase in more acidic or alkaline pH circumstances.

3.2.3. Effects of Operating Temperature on the Lipase Assay Using 4-MUO.

The effects of operating temperature on the lipase-catalyzed hydrolysis of 4-MUO were investigated in a typical temperature range (25–55°C) at pH 7.0 for 60 min (Figure 6). The catalytic activity of each lipase was successfully detected in all temperature conditions, and the highest catalytic activity was shown at 30–40°C, corresponding to the results from the spectrophotometric assay. Among them, PPL showed the highest catalytic activity (0.49 ± 0.02 U/mL) at 35°C, which is near the body temperature. High operating temperature had no significant effect in the detection of the reaction product or the stability of 4-MUO during hydrolysis. Therefore, the present operating temperature range is sufficient to find various lipases in
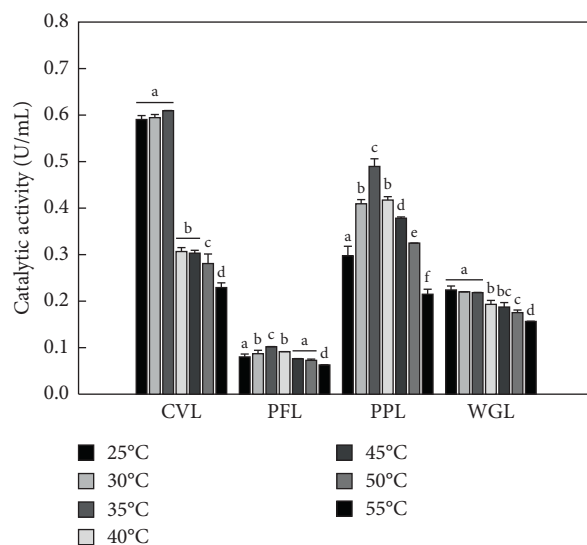
Figure 6: Effects of operating temperature on the catalytic activity of lipases against 4-methylumbelliferyl oleate as a substrate. The operating temperature was in the range of 25–55°C. Error bars indicate the standard error of the mean. Superscripts (a–f) above the bars denote significant differences in catalytic activity ($p < 0.05$, Duncan's multiple range test on ANOVA). CVL, *Chromobacterium viscosum* lipase (0.1 μg/mL); PFL, *Pseudomonas fluorescens* lipase (0.1 μg/mL); PPL, porcine (*Sus scrofa*) pancreatic lipase (10 mg/mL); WGL, wheat germ (*Triticum aestivum*) lipase (1 mg/mL).

small-scale reactions with 4-MUO on microplates without any interruption. Of course, an operating temperature in the range of 30–40°C is generally proper for screening typical lipase activity because most lipases have optimum temperatures ranging from 30 to 50°C. Overall, the effects of three major reaction conditions, which are key influence factors for the high-throughput screening of lipase activity, were comprehensively investigated and optimized using *p*-NPP and 4-MUO as alternative substrates. Based on those results, we conducted high-throughput screening of lipase activity from domestic agricultural products to validate whether our methodology could be uniformly reproduced with a variety of natural lipase sources.

3.3. High-Throughput Screening of Lipase Activity from Domestic Agricultural Products.

Crude protein extracts from 17 agricultural products were screened for lipase activity using spectrophotometric and fluorometric assays simultaneously at optimized conditions. Domestic agricultural products containing more than 10.0 g of protein and 1.0 g of lipids were selected from the 9th Korea National Standard Food Composition Table (Republic of Korea): 4 kinds of mushrooms (*Lentinula*, *Agaricus*, *Hericium*, and *Pleurotus* sp.), 5 kinds of vegetables (*Glycine*, *Allium*, *Cucurbita*, *Capsicum*, and *Brassica* sp.), 5 kinds of cereals (*Coix*, *Fagopyrum*, *Amaranthus*, *Sorghum*, and *Oryza* sp.), 2 kinds of seeds (*Capsicum* and *Helianthus* sp.), and 1 kind of nut (*Arachis* sp.). The protein concentrations of the crude protein extracts were below 20 mg/mL, and the catalytic activity (μU/mL) of each sample was determined as the difference between the initial and final concentrations of the liberated products derived from non-linear regression curves of product concentration versus reaction time. Then, the specific activity was derived by dividing the catalytic activity by protein concentration. We used those

curves to calculate the lipase activity to account for the background absorbance or fluorescence of other compounds in the crude protein extracts that show color or fluorescence. The reactions were conducted at pH 7.0 and 30°C for 60 min using 3 mM *p*-NPP or 4-MUO. The overall lipase activity in the crude protein extracts of the 17 agricultural products is summarized in Tables 1 and 2. Among them, a pileus (i.e., the upper cap-shaped part) of *Pleurotus eryngii* (king oyster mushroom) showed the highest lipase activity in both the spectrophotometric (633.42 μU/mg) and fluorometric (101.77 μU/mg) assays. Except for one study that purified feruloyl esterase (EC 3.1.1.73) from *P. eryngii*, that species has not been mentioned as a source for lipases or esterases [37]. However, as the conspecific fungus *Pleurotus ostreatus* is known to have many lipase and carboxylesterase genes [38], *P. eryngii* could be considered as an excellent source of lipases based on our results. Finally, the tendency of both spectrophotometric and fluorometric results was analogous to each other, although several samples showed different absorbance or fluorescence backgrounds, which consequently affected the lipase activity detected in identical samples. Therefore, it is better to apply both spectrophotometric and fluorometric assays simultaneously when screening for lipase activity to acquire more precise results, especially when screening crude protein extracts.

In addition, *p*-NPP and 4-MUO used in this study are representative compounds among the various *p*-nitrophenyl and 4-methylumbelliferyl fatty acids that can be used as alternative substrates for lipase. These series of compounds generate the same products after hydrolysis of their ester bonds by lipase. However, the physicochemical properties of those compounds are quite different based on the lipophilic moiety (i.e., fatty acid chain length), which significantly affects both the reaction conditions and the catalytic activity of lipase. Most lipases have a similar mode of action to

TABLE 1: Lipase activity in crude protein extracts from domestic agricultural products (spectrophotometric assay).

Classification	Items Name	Specimen	Concentration (mg/mL)	Activity (μU/mL)	Specific activity (μU/mg protein)
Mushrooms	Shiitake mushroom (*Lentinula edodes*)	Pileus	6.0080	148.0607	24.6439
		Stalk	4.6380	73.5127	15.8501
	White mushroom (*Agaricus bisporus*)	Whole	7.4760	801.3916	107.1952
	Lion's mane mushroom (*Hericium erinaceus*)	Whole	4.5490	218.4672	48.0253
	King oyster mushroom (*Pleurotus eryngii*)	Pileus	5.1730	633.4164	379.4340
		Stalk	4.2960	379.4340	633.4164
Vegetables	Soybean sprout (*Glycine max*)	Cotyledon	16.4810	N.D	N.D
		Hypocotyl	5.0780	272.3075	53.6249
	Onion (*Allium cepa*)	Whole	4.4080	197.7594	44.8638
	Pumpkin (*Cucurbita moschata*)	Whole	5.2280	955.6646	182.7974
	Chili pepper (*Capsicum annuum*)	Whole	11.0353	N.D.	N.D.
		Crown	5.0830	1653.8623	325.3713
	Broccoli (*Brassica oleracea*)	Stalk	7.0280	912.8685	129.8902
		Leaf	13.0710	138.3971	10.5881
Cereals	Job's tears (*Coix lacryma-jobi*)	Whole	8.2480	634.6938	76.9512
	Buckwheat (*Fagopyrum esculentum*)	Whole	9.2220	980.1688	106.2859
	Pigweed (*Amaranthus sp.*)	Whole	4.4660	294.3958	65.9193
	Sorghum (*Sorghum bicolor*)	Whole	4.0380	190.5117	47.1797
	Brown rice (*Oryza sativa*)	Whole	5.2450	666.7909	127.1289
Nuts/seeds	Chili pepper seed (*Capsicum annuum*)	Whole	5.6420	1941.3555	344.0900
	Sunflower seed (*Helianthus annuus*)	Whole	5.8240	768.2591	131.9126
	Peanut (*Arachis hypogaea*)	Whole	5.4650	630.8974	115.4433

N.D, not detected.

TABLE 2: Lipase activity in crude protein extracts from domestic agricultural products (fluorometric assay).

Classification	Items Name	Specimen	Concentration (mg/mL)	Activity (μU/mL)	Specific activity (μU/mg protein)
Mushrooms	Shiitake mushroom (*Lentinula edodes*)	Pileus	6.0080	78.7792	13.1124
		Stalk	4.6380	12.2526	2.6418
	White mushroom (*Agaricus bisporus*)	Whole	7.4760	20.9502	2.8023
	Lion's mane mushroom (*Hericium erinaceus*)	Whole	4.5490	275.7866	60.6258
	King oyster mushroom (*Pleurotus eryngii*)	Pileus	5.1730	526.4440	40.8223
		Stalk	4.2960	175.3725	101.7676
Vegetables	Soybean sprout (*Glycine max*)	Cotyledon	16.4810	91.2425	5.5362
		Hypocotyl	5.0780	48.6468	9.5799
	Onion (*Allium cepa*)	Whole	4.4080	33.1211	7.5139
	Pumpkin (*Cucurbita moschata*)	Whole	5.2280	159.3122	30.4729
	Chili pepper (*Capsicum annuum*)	Whole	11.0353	7.8445	0.7109
		Crown	5.0830	426.2458	83.8571
	Broccoli (*Brassica oleracea*)	Stalk	7.0280	168.1837	23.9305
		Leaf	13.0710	120.8350	9.2445
Cereals	Job's tears (*Coix lacryma-jobi*)	Whole	8.2480	68.7360	8.3337
	Buckwheat (*Fagopyrum esculentum*)	Whole	9.2220	206.0473	22.3430
	Pigweed (*Amaranthus sp.*)	Whole	4.4660	73.7128	16.5053
	Sorghum (*Sorghum bicolor*)	Whole	4.0380	40.7260	10.0857
	Brown rice (*Oryza sativa*)	Whole	5.2450	105.8386	20.1790
Nuts/seeds	Chili pepper seed (*Capsicum annuum*)	Whole	5.6420	554.3091	98.2469
	Sunflower seed (*Helianthus annuus*)	Whole	5.8240	7.3494	1.2619
	Peanut (*Arachis hypogaea*)	Whole	5.4650	10.6436	1.9476

hydrolyze triacylglycerols or other ester compounds based on a catalytic triad comprised of amino acid residues (Ser-Asp-His) like chymotrypsin, whereas regioselectivity or stereoselectivity could be expressed in different mechanisms derived from their structural differences and followed environmental changes in active site. Therefore, it needs to be

considered and additionally optimized for the high-throughput screening conditions when using other substrates or finding stereoselective lipase in a further study.

4. Conclusions

In the present study, we comprehensively investigated the effects of reaction conditions on spectrophotometric and fluorometric assays of alternative substrates, and we optimized those conditions for the high-throughput screening of lipase activity in domestic agricultural products. Both assays using alternative substrates worked well at the standard reaction conditions (pH 7.0 and 30°C) for finding a typical lipase. The pH conditions of the reactions should be especially considered to detect the catalytic activity of lipases in more acidic or alkaline pH circumstances. Hence, it is recommended to employ both spectrophotometric and fluorometric assays for the high-throughput screening of lipase activity. Moreover, we propose *P. eryngii* as a novel source of lipases for the first time. Our results could contribute to providing critical information pertaining to the discovery of lipases.

Data Availability

The data used to support the findings of this study are available from the corresponding author upon request.

Conflicts of Interest

The authors declare that they have no conflicts of interest.

Authors' Contributions

K.M.P. and P.S.C. conceived the study and designed the experiments. J.S.H. performed the experiments and analyzed the data. J.Y.P. and H.J.S. wrote the manuscript, and the first draft of the study was reviewed and revised by J.Y.P., H.J.S., C.Y.S., and K.M.P. All authors discussed the contents of the manuscript and approved the submission. Jun-Young Park and Jisa Ha contributed equally as first authors.

Acknowledgments

Supplementary Materials

Figure S1: calibration curves of *p*-nitrophenol (*p*-NP) concentration versus absorption unit (AU) referring to the absorbance at 410 nm. Figure S2: calibration curves of 4-methylumbelliferone (4-MU) concentration versus relative fluorescence unit (RFU) referring to the emission fluorescence at 455 nm. (*Supplementary Materials*)

References

[1] A. K. Singh and M. Mukhopadhyay, "Overview of fungal lipase: a review," *Applied Biochemistry and Biotechnology*, vol. 166, no. 2, pp. 486–520, 2012.

[2] P. K. Ghosh, R. K. Saxena, R. Gupta, R. P. Yadav, and S. Davidson, "Microbial lipases: production and applications," *Science Progress*, vol. 79, no. Pt 2, pp. 119–157, 1996.

[3] J. Polaina and A. L. Maccabe, "Molecular structure and function," in *Industrial Enzymes: Structure, Function and Applications*, pp. 263–281, Springer, Berlin, Germany, 2010.

[4] F. Secundo, G. Carrea, C. Tarabiono et al., "The lid is a structural and functional determinant of lipase activity and selectivity," *Journal of Molecular Catalysis B: Enzymatic*, vol. 39, no. 1–4, pp. 166–170, 2006.

[5] Y. Choi, J.-Y. Park, and P.-S. Chang, "Integral stereoselectivity of lipase based on the chromatographic resolution of enantiomeric/regioisomeric diacylglycerols," *Journal of Agricultural and Food Chemistry*, vol. 69, no. 1, pp. 325–331, 2021.

[6] E. Rogalska, C. Cudrey, F. Ferrato, and R. Verger, "Stereoselective hydrolysis of triglycerides by animal and microbial lipases," *Chirality*, vol. 5, no. 1, pp. 24–30, 1993.

[7] M. Kapoor and M. N. Gupta, "Lipase promiscuity and its biochemical applications," *Process Biochemistry*, vol. 47, no. 4, pp. 555–569, 2012.

[8] X. Duan, M. Xiang, L. Wang, Q. Yan, S. Yang, and Z. Jiang, "Biochemical characterization of a novel lipase from *Malbranchea cinnamomea* suitable for production of lipolyzed milkfat flavor and biodegradation of phthalate esters," *Food Chemistry*, vol. 297, Article ID 124925, 2019.

[9] S. Moayedallaie, M. Mirzaei, and J. Paterson, "Bread improvers: comparison of a range of lipases with a traditional emulsifier," *Food Chemistry*, vol. 122, no. 3, pp. 495–499, 2010.

[10] R. Morales-Medina, M. Munio, A. Guadix, and E. M. Guadix, "Development of an up-grading process to produce MLM structured lipids from sardine discards," *Food Chemistry*, vol. 228, pp. 634–642, 2017.

[11] J.-Y. Park, J. Myeong, Y. Choi et al., "Erythorbyl fatty acid ester as a multi-functional food emulsifier: enzymatic synthesis, chemical identification, and functional characterization of erythorbyl myristate," *Food Chemistry*, vol. 353, Article ID 129459, 2021.

[12] N. Sarmah, D. Revathi, G. Sheelu et al., "Recent advances on sources and industrial applications of lipases," *Biotechnology Progress*, vol. 34, no. 1, pp. 5–28, 2018.

[13] F. Beisson, A. Tiss, C. Rivière, and R. Verger, "Methods for lipase detection and assay: a critical review," *European Journal of Lipid Science and Technology*, vol. 102, no. 2, pp. 133–153, 2000.

[14] R. Gupta, P. Rathi, N. Gupta, and S. Bradoo, "Lipase assays for conventional and molecular screening: an overview," *Biotechnology and Applied Biochemistry*, vol. 37, no. 1, pp. 63–71, 2003.

[15] N. Gomes, C. Gonçalves, M. García-Román, J. A. Teixeira, and I. Belo, "Optimization of a colorimetric assay for yeast lipase activity in complex systems," *Analytical Methods*, vol. 3, no. 4, pp. 1008–1013, 2011.

[16] C. W. Kwon, K.-M. Park, S. J. Choi, and P.-S. Chang, "A reliable and reproducible method for the lipase assay in an AOT/isooctane reversed micellar system: modification of the copper-soap colorimetric method," *Food Chemistry*, vol. 182, pp. 236–241, 2015.

[17] J. Grognux, D. Wahler, E. Nyfeler, and J.-L. Reymond, "Universal chromogenic substrates for lipases and esterases," *Tetrahedron: Asymmetry*, vol. 15, no. 18, pp. 2981–2989, 2004.

[18] K. N. Ingenbosch, A. Rousek, D. S. Wunschik, and K. Hoffmann-Jacobsen, "A fluorescence-based activity assay for immobilized lipases in non-native media," *Analytical Biochemistry*, vol. 569, pp. 22–27, 2019.

[19] N. Gupta, P. Rathi, and R. Gupta, "Simplified *para*-nitrophenyl palmitate assay for lipases and esterases," *Analytical Biochemistry*, vol. 311, no. 1, pp. 98-99, 2002.

[20] T. J. Jacks and H. W. Kircher, "Fluorometric assay for the hydrolytic activity of lipase using fatty acyl esters of 4-methylumbelliferone," *Analytical Biochemistry*, vol. 21, no. 2, pp. 279–285, 1967.

[21] J.-Y. Park, C. S. Kim, K.-M. Park, and P.-S. Chang, "Inhibitory characteristics of flavonol-3-O-glycosides from *Polygonum aviculare* L. (common knotgrass) against porcine pancreatic lipase," *Scientific Reports*, vol. 9, no. 1, p. 18080, 2019.

[22] J. Y. Park, K. M. Park, Y. Yoo et al., "Catalytic characteristics of asn-1(3) regioselective lipase from Cordyceps militaris," *Biotechnology Progress*, vol. 35, no. 2, p. e2744, 2019.

[23] J.-Y. Park, C. H. Kim, Y. Choi, K.-M. Park, and P.-S. Chang, "Catalytic characterization of heterodimeric linoleate 13*S*-lipoxygenase from black soybean (*Glycine max* (L.) Merr.)," *Enzyme and Microbial Technology*, vol. 139, Article ID 109595, 2020.

[24] P. K. Robinson, "Enzymes: principles and biotechnological applications," *Essays in Biochemistry*, vol. 59, pp. 1–41, 2015.

[25] M. C. Reed, A. Lieb, and H. F. Nijhout, "The biological significance of substrate inhibition: a mechanism with diverse functions," *BioEssays*, vol. 32, no. 5, pp. 422–429, 2010.

[26] C. B. Anfinsen, "Principles that govern the folding of protein chains," *Science*, vol. 181, no. 4096, pp. 223–230, 1973.

[27] M. R. Castellar, M. A. Taipa, and J. M. S. Cabral, "Kinetic and stability characterization of chromobacterium viscosum lipase and its comparison with Pseudomonas glumae lipase," *Applied Biochemistry and Biotechnology*, vol. 61, no. 3, pp. 299–314, 1997.

[28] L. Young Phil, C. Guk Hoon, and R. Joon Shick, "Purification and characterization of *Pseudomonas fluorescens* SIK W1 lipase expressed in *Escherichia coli*," *Biochimica et Biophysica Acta (BBA)—Lipids and Lipid Metabolism*, vol. 1169, no. 2, pp. 156–164, 1993.

[29] K. Bagi, L. M. Simon, and B. Szajáni, "Immobilization and characterization of porcine pancreas lipase," *Enzyme and Microbial Technology*, vol. 20, no. 7, pp. 531–535, 1997.

[30] V. S. Kapranchikov, N. A. Zherebtsov, and T. N. Popova, "Purification and characterization of lipase from wheat (*Triticum aestivum* L.) germ," *Applied Biochemistry and Microbiology*, vol. 40, no. 1, pp. 84–88, 2004.

[31] L. E. Janes, A. C. Löwendahl, and R. J. Kazlauskas, "Quantitative screening of hydrolase libraries using pH indicators: identifying active and enantioselective hydrolases," *Chemistry—A European Journal*, vol. 4, no. 11, pp. 2324–2331, 1998.

[32] G. N. Bowers Jr., R. B. McComb, R. G. Christensen, and R. Schaffer, "High-purity 4-nitrophenol: purification, characterization, and specifications for use as a spectrophotometric reference material," *Clinical Chemistry*, vol. 26, no. 6, pp. 724–729, 1980.

[33] S. Seth, D. Chakravorty, V. K. Dubey, and S. Patra, "An insight into plant lipase research—challenges encountered," *Protein Expression and Purification*, vol. 95, pp. 13–21, 2014.

[34] R. F. Chen, "Fluorescent pH indicator. spectral changes of 4-methylumbelliferone," *Analytical Letters*, vol. 1, no. 7, pp. 423–428, 1968.

[35] W. Tsuzuki, A. Ue, and Y. Kitamura, "Effect of dimethylsulfoxide on hydrolysis of lipase," *Bioscience, Biotechnology, and Biochemistry*, vol. 65, no. 9, pp. 2078–2082, 2001.

[36] H. Zhi, J. Wang, S. Wang, and Y. Wei, "Fluorescent properties of hymecromone and fluorimetric analysis of hymecromone in compound Dantong capsule," *Journal of Spectroscopy*, vol. 2013, Article ID 147128, 9 pages, 2013.

[37] A. Nieter, P. Haase-Aschoff, D. Linke, M. Nimtz, and R. G. Berger, "A halotolerant type A feruloyl esterase from *Pleurotus eryngii*," *Fungal Biology*, vol. 118, no. 3, pp. 348–357, 2014.

[38] A. Piscitelli, V. Tarallo, L. Guarino, G. Sannia, L. Birolo, and C. Pezzella, "New lipases by mining of *Pleurotus ostreatus* genome," *PLoS One*, vol. 12, no. 9, Article ID e0185377, 2017.